MATHEMATICAL MODELING ON THE EFFECTS OF VACCINATION AND NON-PHARMACEUTICAL INTERVENTIONS ON COVID-19 CONTROL DYNAMICS

BY

Francis Musili Muli

A Thesis Submitted to the Board of Postgraduate Studies in Fulfilment of the Requirements for the Award of the Degree Of Doctor of Philosophy in Applied Mathematics

SCHOOL OF BIOLOGICAL, PHYSICAL, MATHEMATICS AND ACTUARIAL SCIENCES

JARAMOGI OGINGA ODINGA UNIVERSITY OF SCIENCE AND TECHNOLOGY

Declaration

This thesis is my own work and has not been presented for a degree award in any other institution.

Francis Musili Muli
W262/4167/2020

Signature ..... Date .....

This thesis has been submitted for examination with our approval as the university supervisors.

1. Prof. Benard Okelo
Department of Pure and Applied Mathematics
JOOUST, Kenya

Signature ..... Date .....

2. Prof. Omolo Ongati
Department of Pure and Applied Mathematics
JOOUST, Kenya

Signature ..... Date .....

2. Dr. Richard Magwanga
Department of Biological Sciences
JOOST, Kenya

Signature ..... Date .....

Acknowledgments

I wish to express my appreciation and gratitude to my supervisors, Prof Benard Okelo, Prof.Omolo Ongati, and Dr. Richard Magwanga for their constant advice, guidance and support throughout the research work. I acknowledge my wife Eunice Muthoni and our children Favour Mbenya and Collins Munene for their encouragement. I greatly acknowledge the input of Douglas Mwangi whose input in Python programming was very important to my study. Lastly I thank the Almighty God for without whom we can do nothing.

Dedication

I dedicate this work to my dad Jonathan who instilled diligence in me, and my mum Mary for continuous prayers, support and encouragement.

Abstract

COVID-19 is undoubtedly the most dangerous and highly contagious disease in this century. Intensive researches have and are being done to unearth effective vaccines to deal with future pandemics. In this research, we developed deterministic models for COVID-19 driven by asymptomatic and symptomatic individuals taking into consideration the indispensable role of vaccination in combating disease transmission. Two models were developed, the effective and ineffective vaccine models. The impact of isolating the symptomatic individuals and waning of both natural and vaccine induced immunity for recovered and vaccinated persons respectively were explored. Such considerations were not reconnoitred in the existing literature. The dissection of the proposed models was conferred in terms of the associated reproduction number R_0, which is determined by utilizing the next-generation matrix (NGM) approach and forms the basis upon which the models' stability analysis are established. The analysis shows that COVID-19 free equilibrium (CFE) is locally asymptotically stable for $R_0 < 1$ and unstable if $R_0 > 1$. The local stability of endemic equilibrium was explored using center manifold theorem where the method utilized by Castilo-Chavez and Song was implemented in order to ascertain the prerequisite for the existence of backward bifurcation. For the effective vaccine model, the recovered people's rate of reinfection determined the direction of bifurcation while for the ineffective vaccine, backward bifurcation was driven by the vaccine efficacy. The models' findings demonstrated that raising the rate at which asymptomatic persons are identified and treated significantly reduces COVID-19 transmission in the community. The results also revealed that increased administration

levels of vaccine and strict adherence to isolation for the symptomatic individuals would curtail COVID-19 infections from burgeoning to catastrophic levels that would overrun the capacity of health care support system.

Contents

List of Tables

List of Figures

Index of Notations

Chapter 1

INTRODUCTION

This chapter gives a comprehensive background of the study which generally encompasses the history of viral pandemics in recent past and in particular the novel COVID-19 whose origin is in China. We further give definition of the basic concepts involved, the statement of the problem, the general and explicit objectives as well as the significance of he study.

1.1 Background of the study

Viruses have been considered as innocuous microorganisms in human for a protracted period of time in relation to plants (Balloux et al. [15]). Over the years, the death rate as a result of viral infection in humans has been very low in comparison to other diseases such as Cancer, Cardio-vascular diseases and Tuberculosis (Zheng et al. [125]). Consequently, financing organisations and data scientists have over the years neglected human viral diseases, including the flu. Thus, hardly much research has been sponsored in recent years to work on drug designing or medical research in the field.

Nevertheless, there have been reports that viral infections aggravate the symptoms and possess greater detrimental effects on human health for persons having an auto-immune condition, infectious ailment and compromised immune system (WHO, [114]). The environmental, ecological and social impacts of a changing climate are arguably to be blamed for increased frequency of viral epidemic outbreaks such as the acute respiratory syndrome commonly known as SARS (2002), the Middle East respiratory syndrome (MERS-CoV)(2012), Influenza A virus subtype H1N1 (A/H1N1)(2009) and Ebola virus (2013) (Khan et al. [65], McMichael et al. [75] and Yin et al. [121]). Consequently, it is apparent based on the current patterns that more viral diseases that are very contagious will be discovered in the near future (Shrestha et al. [100]). To date, the world is reeling from the novel COVID-19 pandemic whose devastating effects cannot be underscored.

COVID-19 is an infectious disease that emerged in Wuhan in China in December 2019 and spread rapidly around that country and subsequently to many others. It is a disease caused by a new virus, called SARS-CoV-2 (Ge et al. [45]). Since both the infectious agent and the viral illness are new to the viral world, they are presenting unanticipated difficulties (Li et al. [72] and Wu et al. [115]). The single, positive-stranded RNA virus SARS-CoV-2, also called the Novel Corona virus, is a member of the order Nidovirales and is the cause of the present worldwide COVID-19 pandemic (Cascella [25] and Huang et al. [54]). This disease has generated a completely exceptional new worldwide emergency situation (Chan et al. [29]). On January 30, 2020, WHO designated it as a Public Health Emergency of Global Concern (WHO [114]). Since its beginning,

COVID-19 has been a leading cause of ailment and fatalities in children and adults worldwide. As of 30th June 2021, more than 181.5M infections with 11M recoveries and 3.9M death cases had been reported globally in 220 countries.

Corona virus disease induces a respiratory tract infection. The main cause for concern has been the rapidity with which COVID-19 passes from person to person through touch. As the virus can survive in droplets on surfaces for several days, the available evidence indicates that the virus primarily spreads through close contact (defined as less than one metre between an infected individual and a susceptible individual) (Bai et al. [14] and CDC [27]). As soon as it enters the host, it multiplies throughout the body, turning it into a reservoir (Rothan et al. [93]). Nonetheless, in certain instances, the virus may remain dormant within the body and not manifest any symptoms; however, if this individual carries the virus, they can infect others by releasing droplets of the illness when they cough or sneeze (Rothe et al. [94]).

Clinical laboratory analysis and imaging methods are used for the diagnosis of a COVID-19 infection (Shi et al. [99] and Xu et al. [119]). The current COVID-19 diagnostic tools commonly used include chest computerised tomography (CT) and reverse-transcription polymerase chain reaction (RT-PCR) as discussed in (Chan et al. [30]). According to the research by (Xie et al. [117]), a typical chest CT as COVID-19 diagnostic test is more accurate as compared to RT-PCR when implemented for patients suffering from fever, sore throat, fatigue, coughing or dyspnea. Adverse destructive effects of COVID-19 have been noted especially in individuals with cormobidities or weak immune system. In fact, research

has shown that the degree of immune dysfunction correlates well with COVID-19 infection severity (Callender et al. [24]). Report from WHO indicates that the majority of COVID-19 cases result in a mild or moderate sickness that disappear on its own. Even after they have recovered from the initial infection, some persons may continue to experience persistent symptoms, some of which may be severe. In some instances, in the course of therapy, mechanical breathing and intensive care may be necessary (Abdulamir et al. [1]).

Based on available data and research, WHO had projected that around 15% of COVID-19 cases in the general population were to be severe, and 5% critical, necessitating substantial medical resources and critical-care infrastructure, including the capability to give ventilatory support. Compared to seasonal influenza, this was indicative of a higher degree of severity, which was probably because of many mild cases that went on undiagnosed. The recognized risk factors associated with severe COVID-19 include: age > 60, immune-compromising disorders, diabetes, hypertension, heart disease, and chronic lung illness (Booth et al. [18]). It was observed in a number of nations that the highest COVID-19 mortality rates occurred among the elderly relative to the other age brackets. For example, in China, 80% of fatalities took place in those who were 65 years or older. WHO report ruled out severe COVID-19 infection symptoms among the children. When they occurred, the illness was often minor. There was no significant risk of serious illnesses associated with pregnancy. People are said to be more contagious when symptoms first appear than later in the disease, according to preliminary findings (Wölfel et al. [112] and Liu [73]).

For prevention, WHO recommends cleaning and sanitising commonly handled objects and surfaces every day, concealing coughs and sneezes with tissues or the inside of the elbow and throwing away used tissues right away in the trash, and washing hands with soap and water for about 20 seconds, maintaining social distance, use of face masks and reducing unnecessary travels. Other measures taken include; closure of schools, international traveling stopped, lock down in some countries and curfews among others.

Negative impact of this disease world wide cannot be over emphasized. People's mental health was significantly impacted by the COVID-19 epidemic. The epidemic caused an unprecedented rise in stress, worry, despair, and sleep disruptions in the populace (Amirudin et al. [6] and Kumar et al. [68]). According to WHO [114], the factors that contributed to the mental health difficulties in the face of this pandemic include: isolation and bereavement and grief, loneliness, financial difficulties, severe or chronic sickness, previous physical or mental health concerns, and trouble finding job or being laid off, all served to amplify negative impact of COVID-19 menace. In the face of the pandemic of such magnitude, mental illness or post-traumatic stress disorder was inevitable (Karunathilake [57]) (and the references therein).

According to June 2020 Kenya's COVID-19 statistics, 78% of infected individuals had no symptoms or just had mild ones, making them manageable at home. Home-based isolation and care for COVID-19 patients was implemented in response to the spike in the number of infected individuals and in anticipation of a future increase in COVID-19 cases. This strategy, known as the "Jitenge System" in Kenya, tried to relieve

the increasing strain that COVID-19 patients were exerting on hospitals. The pharmaceutical interventions are highly desirable given the socioeconomic costs of lock downs and physical distancing. With the incessant increase in transmission and rampant fatalities attributed to the widespread COVID-19 infections throughout the globe, the development of vaccines became critically necessary if the fight against the contagious illness was to be successful. The pharmaceutical industry swung into action in attempt to unearth effective vaccines to complement non-pharmaceutical approaches. As of July 2020, there were several COVID-19 vaccines undergoing various phases of testing according to WHO report (WHO [113]). At that time it was yet to be elucidated, the level of efficacy of vaccine that would guarantee substantial decline and ultimately the extinction of this novel virus. Early identification of these efficacies could guide the creation of vaccines and their administration in the population (Hodgson et al. [53]). Immunisation was perceived to be a useful strategy to shield the host from SARS-CoV-2, according to earlier research by (Krammer [66]). Previously, variolation was widely seen as the most effective prophylactic strategy against the disease prior to the development of a vaccine (Brimnes [21]). Variolation, also known as inoculation, is a method of immunization that involves taking materials from the smallpox scab and exposing it to another person (Barquet et al. [16] and Riedel [91]). The name comes from the Latin varius, which means "stained," or from varus, which means "skin mark".

Early in the eighteenth century, variolation was a popular technique, and its implementation remained common in Europe until the discovery by Edward Jenner of the smallpox vaccine (Fenner [43]). Jenner found that

inoculation of cowpox protected against smallpox (Baxby [17]). He used the term vaccine, which comes from vacca, the Latin word for cow, to describe the cowpox virus that induced immunity to smallpox (Kroger [67]). Inspired by the understanding of this old traditional medical practice, Jenner created his own cutting-edge, scientific treatment plan, which eventually helped eradicate the smallpox threat from the planet in the 20th century, marking a significant advancement in the history of infectious illnesses and medical research.

In 1885, Louis Pasteur of France expanded the term vaccine to include all inoculating agents, not only those restricted to the inoculation of smallpox and the term vaccination, explicitly defined as the act of administering thereof (Kroger [67] and Stern et al. [102]). Smallpox (variola) virus, a fatal childhood disease, is said to have killed more people than any other microbe in recorded history. It's eradication globally became historic and of tremendous success story as far as public health is concerned. Currently, a vaccine is defined as a suspension of live (often attenuated) or inactivated microorganisms (such as viruses or bacteria) or fractions thereof that are given to a patient in order to create immunity and avoid infectious diseases or their after effects (Kroger [67]).

Invention of vaccines has immensely contributed the most significant developments in the medical field. As pandemics arise, they are a component of a complex public health response. The physiological rationale for immunization is sound. Immune system activation after vaccination results in the induction of both innate and adaptive immune responses, which, in the case of a humoral reaction, lead to the creation of antibodies or, in the event of a subsequent exposure, the development of memory cells

that identifies the same antigen. Recurring doses at regular intervals can increase the vaccine's efficiency and efficacy (CDC [28]). Before a vaccine is approved for public utilization, scientist expose it to extensive and elaborate trials in order to determine its effectiveness, safety, and efficacy.

Numerous more illnesses now have novel vaccinations available, such as polio, measles and pertussis (Plotkin [89]), but the smallpox vaccine is the only one so far that has led to the eradication of a disease from the human population. Vaccination has both direct and indirect effects. As a direct result of vaccination, the vaccinated individual is less susceptible to infection to some degree. The indirect effect of vaccination is enjoyed by all individuals, vaccinated or otherwise, and comes from a reduction of the population who may spread the infection. Thus, the direct effect acts on an individual level, and indirect effects act at the population level.

The concept that population protection takes place without the need for everyone to be vaccinated is known as herd immunity, defined as the resistance of a group to attack by a disease to which a large proportion of the members are immune, thus lessening the likelihood of a patient with a disease coming into contact with a susceptible individual (Fox [44]).

The use of mathematics in the assessment of smallpox vaccination was the start of a field now known as mathematical epidemiology (Anderson et al [7], Brauer et al. [20], Diekmann et al. [37], Keeling et al. [60] and Wang et al. [110]). This field has expanded to become the study of the spread of infectious disease, in time and space, using mathematical techniques.

1.2 Basic concepts

There are mathematical concepts and tools that are used for developing and analysing mathematical models.

Definition 1.1. (Morens et al. [76], Pandemic)

The World Health Organization (WHO) declares a disease a pandemic when the diseases growth is exponential. This means growth rate sky-rockets, and each day cases grow more than the day prior. COVID-19 being termed as pandemic means that the virus covers a wide area, affecting several countries and populations. Pandemic differs with an epidemic in that an epidemic is an unexpected increase in the number of disease cases infecting a substantial proportion of a population in a specific geographical area and possibly causing severe illnesses and deaths over a short period of time before subsiding. Endemic on the other hand refers to diseases that persist in the population for a sustained and probably an indefinite period of time, usually only causing illness to a relatively small percentage of the population (Anderson et al. [7]).

Definition 1.2. Bilinear incidence rate

Incidence rate is the number of individuals who become infected per unit time in epidemiology. It is also referred to as the rate of infection. The incidence rate are defined in different ways, one of which is the bilinear incident rate. This depends on the law of mass action, where by the rate of infection is directly proportional to the product of the susceptible and infected population βSI.

Definition 1.3. Equilibrium points and their stability

An equilibrium point or steady state of a dynamical system from an autonomous system of ordinary differential equations($ODEs$) is defined as a solution that does not change with time (Scholarpedia [98]). Thus equilibrium points are constant solutions of Differential equations (Boyce et al. [19]). The point $\bar{x} \in \Re^n$ is an equilibrium point for the differential equation:

$$\frac{dx}{dt} = f(t, x) \tag{1.2.1}$$

if $f(t, \bar{x}) = 0$ for all t and is uniquely determined by its initial conditions $x(0) = x_0$ and the solution is denoted by $x(t, x_0)$.

The Jacobian matrix of a system of ordinary differential equations is the matrix of first order partial derivatives of a vector-valued function (Arrowsmith [10]). In general Jacobian matrix gives the gradient of a scalar function of multiple variables , which itself generalises the derivative of a scalar function of single variable.

Definition 1.4. *Let* $\boldsymbol{F} : \mathbb{R}^m \to \mathbb{R}^m$ *be a function that takes the vector* $x \in \mathbb{R}^n$ *and produce the vector output of* $\boldsymbol{F(x)} \in \mathbb{R}^m$*, then the Jacobian matrix* J *of function* $\boldsymbol{F}$ *is* $m \times n$ *matrix, such as:*

$$J = \frac{d\mathbf{F}}{dx} = \left[\frac{\partial \mathbf{F}}{\partial x_1} \cdots\cdots \frac{\partial \mathbf{F}}{\partial x_n}\right] = \begin{bmatrix} \frac{\partial F_1}{\partial x_1} & \frac{\partial F_1}{\partial x_2} & \cdots & \frac{\partial F_1}{\partial x_n} \\ \frac{\partial F_2}{\partial x_1} & \frac{\partial F_2}{\partial x_2} & \cdots & \frac{\partial F_2}{\partial x_n} \\ \vdots & \vdots & \ddots & \vdots \\ \frac{\partial F_m}{\partial x_1} & \frac{\partial F_m}{\partial x_2} & \cdots & \frac{\partial F_m}{\partial x_n} \end{bmatrix}$$

where the entries of Jacobian matrix are evaluated at $x = (x_1, ..., x_n)$.

$\bar{x}$ is an equilibrium point if $f(\bar{x}, t) = 0$. So the stability of $\bar{x}$ depends on

the eigenvalues of $Df(\bar{x})$. The solution $\bar{x}$ is locally stable if all solutions which start near x^* remain near $\bar{x}$. If solutions that start near $\bar{x}$ tend towards $\bar{x}$ as $t \to \infty$, then $\bar{x}$ is locally asymptotically stable.

Definition 1.5. *The equilibrium point* $\bar{x} \equiv 0$ *of equation* (1.5.1.1) *is stable at* $t = t_0$ *if for any* $\epsilon > 0 \exists \delta(t_0, \epsilon) > 0$ *such that* $\| x(t_0) \| < \delta \Longrightarrow \| x(t_0) \| < \epsilon, \forall \epsilon > t_0$

Definition 1.6. *An equilibrium point* $\bar{x} \equiv 0$ *of equation* (1.4.1.1) *is asymptotically stable at* $t = t_0$*, if*

(i) $\bar{x} \equiv 0$ *is stable and*

(ii) $\bar{x} \equiv 0$ *is locally attractive(sink),* $\exists \delta(t_0)$ *such that* $\| x(t_0) \| < \epsilon \Longrightarrow \lim_{t \to \infty} x(t_0) = 0$

1.2.1 Definity of functions

Definition 1.7. Positive Definite (Semi-Definite) Functions(PDF) A continuously differentiable function $V : \mathbb{R}^n \to \mathbb{R}$ is regarded as positive definite within the region $D \in \mathbb{R}^n$ containing the equilibrium point $\bar{x}$ if:

(i) $V(\bar{x}_i) = 0, \forall i = 1, 2, ...n$

(ii) $V(x_i) > 0, x_i \in D$ and $x_i \neq \bar{x}_i$

A function is regarded as positive semi-definite if the condition (ii) above is replaced by $V(x_i) \geq 0$.

Definition 1.8. Negative Definite (Semi-Definite) Functions(NDF) A continuously differentiable function $V : \mathbb{R}^n \to \mathbb{R}$ is regarded as negative definite within the region $D \in \mathbb{R}^n$ containing the equilibrium point $\bar{x}$ if:

(i) $V(\bar{x}_i) = 0, \forall i = 1, 2, ...n$

(ii) $V(x_i) < 0, x_i \in D$ and $x_i \neq \bar{x}_i$

A function is regarded as negative semi-definite if the condition (ii) above is replaced by $V(x_i) \leq 0$.

1.2.2 Lipchitz Continuity

According to (Boyce et al. [19]), the deficiency of analytical methods for solving non-linear ordinary differential equations has necessitated the need for the study of existence and uniqueness of these types of ODEs. Consider an Initial Value Problem (IVP):

$$\frac{dy}{dx} = f(x, y), \quad y(x_0) = y_0. \tag{1.2.2}$$

Much of the theory for the IVP (1.2.2) above involves the so called Lipschitz condition. This condition takes a form of fundamental inequality and it plays a pivotal role in providing information about solutions to non-linear ODEs such as existence, uniqueness and approximation.

Definition 1.9. A function $f(x, y)$ is said to satisfy Lipschitz condition on a set Ω if there is a constant $K_f > 0$ such that:

$$|f(x, y_2) - f(x, y_1)| < K_f|y_2 - y_1|, \quad \forall (x, y_1), (x, y_2) \in \Omega \tag{1.2.3}$$

where K_f is the Lipschitz constant for f in the domain Ω.

Lipschitz Existence and Uniqueness Theorem (Strogast [103]): *Let* $f(x,y)$ *in* (1.2.2) *be continuous on a rectangle* $\{\bar{\Omega} = (x,y) : \ x_0 - \delta < x < x_0 + \delta; \ \ y_0 - b < y < y_0 + b\}$, *then* $\exists$ *a solution in* $\bar{\Omega}$. *Furthermore, if* $f(x,y)$ *is Lipschtiz continuous with respect to* y *on a rectangle* R *(possibly smaller than* $\bar{\Omega}$*), given as* $R := \{(x,y); \ \ x_0 - a < x < x_0 + a; \ \ y_0 - b < y < y_0 + b, \ \ a < \delta\}$, *the solution in* R *shall be unique.*

Lemma 1 (Strogast [103]). Let $\bar{\Omega}$ be a rectangle: $R := \{(x,p) : x \in [a,b], \ \ |p - A| \leq B\}$ or the infinity strip: $S := \{(x,p) : x \in [a,b], \ \ |p| < \infty\}$. If $f : \bar{\Omega} \to \mathbb{R}$ and $\frac{\partial f}{\partial y}$ exists, is continuous and there is some constant $L_f \geq 0$ such that $|\frac{\partial f}{\partial y}(x,y)| \leq L_f$, $\forall (x,y) \in \bar{\Omega}$, then (1.2.3) holds with $K_f = L_f$.

1.2.3 Lyapunov Stability

Definition 1.10. Let $\bar{x}$ be and equilibrium point of some non-linear system (1.2.1) in some neighborhood $\Omega \in \mathbb{R}^n$. We also let $V(x)$ to be a continuously differentiable function in the domain of $\Omega \in \mathbb{R}^n$ that contains the equilibrium point $\bar{x}$ of the system (1.2.1). A function $V(x)$ is referred to as a Lyapunov function if it satisfies the following properties:

(i) It has a local minimum in $\bar{x}$ i.e $V(x) = 0$, when $x = \bar{x}$.

(ii) $V(x) > 0$, $\forall x \in \Omega \backslash \{\bar{x}\}$

(iii) The derivative of $V(x)$ along the trajectories of (1.2.1) (denoted by $\dot{V}(x)$), is given by: $\dot{V}(x) = \sum_{i=1}^{n} \frac{\partial V}{\partial x_i} \dot{x}_i = \sum_{i=1}^{n} \frac{\partial V}{\partial x_i} f_i(x)$

Lyapunov Stability Theorem(Khalil [64], Theorem 3.1):*Let* $x = \bar{x}$ *be an equilibrium point for* (1.2.1) *and* $\Omega \subset \mathbb{R}^n$ *be a domain containing* $x = \bar{x}$. *Let* $V : \Omega \in \mathbb{R}^n$ *be a continuously differentiable function, such that:*

$$V(x) = 0, \quad at \quad x = \bar{x} \quad and \quad V(x) > 0, \quad \forall x \in \Omega \backslash \{\bar{x}\} \tag{1.2.4}$$

$$\dot{V}(x) \leq 0, \forall x \in \Omega \backslash \{\bar{x}\} \tag{1.2.5}$$

Then $\bar{x}$ *is stable equilibrium point.*

Definition 1.11. The system (1.2.1) is locally asymptotically stable (L.A.S) if $\dot{V}(x) < 0$, $\forall x \in \Omega \backslash \{\bar{x}\}$

Definition 1.12. The system (1.2.1) is globally asymptotically stable (G.A.S) if for $\Omega = \mathbb{R}^n$, (where the region Ω is the entire space), $V(x) \to \infty$ as $\|x\| \to \infty$.

1.2.4 Non-Pharmaceutical interventions

In epidemiological view point, non-pharmaceutical interventions are any strategies that stops an epidemic disease from spreading without the need for prescription medication treatments or vaccines. In the face of COVID-19, these measures include washing hands with soap and water for about 20 seconds, covering coughs and sneezes with a tissue or the inside of the elbow and disposing of used tissue papers immediately, cleaning and disinfecting frequently touched objects and surfaces, maintaining social distances, use of face masks and reducing unnecessary travels.

1.2.5 Vaccines

A vaccine is a substance, usually made from the inactivated or weakened form of the causative agent or from its components or products, that is used to boost immunity to a certain infectious disease or pathogen.

1.2.6 The basic reproduction number

The basic reproduction number is the average number of cases that one case produces in an uninfected community or a population that is fully susceptible over the infectious period (Tulu et al.[107]). The threshold parameter, also known as the basic reproductive ratio, is another name for the basic reproduction number and is denoted by R_0.

The next generation matrix approach is utilized to compute the basic reproduction number for the compartmental model of disease spread. This approach was created by (Diekmann et al. [38] and Driessche et al. [39]); where the population was segmented into n compartments and $m < n$ infected classes. We let x_i; where $i = 1, 2, 3, ..., m$, to be the number of infected persons in the i^{th} disease infected compartment at time t. Then the epidemic model is given by

$$\frac{dx_i}{dt} = F_i(x) - V_i(x),$$

where $F_i(x)$ is the fertility matrix that illustrates the pace at which new infections emerge inside the compartment. The transmission matrix, i and $V_i(x)$, reflects the rate of individual transfer and is separated into two subcompartments, $V_i^-(x)$ and $V_i^+(x)$, which indicate the rate of individual

transfer into and out of compartment i. Here is the definition of the matrix $m \times n$ of F and V.

$$F = \frac{\partial F_i}{\partial x_j}(x_0)$$

and

$$V = \frac{\partial V_i}{\partial x_j}(x_0),$$

then the next generation matrix is FV^{-1}, and the model's fundamental reproduction number R_0, is the matrix's biggest eigenvalue or spectral radius.

1.2.7 Forward bifurcation

Its quite indisputable that the reproduction number R_0 is a crucial factor in determining whether an infection can typically self-replicate and propagate for $R_0 > 1$ in a susceptible population or whether the disease will dissipate for $R_0 < 1$. Basically, the classical infectious disease models exhibit two inherent equilibria namely, a disease free equilibrium point, DFE and an endemic equilibrium point, EEP . The stability of these two equilibria switch at the (transcritical) bifurcation point which takes place at the value when $R_0 = 1$. At this threshold value when $R_0 = 1$, the DFE transits to unstable equilibrium whereas the endemic equilibrium assumes a stable state. The figure (1.2.1) gives an illustration of forward bifurcation at the point $R_0 = 1$. The star notation denotes the equilibrium values.

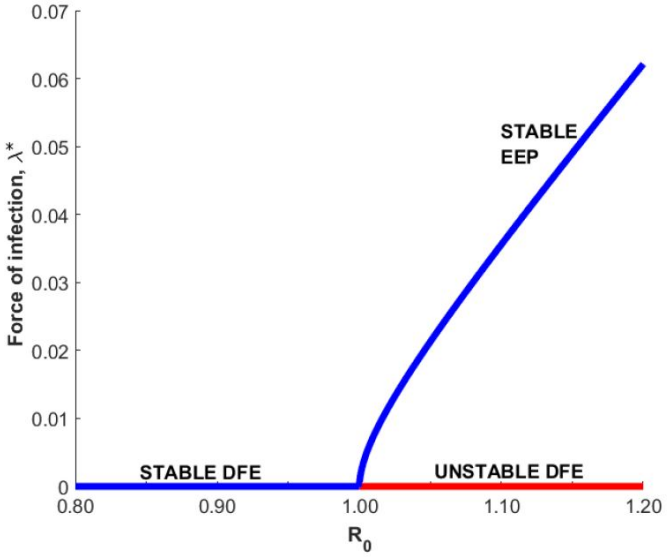

Fig. 1.2.1. Graphical illustration of force of infection $\lambda^* = \frac{\beta I_h^*}{N}$ against R_0 for the forward bifurcation

1.2.8 Backward bifurcation

The notion assumed for decades that $R_0 < 1$ indicating that an infectious illness has disappeared from the community has of late been challenged with several analytical and theoretical studies vehemently demonstrating that this condition is not always tenable. Consequently, the phenomenon of backward bifurcation presents the possibility of concurrent existence of both the stable DFE and stable EEP at $R_0 < 1$. This implies that even though the requirement of reproduction number being less than unity for elimination of an epidemic, the population may still be at endemic equilibrium zone where disease persists for an indefinite period of time. The concurrent existence of the two stable equilibrium causes the final equi-

librium a population reaches to depend on the initial state (the number of individuals) of its sub-populations. The figure (1.2.2) gives an illustration of a typical backward bifurcation at the point $R_0 = 1$. We note that three equilibria exist concurrently for the range $0 < R_c < R_0 < 1$, where R_c is the critical value, which in this case is approximately 0.82.

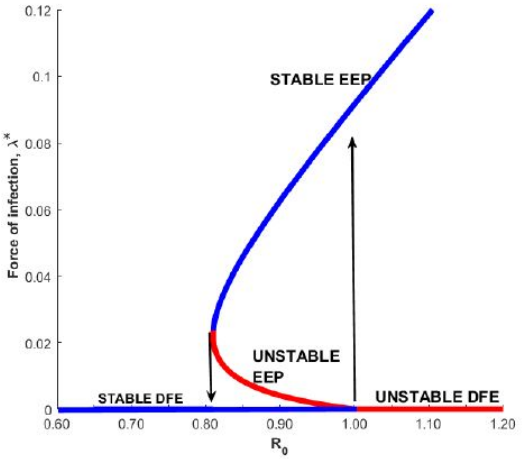

Fig. 1.2.2. Graphical illustration of force of infection $\lambda^* = \frac{\beta I_h^*}{N}$ against R_0 for the backward bifurcation

1.3 Statement of the Problem

Emerging infectious illnesses are a major source of worry for public health agencies because they have devastating effects on public health and place a heavy financial burden on the community. The appearance of the novel SAR-CoV 2 has disrupted the global economy, the food system, education, employment, tourism, and several other aspects of life. It is therefore imperative to evaluate the effectiveness of methods utilized in attempt to

stem the spread this contagious diseases. The study on the dynamics of antibody response to $BNT162b2$ COVID-19 vaccine found out that the antibody levels declined six months after vaccination, an indication of waning of immune response to COVID-19 infection over time. At the sixth month after the administration of the second dose, the spike antibody levels were similar to the levels in persons vaccinated with one dose or in COVID-19 convalescent persons. In this study we seek to address the impact of the waning immunity of COVID-19 vaccine on the long-term transmission dynamics of this infectious disease, owing to the fact that the fast roll out of vaccine brings a false sense of safety which may lead to relaxation of non-pharmaceutical measures. Most studies have underscored the fact that for minimization of SARS-CoV-2 infection, at-risk populations are to be targeted in efforts to boost vaccine effectiveness. Consequently, this study endeavors to establish the vaccine efficacy and the general population coverage capable of abasing COVID-19 infections and ultimately restoring normalcy. In this study, we have as well included the possibility of COVID-19 asymptomatic patients becoming symptomatic if left untreated. This has been assumed by many researchers yet this cannot be ignored since any infection compromises innate immune system, and so one may become vulnerable with the persistence of infection as well as the emergence and re-emergence of different variants of COVID-19.

1.4 Objectives of the study

1.4.1 General objective

The main objective of this study is to develop and analyze a mathematical model that describes the effect of vaccination and non-pharmaceutical interventions on COVID-19 control dynamics.

1.4.2 Specific objectives

The specific objectives of this study are to:

(i). Formulate model 1 that captures the effect of vaccine offering full protection against COVID-19 infection as well as the re-infection of the recovered patients due to waning of natural immunity on long term COVID-19 control dynamics.

(ii). Formulate model 2 that captures the effect of ineffective vaccine as well as isolation of symptomatic individuals on the long term COVID-19 control dynamics.

(iii). Establish the existence, stabilities of the equilibrium points and perform sensitivity analysis for each model.

(iv). Fit the models to the real COVID-19 statistical data from Kenya and perform simulations to ascertain the influence of the most vital parameters of each model.

1.5 Significance of the study

The only set of pandemic countermeasures that are consistently and universally accessible are non-pharmaceutical interventions (NPIs) . NPIs could potentially slow down the spread of the COVID-19 pandemic by delaying the virus's introduction into a population, delaying the epidemic's height and peak if it has already begun, reducing the spread of the virus through environmental or personal protective measures, and lowering the overall number of infections and, consequently, the overall number of severe cases. Mathematical formulations that are clear, logical, and precise are essential in unearthing containment measures that are cost effective and with high degree of precision in response to any disease outbreak. Consequently, the goal of this study is to create and evaluate a deterministic model that would qualify and quantify the possible impacts of government's COVID-19 control and preventive measures such as administration of COVID-19 vaccine to the susceptible and booster vaccine to the vaccinated population, early identification and treatment of asymptomatic and effective isolation of symptomatic individuals on COVID-19, thereby offering insight to the healthcare industry on the strategies that would ultimately leads to scaling down COVID-19 infections.

Chapter 2

LITERATURE REVIEW

2.1 Introduction

This chapter provides a thorough historical overview of the evolution of mathematical epidemiology. We also provide a detailed analysis of a couple of COVID-19 models that have been developed and comprehensively examined by different studies. The research gaps identified have informed our study objectives.

2.2 Development of mathematical epidemiology models

Ross et al [92] and McKendrick[63], developed the first models of mathematical epidemiology. Ross demonstrated how malaria is transmitted by mosquito bites using his model. He also noted that by lowering the mosquito population, malaria may be prevented based on his model. There is a higher probability that Ross was the pioneer of the threshold

concept which has been essential to epidemiology ever since it was first introduced. This threshold behavior is present in all mathematical models, including the very heterogeneous ones. This threshold is expressed as follows in epidemiological terms: A disease will die out if the average number of secondary infections brought about by a single infective introduction in a population that is fully susceptible is less than unity, and an epidemic will emerge if it is more than unity. Subsequently, this threshold was referred to as a fundamental reproduction number, R_0 (Heesterbeek [52]).

In their work on the general compartmental model, Kermack and McKendrick significantly expanded the idea of basic reproduction number, for both illnesses where recovery leads to lifelong immunity and diseases where reinfection is possible. Bailey et al. [14] significantly expanded the field of mathematical modelling by incorporating an exposed (latent) sub-population in their model. During this time, the population's afflicted individuals do not spread the infection to others. Hammer [51], formulated a model incorporating mass-action incidence. According to this study, the average number of contacts required to spread an infection within a unit of time for each individual is proportionate to the density of the population..

2.3 Mathematical model formulation of infectious diseases

The first compartmental model (SIR), which consists of a system of three coupled nonlinear ordinary differential equations, was developed by Kermack et al. [63] as an extension of Ross's work. This model was simply presented as:

$$\begin{aligned}\frac{dS}{dt} &= -\beta SI \\ \frac{dI}{dt} &= \beta SI - \gamma I \\ \frac{dR}{dt} &= \gamma I\end{aligned}$$

in which t is the time, $S(t)$ represents susceptible individuals, $I(t)$ represents infected individuals, and $R(t)$ represents those who have recovered. These equations were created under a number of presumptions: First, each member of the population must be treated as having an equal chance, at rate a, of catching the illness as every other member of the population, and an equal percentage b of persons they come into contact with in a given amount of time. Then, let β represent the result of multiplying a by b. This is equivalent to the product of transmission chance and the contact rate. The percentage of infectious agents that leave this class per unit time to enter the removed class is γ, which stands for the mean recovery/death rate or $\frac{1}{\gamma}$ for the mean infective period. The rate of infection in this case is said to assume the law of mass action.

Norman et.al. [82] developed a SIRD model. They employed this model to do a numerical analysis of the susceptible-infected-recovered-diseased (SIRD) populations in order to explore the impact of seasonality in driving cycles in recurrent epidemics. Typically, this kind of model is provided as:

$$\begin{aligned}
\frac{dS}{dt} &= -\frac{\beta SI}{N} \\
\frac{dI}{dt} &= \frac{\beta SI}{N} - \kappa I - \mu I \\
\frac{dR}{dt} &= \kappa I \\
\frac{dD}{dt} &= \mu I
\end{aligned}$$

A lot of work has gone into creating more accurate mathematical models in recent years to study the dynamics of infectious disease transmission, including SARS, cholera, Ebola, malaria, HIV, and TB. When examining the SARS outbreak, Chowell et al. [33] employed the sensitivity and uncertainty analysis of the basic reproductive number R_0 to evaluate the role that the model parameters play in outbreak control. The findings indicate that the most significant fractional effects on R_0 are caused by the transmission rate and the effectiveness of isolation. The study on the spread of SARS included the introduction of small-world networks. It was demonstrated that the outbreak's severity would be limited if all infected persons were isolated as soon as they were detected (Nainggolan et al. [80] and Small et al. [101]). Additionally, Gumel [49] looked at the

role of disease transmission parameters in the reduction of R_0 and the prevalence of the disease in order to discuss the control of SARS. He also attempted to obtain a threshold for the basic reproductive number R_0 for evaluating the strategies of isolation and quarantine.

In Wan et al. [109] study, a model was proposed to assess the efficacy of interventions and self-protective measures as they evolved, to calculate the risk of partially lifting control measures, and to forecast the virus's epidemic trend in mainland China and excluding Hubei. The authors came to the conclusion that the containment tactics implemented by the Chinese government were successful and cautioned against removing personal protection too soon since doing so might cause the illness to spread for a protracted period of time resulting to more infections in the community.

Xiefei et al. [118] investigated isolation and quarantine strategies that were both optimum and suboptimal during the SARS pandemic. They shown that early on in an epidemic, the most effective use of isolation and quarantine measures may have a significant influence on both optimum and suboptimal management. If not, it would not be possible to tame the spread of SARS.

An investigation on the effects of quarantine during an Ebola virus outbreak was conducted by Attila et al. [13]. They found in their study that the primary drivers of the dynamics of disease transmission are the factors pertaining to the efficiency of quarantine, namely the parameter linked to the decrease in infectiousness of sick persons under quarantine and the contact rate during quarantine. Overall, their research shown

that, if a quarantine intervention method is implemented alone and has a high enough coverage and efficacy level, it may effectively contain or eradicate the Ebola virus in a community.

The majority of these studies demonstrate that, in cases where treatment or immunisation alternatives are not yet available, isolating the diseased person is one of the most effective NPIs used to control an infectious disease (Sun et al. [120]).

An epidemic generally exhibits a similar trend that may be expressed numerically. At first, there is a gradual increase in the number of infected patients, which often shows exponential trend. Once it reaches the crest, it turns and starts to descend steadily. In the end, the outbreak diminishes to zero, suggesting that the pandemic is over..

2.4 Mathematical models of COVID-19

Following the December 2019 COVID-19 outbreak in Wuhan City, China, the globe has seen its unprecedented terrible effects. According to data from published epidemiology and virology studies, respiratory droplets, direct contact with infected individuals, or contact with contaminated objects and surfaces are the main ways that COVID-19 is spread from infected individuals to those who are in close proximity according to Chan et al. [29] and Onge et al. [87]. In China and the Republic of Korea for example, stringent preventive measures including lock downs of cities, closures of public transportation, schools, and businesses, tracking down and isolating infected people, rapid media information distribution, and

other measures were implemented. These preventive actions resulted in an abrupt decrease in the COVID-19 disease transmission rate and proved to be a successful method of viral containment (WHO [114]). In an effort to reduce the burden of this disease on the general public, mathematical models have been and are still being developed inorder to provide insight into the best preventative and control methods.

Vitaly et al. [108] proposed a Susceptible-infected-recovery type model(SIR). This model is analogous to that of Kermack and Mckendrick except for the addition of parameter σ signifying COVID-19 induced death rate. From parameters used, there are some parameters that were not included in this model such as natural death and Exposure class which should be taken care of since COVID-19 disease has latency state.

A mathematical model was developed and studied by Kassa et al. [58] for the transmission of COVID-19. At $R_0 < 1$, the model displayed a backward bifurcation when the recovered individuals did not acquire a lasting immunity against the illness. It was demonstrated that the model lacked backward bifurcation in the absence of reinfection and that the DFE is globally asymptotically stable for $R_0 < 1$. Using the suggested model, a number of mitigation techniques were examined, and it was shown that the infectious group of asymptomatic people may be a significant factor in the disease's future recurrence. They advised that in order to manage the illness in the event that vaccine is not available, nations should build the capacity to identify and quarantine at least 30% of the infected population while also treating at least 50% of symptomatic patients in isolation.

The study by Keno et al. [62] investigated the optimal control strategies of COVID-19 dynamics. The study findings suggested that the simultaneous administration of vaccine to the susceptible population and and increasing the rate of treatment of the infectives is the best approach for abasing COVID-19 transmissions. A deterministic model comprised of a system of ODEs for the dynamics of the COVID-19 population in Nigeria was suggested by Olaniyi et al. [85]. According to the study, a 50% reduction in effective transmission rate can bring the R_0 value for the nation's disease outbreak below one.Additionally, the scientists employed the Pontryagin Maximum Principle to examine the effects of time-dependent management and preventative control strategies in reducing the disease's spread. It was discovered that putting the coordinated control measures into practice could significantly lower the number of infected persons.

A COVID-19 model incorporating the isolation class was formulated by Anggriania et al. [8]. The findings showed that human to human contact is the potential cause of outbreak of COVID-19. The study pointed to the fact that the general isolation (self-isolation at home and hospitalization) of the infected human can significantly bring down the risk of future COVID-19 spread. Takasar et al. [105] formulated a five compartmental COVID-19 model based on SEIQR. They used sensitivity analysis to identify the causes of the disease's spread and persistence in the community. They focused on the characteristics that cause a greater variance in the fundamental reproduction number. According to the study's findings, the most sensitive metric is the contact rate between susceptible and infectious persons, which is followed by the infectious individuals' recovery rate. This investigation was predicated on an ideal quarantine situation.

The schematic diagram was as below:

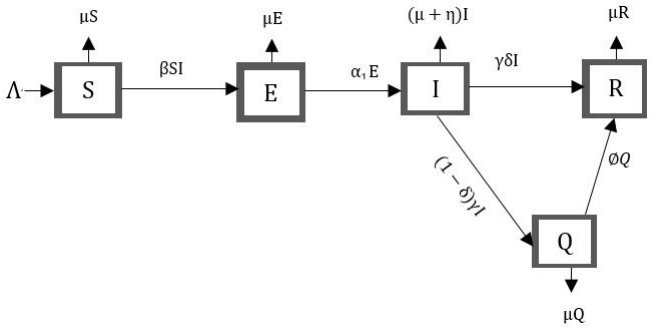

Fig. 2.4.1. Flow diagram

The research conducted by Leung et al. [71] revealed that social separation is the most efficient in containing pandemics with a basic reproductive number of $R_0 = 1.5 - 2.5$. A fundamental reproduction number $R_0 = 2.6$ is calculated for the COVID-19 pandemic, as shown by Zhao et al. [124], with an uncertainty range of 1.5 to 3.5. R_0 indicates the average number of new instances resulting from an existing case. When $R_0 > 1$, this corresponds with the exponential spread of the virus at that time, but for $R_0 < 1$ the spread stops on its own.

Sasmita et al.[96] developed a mathematical model of type SEI_1I_2RS.

In this study, it was highlighted that the key to successful outbreak control is to find the infectious case as fast as possible, so that the patient can be treated as well as socially restricted, separating the carrier cases from other individuals that may be susceptible to the disease.

Abdul et al.[2] developed a mathematical model that illustrated the dynamics of COVID-19 transmission impacts and mitigation strategies in

Tanzania (see Figure 2.4.1). They developed a human population-based Susceptible-Masked-Unmasked-Exposed-Infected-Hospitalized-Recovered ($SMUEIHR$) model type. The sensitivity analysis emphasized the significance of mask use in COVID-19 management, particularly when workers are interacting with isolated patients receiving supportive care and medicine, or when they are exposed to a busy area. The schematic diagram was as below:

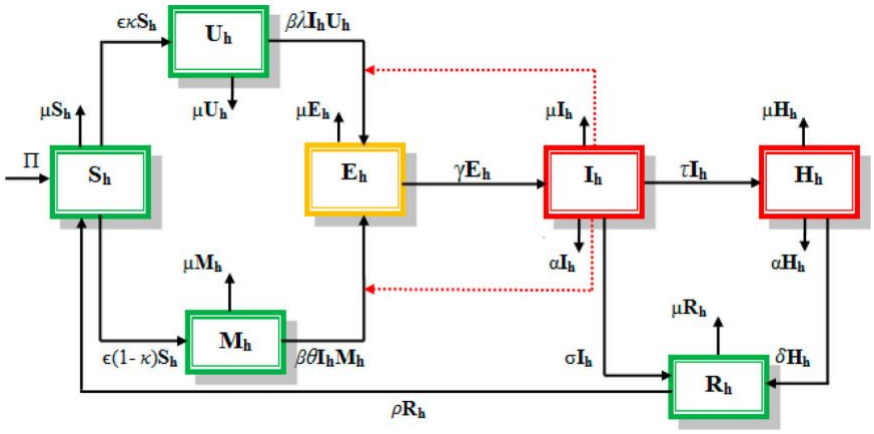

Fig. 2.4.2. Flow diagram

The dynamics of each phase with time was described with seven ordinary differential equations as shown below.

$$
\begin{aligned}
\frac{dS_h}{dt} &= \pi + \rho R_h - (\epsilon + \mu) S_h \\
\frac{dM_h}{dt} &= \epsilon(1-\kappa) S_h - (\mu + \beta\theta I_H) M_h \\
\frac{dU_h}{dt} &= \epsilon\kappa S_h - (\mu + \beta\lambda I_h) U_h \\
\frac{dE_h}{dt} &= \beta(\theta M_h + \lambda U_h) I_h - (\mu + \gamma) E_h \\
\frac{dI_h}{dt} &= \gamma E_h - (\mu + \alpha + \tau + \sigma) I_h \\
\frac{dH_h}{dt} &= \tau I_h - (\mu + \alpha + \delta) H_h \\
\frac{dR_h}{dt} &= \sigma I_h + \delta H_h - (\mu + \rho) R_h
\end{aligned}
$$

Mugisha et al. [77] proposed a SEI_aI_sHR model incorporating implications of complacency and early easing of lock-down. This model evaluated the effects of complacency, disregarding standard operating procedures (SOPs) to stop the spread of illness, and deciding when and how much to lessen lock-down. The study's conclusions demonstrated that the Ugandan government's prompt adoption of COVID-19 preventative and control measures prevented thousands of cases that would have quickly overwhelmed the country's healthcare system. Due to weariness and laxity, this would have negatively impacted the quality of care provided, increasing the number of deaths and hospital-acquired illnesses. This model assumed constant external disease pressure.

The schematic diagram was as below:

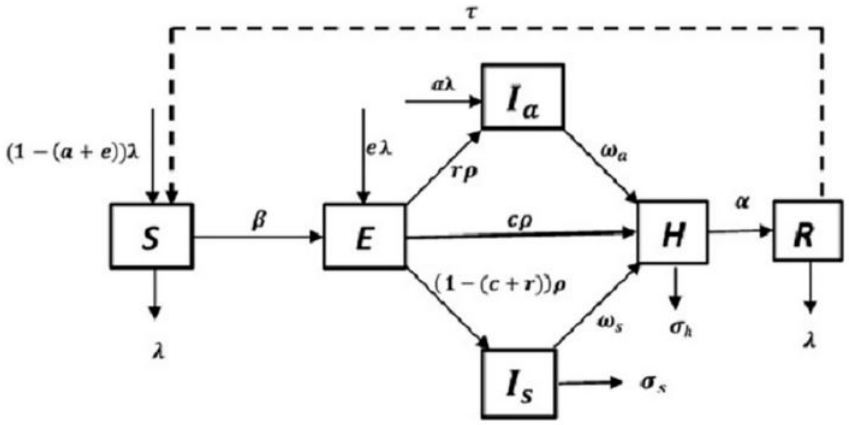

Fig. 2.4.3. Flow diagram

The study utilized the system od ODES below:

$$\frac{dS}{dt} = (1-(a+e))N - \frac{\beta bS(qI_a + I_s + gH)}{N} + \tau R - \lambda S$$
$$\frac{dE}{dt} = e\lambda N + \frac{\beta bS(qI_a + I_s + gH)}{N} - \rho E$$
$$\frac{dI_a}{dt} = a\lambda N + \gamma\rho E - \omega_a I_a$$
$$\frac{dI_s}{dt} = (1-(c+r))\rho E - \sigma_s I_s - \omega_s I_s$$
$$\frac{dH}{dt} = c\rho E + \omega_a I_a + \omega_s I_s - \sigma_h H - \alpha H$$
$$\frac{dR}{dt} = \alpha H - \tau R - \lambda R$$

where the parameters and variables were described in table 2.4.1 below.

Table 2.4.1: Definition of Parameter and variables

$a(t)$	Percentage of asymptomatic new arrivals
$e(t)$	Percentage of latently infected new arrivals
λ	Rate of recruitment per capita.
β	Rate of disease transmission.
b	The proportion of available vulnerable persons.
g	Infectivity factor for patients in hospitals.
q	Infectivity factor in people without symptoms.
α	Hospitalised patients' rate of recovery.
ρ	Rate of change from the latent to the infectious stage.
r	Percentage of latently.
σ_s	Disease induced mortality rate of infectious persons
σ_h	Hospitalized patient death rate due to illness.
τ	Rate of waning of COVID-19 disease induced immunity
ω_a	Hospitalization rate of asymptomatic infectious
ω_s	Hospitalization rate of asymptomatic infectious
c	Percentage of latent infectives who are traced and isolated

Idris et al. [55] created a simulation of the dynamics of COVID-19 transmission in Nigeria with both symptomatic and asymptomatic people. The fixed point theorem approach was employed in their investigation to prove the model solution's existence and uniqueness. Their findings indicate that the two most sensitive factors in the R_0 are the contact rate between susceptible people and the rate at which individuals shift from the exposed class to the symptomatically infected class. They thus proposed that it should be of great concern to everyone that, in the battle against the pandemic, exposure resulting from contact with infected persons be

limited, particularly those who are asymptomatic I_A. The schematic diagram was as below:

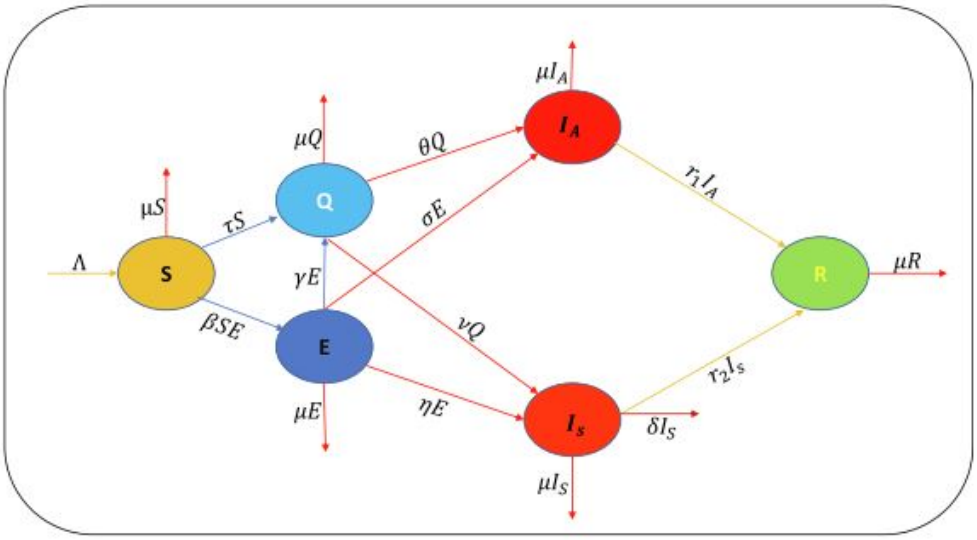

Fig. 2.4.4. Flow diagram

In this research,it was assumed that the the transmission was as a result of bilinear interactions between the susceptible population and the exposed or those latency compartment. They as well assumed that the recovered individuals gain permanent immunity to COVID-19. Recent studies have pointed that this pandemic is highly transmitted by both symptomatic and asymptomatic individuals.

Matthew et al. [74] developed and analyzed a ($SEAIQR$) mathematical model that encapsulates the essential COVID-19 compartments and parameters. This study proved that isolation and identification of the infected persons are more effective therapeutic options. Since asymp-

tomatic carriers do not exhibit clinical symptoms, it is challenging to identify them. Therefore, screening of people who have traveled to or resided in COVID-19 epidemic areas, or population-wide testing, should be carried out in order to identify the asymptomatic carriers who evade contact tracing. This study assumed a permanent acquisition of immunity after recovery from COVID-19 infection. The proposed schematic diagram was as in the figure below:

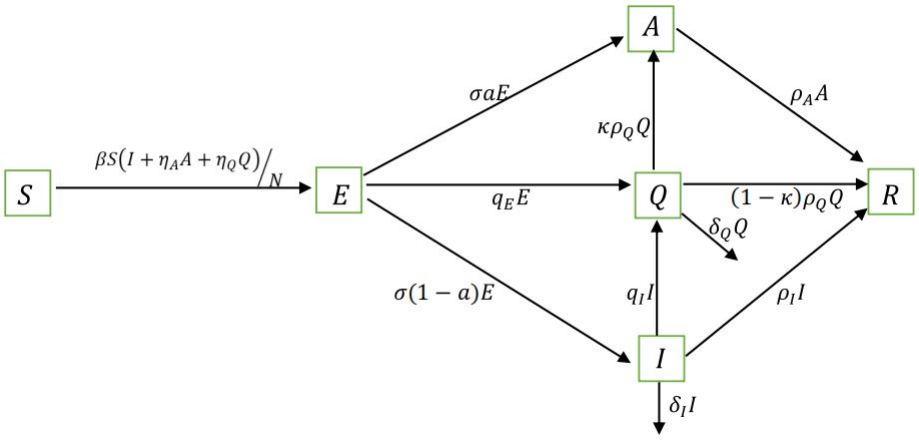

Fig. 2.4.5. Schematic diagram

The following set of equations was used in the model's formulation:

$$
\begin{aligned}
\frac{dS(t)}{dt} &= -\frac{\beta S(I+\eta_A A+\eta_Q Q)}{N} \\
\frac{dE(t)}{dt} &= \frac{\beta S(I+\eta_A A+\eta_Q Q)}{N} - \delta E \\
\frac{dA(t)}{dt} &= \sigma a E + k\rho_Q Q - \rho_A A \\
\frac{dI(t)}{dt} &= \sigma(1-a)E - q_I I - \delta_I I - \rho_I I \\
\frac{dQ(t)}{dt} &= q_E E + q_I I - \rho_Q Q - \delta_Q Q \\
\frac{dR(t)}{dt} &= \rho_I I + (1-K)\rho_Q Q + \rho_A A
\end{aligned}
\tag{2.4.1}
$$

As shown in Isaacs et al. [56] and Wu et al. [116], reinfection by the corona virus family is conceivable. Even while the exact duration required for an individual who has recovered from COVID-19 to lose immunity is yet unknown, its significance cannot be ignored at this time. As a result, it makes sense to take into account an epidemiological model formulation similar to the Susceptible-Infected-Recovered-Susceptible (SIRS) type when creating a mathematical model for COVID-19 dynamics.

Gumel [49] formulated partial immunity SIR epidemic model in which infection confers partial immunity to reinfection.

A research was conducted by Alshammari [4] on a mathematical model to study the spread of COVID-19 in the Kingdom of Saudi Arabia. A dynamical model known as susceptible, exposed, symptomatic, asymptomatic, hospitalized, and recovered (SEYNHR) was developed. The mean asymptomatic infectious time Φ_N and the mean symptomatic infectious period Φ_Y were considered to be equal in this investigation. The Saudi Arabian Ministry of Health (MOH) reported COVID-19 confirmed cases from March 2 to April 14 for the model's parameterization. The

number of hospital intensive care unit (ICU) beds that would be needed if the COVID-19 spread trend was not stopped was predicted by the research. The study further emphasized that the number of new COVID-19 symptomatic patients Φ_Y is mostly determined by the effective contact rate from asymptomatic to susceptible β_2.

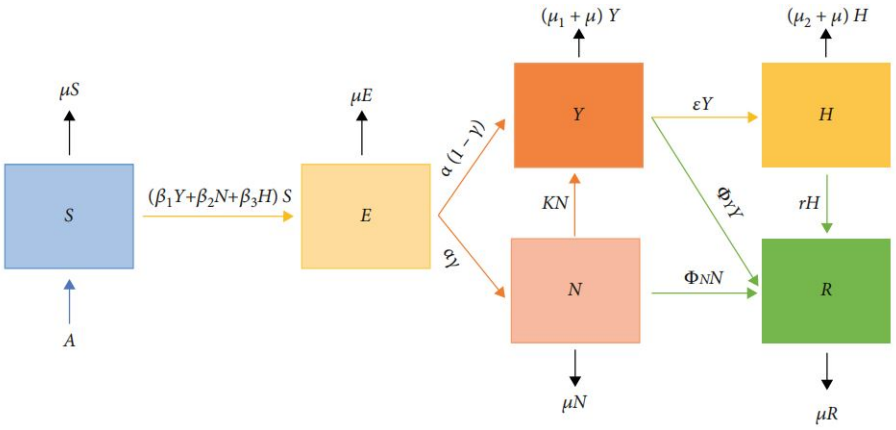

Fig. 2.4.6. Schematic diagram

From the above, it can be deduced that since Covid-19 outbreak in Wuhan, China, many researches in terms of mathematical simulations have been conducted in an effort to unravel optimal mitigation measures to the spread of this respiratory disease.

2.5 Vaccination as disease transmission control measure

A pathogen include bacterium virus, parasite or fungus that is capable of causing disease or illness when it enters the body of its host. A pathogen's makeup consists of several sub-components that are specific to the pathogen in question and the sickness it causes. An antigen is the portion of a disease that causes the production of antibodies. An essential component of the immune system are the antibodies produced in reaction to the antigen of the infection. The antibodies acts as a safeguard of an individual against any attack by a specific pathogen. This is due to the fact that every antibody in our system is designed to specifically detect a single antigen. Numerous varieties of these antibodies are stored in our bodies. It takes time for the immune system to react to a new antigen and develop antibodies that are unique to that antigen in the human body. Thus, the vulnerable has the potential to get sick.

After the production of antigen-specific antibodies, the immune system as a whole uses these antibodies to eliminate the pathogen and halt the sickness. Except in cases when two infections are very similar to one another, antibodies to one pathogen often do not protect against another. The body develops memory cells that make antibodies in response to an antigen, and these cells survive long after the pathogen is eliminated by the antibodies. When the body encounters the same pathogen again, memory cells prepare the body to produce antibodies in response to the antigen, which speeds up and improves the effectiveness of the immune response. This implies that the individual's immune system will be ready

to fight off illness the moment they come into contact with the harmful infection in the future.

Vaccines consist of dormant or weakened components of a certain organism (antigen), which causes the body to mount an immune response. Vaccines that are more recent have the production blueprint for antigens instead of the actual antigen. This weakened version will not cause the disease in the person receiving the vaccine, but it will stimulate their immune system to react much as it would have on its initial reaction to the actual pathogen. This is true regardless of whether the vaccine is composed of the antigen itself or the blueprint so that the body will produce the antibody. Some vaccines require multiple doses, given weeks or months apart. This is sometimes needed to allow for the production of long-lived antibodies and development of memory cells. In this way, the body is trained to fight the specific disease-causing organism, building up memory of the pathogen so as to rapidly fight it if and when exposed in the future.

Vaccination enables one to be protected against infection from a specific disease target. However, not everyone qualifies for immunisation. Particular vaccinations may not be administered to people who have severe allergies to particular vaccine components or underlying medical illnesses (such HIV or cancer) that impair their immune systems. If these persons live with and among other vaccinated people, they can still be protected. The infection finds it difficult to spread in a society where a large proportion of the population has received vaccinations since these individuals are immune. Therefore, the likelihood of those who cannot receive vaccinations getting exposed to the dangerous germs decreases with the number

of those who receive vaccinations. We refer to this as herd immunity.

It is worth noting that herd immunity does not offer complete protection to individuals who cannot safely get vaccinations, and that no vaccine offers 100% protection. However, if others around them receive vaccinations, these individuals will be well protected due to herd immunity. Those in the community who are unable to receive vaccinations are also protected by vaccinations.

The majority of patients lost 50% of their Nct-antibodies after six months, 75% after a year, and 100% of their baseline antibodies four years after infection, according to recently published research on serological testing for seasonal Human Coronavirus 229E (HCoV-229E) that examined antibody dynamics after infection (Edridge et al. [40]). The possibility of achieving a functioning herd immunity thus appears implausible in light of these data. Moreover, the concept of herd immunity is called into question by the quick reduction of protective immunity.

As the COVID-19 pandemic unfolded, a number of vaccines were approved by World Health Organization's (WHO) Emergency Use List (EUL). They included AstraZeneca, Johnson and Johnson, Modena and Pfizer. To date there are more vaccine candidates that are presently undergoing pre-clinical and clinical testing (WHO [113]).

2.6 Mathematical model involving vaccination as a control measure

The efficacy of vaccination was examined in terms of vaccination efficiency, vaccination schedule, and easing societal policies that reduce disease transmission in the study by Webb [111] on A COVID-19 epidemic model predicting the effectiveness of vaccination in the US. The model showed that the degree to which social policies that limit the spread of illness are loosened would have a significant impact on how quickly the epidemic abates once vaccination programmes are put in place. A model similar to SIRU was developed. This model took into account the following compartments: $S(t)$ for the susceptible individuals at time t, $I(t)$ for the infectious individuals at time t who are asymptomatic, $R(t)$ for the infectious individuals at time t who are symptomatic and will be reported, and $U(t)$ for the infectious individuals at time t who are symptomatic but have not yet been reported. According to the model, the COVID-19 outbreak in the US was not totally disappear in 2022 even with the introduction of vaccination strategies, but rather will decline considerably. However, if in the future a new, more virulent, and vaccine-resistant strains of COVID-19 evolve and are brought into the US from outside, the study predicted that the COVID-19 pandemic in the US may take a completely different turn.

The model's flow diagram is displayed below:

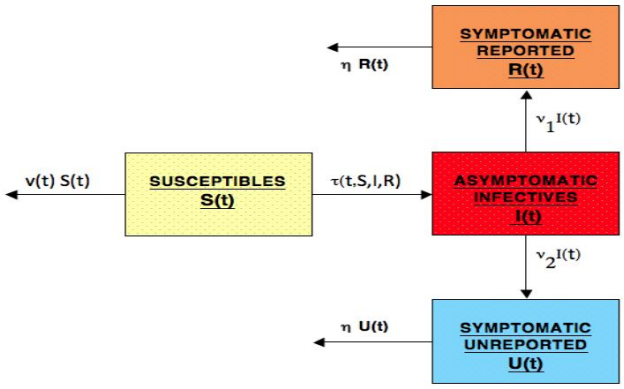

Fig. 2.6.1. Schematic diagram

A research by Ghostine et al. [46] aimed at studying the vaccination's effect on the COVID-19 pandemic. This study examined a population-level SEIR model with seven state variables, including susceptible, $S(t)$, exposed (infected but not yet infectious), $E(t)$, infectious (not yet quarantined), $I(t)$, quarantined (confirmed and infected), $Q(t)$, The numbers of susceptible, exposed (infected but not yet infectious), infectious (not yet quarantined), quarantined (confirmed and infected), recovered, $R(t)$, dead, $D(t)$ and vaccinated, $V(t)$ sub-populations. The diagramatic representation of the flow diagram is as below:

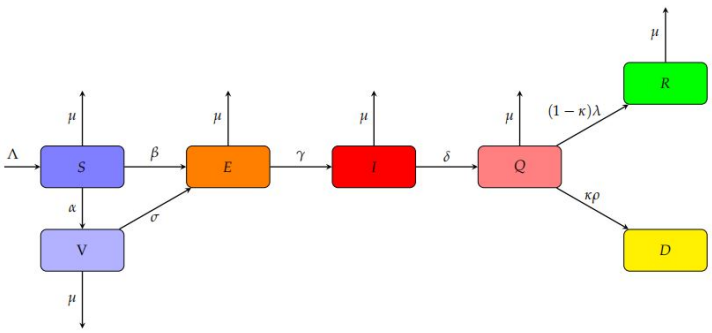

Fig. 2.6.2. Schematic diagram

The following set of nonlinear ordinary differential equations then governs the model:

$$\begin{aligned}
\frac{dS(t)}{dt} &= \Lambda - \beta S(t)I(t) - \alpha S(t) - \mu S(t) \\
\frac{dE(t)}{dt} &= \beta S(t)I(t) - \gamma E(t) + \delta\beta V(t)I(t) - \mu E(t) \\
\frac{dI(t)}{dt} &= \gamma E(t) - \delta I(t) - \mu I(t) \\
\frac{dQ(t)}{dt} &= \delta I(t) - (1-\kappa)\lambda Q(t) - \kappa\rho Q(t) - \mu Q(t) \\
\frac{dR(t)}{dt} &= (1-\kappa)\lambda Q(t) - \mu R(t) \\
\frac{dD(t)}{dt} &= \kappa\rho Q(t) \\
\frac{dV(t)}{dt} &= \alpha S(t) - \sigma\beta V(t)I(t) - \mu V(t)
\end{aligned} \tag{2.6.1}$$

The results from this study show that when vaccination campaign is intensified, there is a notable decrease in the quantity of verified cases and fatalities.

2.6.1 Gaps to be addressed by this study

From the literature review on mathematical modeling of COVID-19 infection, transmission and control dynamics, we were able to identify the research gaps which informed our study.

Our proposed model mirrors that studied by Alshammari [4] but with the inclusion of the vaccinated state. The first model considers a case of a perfect vaccine in the sense that the vaccine administered confers 100% immunity to COVID-19 infection. Additionally, this model explores the impact of reinfection of the recovered population as a result of the waning of natural immunity. The second model accounts for the scenario when the vaccination is ineffective in preventing COVID-19 infection, albeit at a lower incidence than in susceptible cohort. Furthermore, we make an assumption that the relative infectiousness of the symptomatic isolated population relative to that of asymptomatic and non-isolated symptomatic patients is negligible. The bi-linear force of infection as utilized by Alshammari [4] is replaced with the standard incident rate. We further fit the proposed model to the real COVID-19 statistical data in Kenya obtained from the worldmeters and can be accessed freely via the link given in Worldometers [34]. The underlying premise of both models is that the vaccine-induced immunity wanes, increasing ones' susceptibility to COVID-19 infections.

Chapter 3

RESEARCH METHODOLOGY

3.1 Introduction

This chapter lays emphasis on different approaches employed in this research. We first give an overview of dynamical systems with deliberate focus on continuous -time systems constructed using ordinary differential equations(ODEs). We then introduce the theory of stability of equilibrium point(s) with special emphasis on Routh-Hurwitz criterion, Lyapunov functions and computation of reproduction number R_0.

3.2 Dynamical systems

According to Layek [70], dynamics is defined as the study of time evolution processes. A dynamical system is therefore a mathematical formulation that describes the changes in state of a system through time. There are

three components of dynamical system namely: a time domain, a state space domain(or phase space) and an evolution operator (or function).

3.2.1 Time domain

Dynamical systems can either be analysed via continuous time domain ($t \subseteq \mathbb{R}$) or discrete time domain ($t \subseteq \mathbb{Z}$).

3.2.2 State space

Is the collection of all possible states of a dynamical system. Generally, a system of n first order differential equation in the space $\mathbb{R}^n$ is a dynamical system of n dimensions which describes the time behaviour of the process of evolution. In this study we consider continuous dynamical system of the form $\mathbf{x} \subseteq \mathbb{R}^n$ where $\mathbf{x} = [x_1, x_2, x_3, ..., x_n]$ and is defined by the differential equation:

$$\frac{d\mathbf{x}}{dx} = F(\mathbf{x}) = \begin{cases} \dot{x}_1 = f_1(x_1, x_2, ..., x_n) \\ \dot{x}_2 = f_2(x_1, x_2, ..., x_n) \\ \vdots \\ \dot{x}_n = f_n(x_1, x_2, ..., x_n) \end{cases} \tag{3.2.1}$$

3.2.3 Evolution Operator

We consider a system $\dot{\mathbf{x}} = f(\mathbf{x})$, with $x \in \mathbb{R}^n$ with initial conditions $\mathbf{x}(t_0) = \mathbf{x}_0$. Let $G \subset \mathbb{R}^n$ be an open set. For $x_0 \in G$, let $\varphi(t, x_0)$ be a solution to the above system of ODEs. The mapping $\varphi_t : \mathbb{R}^n \to \mathbb{R}^n$

defined by $\varphi_t(\mathbf{x}) = \varphi(t, \mathbf{x}_0)$ is referred to as an evolution operator of the system. The mapping φ_t for both linear and nonlinear systems possess the following properties:

(i). $\varphi_0(\mathbf{x}) = \mathbf{x}$ (The identity operator).

(ii). $\varphi_s(\varphi_t(\mathbf{x})) = \varphi_{(s+t)}\mathbf{x}$, for all $s, t \in \mathbb{R}^n$ This implies that the evolution of the system over $t + s$ units of time, starting from a point x, is synonymous to that in which the system first evolve over s units of time and then evolve over t units of time.

(iii). $\varphi_t(\varphi_{-t}(\mathbf{x})) = \varphi_{-t}(\varphi_t(\mathbf{x})) = \mathbf{x}$, for all $t \in \mathbb{R}^n$.

Dynamical systems may thus be viewed as group of non-linear or linear operators evolving as $\varphi_t(\mathbf{x}), t \in \mathbb{R}^n, \mathbf{x} \in \mathbb{R}^n$.

Example 3.1. Find the evolution operator $\varphi_t(x)$ for one dimensional system $\dot{\mathbf{x}} = 1 - x^2$. Hence verify the properties $(i) and (ii)$ above.

Solution

$\frac{dx}{dt} = 1 - x^2 \Longrightarrow \frac{1}{2}\log|\frac{1+x}{1-x}| = t + c, \quad x \neq 1, -1$

$\frac{1+x}{1-x} = Ae^{2t} \Longrightarrow x(t) = \frac{Ae^{2t}-1}{1+Ae^{2t}}$

We assume the initial value at $t = 0$ i.e $x(0) = x_0$ so as to compute the value of the constant of integration. Thus $A = \frac{x_0+1}{1-x_0}$. We substitute the value of A to get $x(t) = \frac{(x_0+1)e^{2t}-1+x_0}{1-x_0+(x_0+1)e^{2t}} \quad \forall x, t \in \mathbb{R}$

The above solution is defined $\forall t \in \mathbb{R}$ and for $x_0 \neq -1, 1$. It is worth noting that the points $x = -1, 1$ are the equilibrium points of the given system. The evolution operator the given one dimentional system is:

$x(t) = \frac{(x+1)e^{2t}-1+x}{1-x+(x+1)e^{2t}} \quad \forall x, t \in \mathbb{R}$

When $t = 0$, $\varphi_0(x) = \frac{(x+1)-1+x}{1-x+(x+1)} = x$ which is the identity operator.

We now prove that $\varphi_s(\varphi_t(\mathbf{x})) = \varphi_{(s+t)}\mathbf{x}, \forall t, s \in \mathbb{R}^n$

$\forall x, s, t \in \mathbb{R}^n$, we have $\varphi_t(\varphi_s(x)) = \varphi_t(y) = \frac{(y+1)e^{2t}-1+y}{1-y+(y+1)e^{2t}}$

where $y = \varphi_s(x) = \frac{x+1)e^{2t}-1+x}{1-x+(x+1)e^{2s}}$. Substituting this value of y in the above expression gives:

$\varphi_t(\varphi_s(x)) = \frac{(x+1)e^{2(s+t)}-1+x}{1-x+(x+1)e^{2(s+t)}} = \varphi_{t+s}(x)$. Hence the proof.

The set states $\varphi_t(x_0)|t \geq 0$ defines an orbit, also called a trajectory, starting at x_0 and ordered by time.

3.3 Routh-Hurwitz criterion

The Routh-Hurwitz criterion is a method that attempts to examine the stability of a linear system by analysing the roots of a given characteristic polynomial. Suppose we have equation characteristic of the form:

$$P_n(\lambda) = a_0\lambda^n + a_1\lambda^{n-1} + a_2\lambda^{n-2} + Q + a_{n-1} + a_n = 0 \qquad (3.0)$$

This matrix is referred to as Hurwitz matrix. All elements in this matrix with subscripts more than n or less than 0 are replaced with zero.

Let $H_1 = a_1$, $H_2 = \begin{pmatrix} a_1 & a_3 \\ a_0 & a_2 \end{pmatrix}$, $H_3 = \begin{pmatrix} a_1 & a_3 & a_5 \\ a_0 & a_2 & a_4 \\ 0 & a_1 & a_3 \end{pmatrix}$.....and

$$H_n = \begin{pmatrix} a_1 & a_3 & a_5 & a_7 & M & a_{2n-1} \\ a_0 & a_2 & a_4 & a_6 & M & a_{2n-2} \\ 0 & a_1 & a_3 & a_5 & M & a_{2n-3} \\ 0 & 0 & a_2 & a_4 & M & a_{2n-4} \\ K & K & K & K & M & K \\ 0 & 0 & 0 & 0 & M & a_n \end{pmatrix}$$

For the equation (3.0) to be asymptotically stable, all the principal minors of the matrix H below must be positive and also nonzero, thus $D_1, D_2, D_3, D_4, ..., D_n > 0$.

Example 3.2. For the fourth order system where $(n = 4)$, matrix (3.0) become a 4×4 matrix:

$$P_n(\lambda) = a_0\lambda^4 + a_1\lambda^3 + a_2\lambda^2 + a_3\lambda + a_4 = 0 \tag{3.1}$$

Here we have $D_1 = a_1$, $D_2 = \begin{vmatrix} a_1 & a_3 \\ a_0 & a_2 \end{vmatrix} = (a_1a_2 - a_0a_3) > 0,$

$$D_3 = \begin{vmatrix} a_1 & a_3 & 0 \\ a_0 & a_2 & a_4 \\ 0 & a_1 & a_3 \end{vmatrix} = \{a_1(a_2a_3 - a_1a_4) - a_0{a_3}^2\} > 0$$

$$D_4 = \begin{vmatrix} a_1 & a_3 & 0 & 0 \\ a_0 & a_2 & a_4 & 0 \\ 0 & a_1 & a_3 & 0 \\ 0 & 0 & a_2 & a_4 \end{vmatrix} = \{a_1a_4(a_2a_3 - a_1a_4) - a_0{a_3}^2a_4\} > 0.$$

Thus for a polynomial of the fourth degree, the necessary and sufficient condition for all roots to have the roots having negative real parts are $a_1 > 0, a_2 > 0, a_3 > 0$ and $a_4 > 0$.
In this approach, the analysis can be performed in terms of the system parameters and the stability conditions can then be derived.

3.3.1 Liénard-Chipart criterion

This rule is a modification of Routh-Hurwitz stability criterion. Its evident that it may not be easy to compute the determinants especially for polynomials of a degree $n > 4$. A. Liénard and M.H Chipart observed that the polynomial (3.0) is Hurwitz stable iff one of the conditions below are satisfied:

(i). $a_n > 0$, $a_{n-2} > 0$,.....; $D_1 > 0$, $D_3 > 0$,....

(ii). $a_n > 0$, $a_{n-2} > 0$,.....; $D_2 > 0$, $D_4 > 0$,....

(iii). $a_{n-1} > 0$, $a_{n-3} > 0$,.....; $D_1 > 0$, $D_3 > 0$,....

(iv). $a_{n-1} > 0$, $a_{n-3} > 0$,.....; $D_2 > 0$, $D_4 > 0$,....

Its thus evident that this criterion has a computational advantage over the Routh-Hurwitz since the number of determinants to be evaluated is reduced to almost half.

Example 3.3. Find the range U that will make the system $\frac{T(s)}{V(s)} = \frac{U}{s^3+4s^2+s+U}$ is stable.

Solution

From the characteristic equation $\frac{T(s)}{V(s)} = \frac{U}{s^3+4s^2+s+U}$, the corresponding 3×3 Hurwitz matrix: $H_3 = \begin{pmatrix} 4 & K & 0 \\ 1 & 1 & 0 \\ 0 & 4 & K \end{pmatrix}$. We apply liénard rule to identify the value of K that guarantees this system to be stable. This is because K is a gain and always positive and nonzero. In this case its prudent to consider D_2 only. Thus $D_2 = \begin{vmatrix} 4 & K \\ 1 & 1 \end{vmatrix}$ This gives $0 < k < 4$

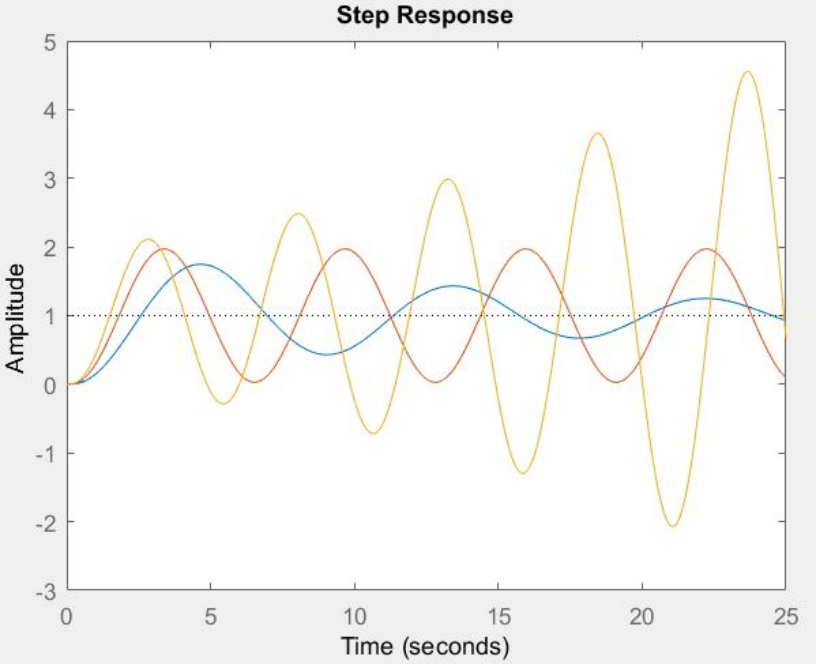

Fig. 3.3.1. Graph for various values of K

The curve with decaying amplitude is for the value of $K = 2$ i.e within the admissible values of K that makes the function stable. The curve with constant amplitude is for $K = 4$ while the curve with increasing

amplitude is for $K = 6$ and represents unstable condition as $t \to \infty$.

3.4 Lipschitz Continuity

According to Boyce et al. [19], lack of general formula for evaluating non-linear ordinary differential equations of the form (3.2.1) has elicited some pertinent questions about the existence and uniqueness of solutions to such systems of equations. The knowledge on Lipschitz continuity theorem is thus of paramount importance.

Definition 3.4. Given a general function $f : \Psi \to \Upsilon$ where Ψ may be an interval of rational numbers $\{x \in \Psi : a \leq x \leq b\}$ for some rational numbers a and b. If x_1 and x_2 are two numbers in Ψ, then $|x_2 - x_1|$ is the change in the input and $|f(x_2) - f(x_1)|$ is the corresponding change in the output. We say that f is Lipschitz continuous on Ψ, if there is a constant K_f referred to as Lipschitz constant such that.

$$|f(x_1) - f(x_2)| \leq K_f|x_1 - x_2| \quad \forall x_1, x_2 \in \Psi$$

Example 3.5. Show that the function $f(x) = x^{n+1}$ is Lipschitz continuous on any interval $\Psi = [-b, b]$, where n is a positive rational number. Hence determine the Lipschitz constant K_f.

Solution

Given x_1 and x_2 in Ψ, we estimate $|f(x_2) - f(x_1)| = |x_2^{n+1} - x_1^{n+1}|$ in terms of $|x_2 - x_1|$. We utilize the fact that:

$$x_2^{n+1} - x_1^{n+1} = (x_2 - x_1)(x_2^n + x_2^{n-1}x_1 + x_2^{n-2}x_1^2 + ... + x_2x_1^{n-1} + x_1^n)$$

Thus $(x_2 - x_1)\sum_{j=0}^{n} x_2^{n-j}x_1^j = \sum_{j=0}^{n-1} x_2^{n+1-j}x_1^j - \sum_{j=0}^{n} x_2^{n-j}x_1^{j+1}$

It should be noted that most of the terms in middle of the two sums to the right will cancel out. This can be exemplified by separating the first term of the first sum and then separating the last term in the second sum to give:

$(x_2 - x_1)\sum_{j=0}^{n} x_2^{n-j}x_1^j = x_2^{n+1} + \sum_{j=1}^{n} x_2^{n+1-j}x_1^j - \sum_{j=0}^{n-1} x_2^{n-j}x_1^{j+1} - x_1^{n+1}$

Changing the index in the second sum gives:

$(x_2 - x_1)\sum_{j=0}^{n} x_2^{n-j}x_1^j = x_2^{n+1} + \cancel{\sum_{j=1}^{n} x_2^{n+1-j}x_1^j} - \cancel{\sum_{j=1}^{n} x_2^{n+1-j}x_1^j} - x_1^{n+1}$

Thus: $(x_2 - x_1)\sum_{j=0}^{n} x_2^{n-j}x_1^j = x_2^{n+1} - x_1^{n+1}$

$|f(x_2) - f(x_1)| = |\sum_{j=0}^{n} x_2^{n-j}x_1^j||x_2 - x_1|.$

Utilizing the triangular inequality to the term $|\sum_{j=0}^{n} x_2^{n-j}x_1^j|$ gives:

$|\sum_{j=0}^{n} x_2^{n-j}x_1^j| \leq \sum_{j=0}^{n} |x_2|^{n-j}|x_1|^j = \sum_{j=0}^{n} b^n$

Thus $|f(x_2) - f(x_1)| \leq nb^n|x_2 - x_1|$

The function $f(x) = x^{n+1}$ is thus Lipschitz continuous with Lipschitz constant being $K_f = nb^n$

Lipschitz function can be generalized to higher dimensions. Consider $\Omega \subseteq \mathbb{R}^n, f : \Omega \to \mathbb{R}^m$. We say that f is Lipschitz on Ω if $\exists\ K_f > 0$ such that for any $\vec{x}$, $\vec{y} \in \Omega$, where $\vec{x} = (x_1, x_2, ..., x_n)$ and $\vec{y} = (y_1, y_2, ..., y_n)$, we have: $\{\sum_{i=1}^{m}[f_i(\vec{x}) - f_i(\vec{y}]^2\}^{\frac{1}{2}} \leq K_f\{\sum_{i=1}^{n}[\vec{x}_j - \vec{y}_j]^2\}^{\frac{1}{2}}$.

The value of K_f has to be the same in the above inequality for any $\vec{x}, \vec{y} \in \Omega$.

3.4.1 Picard-Lindelöf Theorem

Let $\bar{\Omega}$ be a nonempty open set in $\mathbb{R}\times\mathbb{R}$, let $(x_0, y_0) \in \bar{\Omega}$ and let $f : \bar{\Omega} \to \mathbb{R}$. Let the following conditions be satisfied:

(i) .f(x,y) is continuous in a compact rectangle of the form $\bar{\Re} = \{(x, y) : |x - x_0| \leq a, \ \ |y - y_0| \leq b\} \in \bar{\Omega}$ and hence $\exists$ a $\aleph > 0$ such that $|f(x, y)| \leq \aleph \quad \forall (x, y) \in \bar{\Re}$.

(ii) .f(x,y) satisfy a uniform Lipschitz condition in $\bar{\Re}$ such that: $|f(x, y_1) - f(x, y_2)| \leq K_f|y_1 - y_2|$.

(iii) . $y_0(x)$ is continuous in $|x - x_0| \leq a$, and $|y_0(x) - y_0| \leq b$.

Then the initial value problem (IVP) $\frac{dy}{dx} = f(x, y)$, $y(x_0) = y_0$, has a unique solution $y(x)$ and this solution is valid in the interval:
$\bar{I} : |x - x_0| \leq \bar{h}$=$min\{a, \frac{b}{\aleph}\}$.

Example 3.6. Given the non-linear differential equation: $(1-x^2y)y^{'}(x) = 2e^{-xy^2+1}$ and the initial condition: $y(1) = -2$, identify the interval on which this IVP has a unique solution.

Solution

The above differential equation cannot explicitly be solved. This equation can be rewritten as: $y^{'}(x) = \frac{2e^{-xy^2+1}}{(1-x^2y)}$. In this problem the function f is defined by: $f(x, y) = 2e^{-xy^2+1}(1 - x^2y)^{-1}$ and x_0, y_0 are given by $x_0 = 1, y_0 = -2$. We consider triangle $\bar{\Re}$ centered at $(1, -2)$. The rectangle $\bar{\Re}$ need to be carefully selected so that the denominator of functions

f and $\frac{\partial f}{\partial y}$ does not vanish. We let $a = \frac{1}{4}$ and $b = \frac{1}{5}$ so that we have the triangle: $\bar{\Re} = \{(x, y) : \frac{3}{4} \leq x \leq \frac{5}{4}, \ \frac{-11}{5} \leq y \leq \frac{-9}{5}\}$. We notice that $(1 - x^2y) \geq 2$ for $(x, y) \in \bar{\Re}$. Thus $|(1 - x^2y)^{-1}| < \frac{1}{2}$ and $2e^{-xy^2+1} \leq 2e^{\frac{-81}{50}+1} < 2$. Thus $|f(x, y)| = |\frac{2e^{-xy^2+1}}{1-x^2y}| \leq 1, \ \ \forall (x, y) \in \bar{\Re}$.

We now verify the Lipschitz condition by computing:

$\frac{\partial f}{\partial y}(x, y) = \frac{-4xye^{-xy^2+1}}{1-x^2y} - \frac{2x^2e^{-xy^2+1}}{(1-x^2y)^2}$.

We observe that $| - 2xy| \leq 6$ and $\frac{x^2}{1-x^2y} < 1$. Thus we have:

$|\frac{\partial f}{\partial y}(x, y)| \leq |\frac{-4xye^{-xy^2+1}}{1-x^2y}| + | - \frac{2x^2e^{-xy^2+1}}{(1-x^2y)^2}| \leq 7$. Hence the Lipschitz condition is satisfied with constant $K_f = 7$.

We now have: $h \leq min\{a, \frac{b}{\aleph}\} = min\{\frac{1}{4}, \frac{1}{5}\} = \frac{1}{5}$. It is thus evident that the given IVP has exactly one solution which lies in the interval $[1 - \bar{h}, 1 + \bar{h}]$. We can exemplify this by choosing, say, $h = 0.125$. This shows that a unique solution exists in the interval $[0.875, 1.125]$.

3.5 Linear stability analysis

The stability of a dynamical system can be analysed by using a perturbation approach, a method which investigates the effects of 'small' perturbation close to an equilibrium point. The local stability using the principle of linearised stability has been described by many textbooks (Alligood et al. [3], Arnold [9] and Seydel [97].

Consider the dynamical system

$$\dot{x}(t) = f(x(t)) \tag{3.5.1}$$

which has an equilibrium point $\bar{x}$.

We consider starting the system (3.5.1) above from initial condition $x(t_0) = \bar{x}$. The resulting $x(t)$ satisfies $x(t) = \bar{x}$ for all $t > t_0$. We define a deviation variable $\delta_x(t) = x(t) - \bar{x}$. This implies that:

$$x(t) = \delta_x(t) + \bar{x} \tag{3.5.2}$$

But $\dot{x(t)} = \dot{\delta_x(t)}$ thus:

$$\dot{\delta}_x(t) = f(\bar{x} + \delta_x(t)) \tag{3.5.3}$$

Applying Taylor's expansion on the right hand side of Equation (3.5.3) gives:

$$\dot{\delta}_x(t) = f(\bar{x}) + \frac{df}{dx}|_{x-\bar{x}}\delta_x(t) + \frac{1}{2}\frac{d^2f}{dx^2}|_{x-\bar{x}}\delta_x^2(t) + \frac{1}{6}\frac{d^3f}{dx^3}|_{x-\bar{x}}\delta_x^3(t) + ... \tag{3.5.4}$$

We consider the fact that $f(\bar{x}) = 0$. Since $x(t) \to \bar{x}$, $\delta_x(t) \to 0$. We thus ignore all higher order terms (of second order and above) to get: $\dot{\delta}_x(t) \simeq \frac{df}{dx}|_{x-\bar{x}}\delta_x(t)$.

For the functions of multiple states as in Equation(3.2.1), we consider the equilibrium points given by $\bar{x_1}, \bar{x_2}, ..., \bar{x_m}$ so that $f_i(\bar{x_1}, \bar{x_2}, ..., \bar{x_m}) = 0$ for all $i \in \{1, 2, ..., m\}$. The linearisation of f_i about the equilibrium point is thus given by $\dot{\delta}_x(t) \simeq \sum_{j=1}^{m} \frac{\partial f_i}{\partial x_j}|_{x_j=\bar{x}_j}\delta_{x_i}(t)$. The above is a linear time-invariant, differential equation since $\dot{\delta}_x(t)$ is a linear combination of $\delta_{x_i}(t)$. The above equation can be rewritten as:

$$\dot{\delta}_x(t) \simeq A\delta_{x_i}(t). \tag{3.5.5}$$

Where $A = \sum_{j=1}^{m} \frac{\partial f_i}{\partial x_j}|_{x_j=\bar{x}_j}$ is a constant matrix referred to as a Jacobian matrix defined by:

$$J = \begin{pmatrix} \frac{\partial f_1}{\partial x_1} & \frac{\partial f_1}{\partial x_2} & . & . & . & \frac{\partial f_1}{\partial x_m} \\ \frac{\partial f_2}{\partial x_1} & \frac{\partial f_2}{\partial x_2} & . & . & . & \frac{\partial f_2}{\partial x_m} \\ . & . & . & . & . & . \\ . & . & . & . & . & . \\ . & . & . & . & . & . \\ \frac{\partial f_m}{\partial x_1} & \frac{\partial f_m}{\partial x_2} & . & . & . & \frac{\partial f_m}{\partial x_m} \end{pmatrix}$$

The linear system in equation (3.5.5) is called the Jacobian linearisation of the original non-linear system about the equilibrium point $\bar{x}$.

Theorem 3.7. *(Ezzinbi [42])(**Linearization Principle**).* Let $f : \mathbb{R}^n \to \mathbb{R}^n$ be a c^2 function and $\bar{x}$ be the equilibrium of a differential equation (3.2.1). Let $A = \frac{\partial Df}{\partial Dx}|_{x=\bar{x}} = [\frac{\partial f_i}{\partial x_j}]$ be the linearization of f, and $\varrho A \subseteq Re(\Lambda_i) < 0$. Then $\bar{x}$ is locally exponentially stable for (3.2.1). If there exists $\Lambda_i \in \varrho(A)$ such that $Re(\Lambda_i) > 0$ then $\bar{x}$ is unstable equilibrium point.

The stability of $\bar{x}$ is thus determined by the eigenvalues Λ_i of the Jacobian matrix. The perturbation $\delta_{x_i}(t)$ tends to zero if the real parts of Λ_i are negative, and increases if the real parts of the Λ_i has a positive value. It is also worthy noting that incase one of the Λ_i has a zero real part, the second order terms of delta state $\delta^2_{x_i}(t)$ cannot be ignored and thus must

be put into consideration when determining the stability of $\bar{x}$.
The eigenvalue problem is represented by:

$$\mathbf{A}\mathbf{v} = \Lambda\mathbf{v} \tag{3.5.6}$$

for a square matrix $\mathbf{A}$, eigenvalue Λ, and (nonzero) eigenvector $\mathbf{v}$. Equation (3.5.6) can be rewritten as :

$$(\mathbf{A} - \Lambda\mathbf{I})\mathbf{v} = 0 \tag{3.5.7}$$

where $\mathbf{I}$ represents identity matrix. Equation (3.5.7) has the implication that $(\mathbf{A} - \Lambda\mathbf{I})$ is invertible matrix thus its determinant is equal to zero. The eigenvalues can be determined by solving the characteristic equation $\det(\mathbf{A} - \Lambda\mathbf{I}) = 0$
The corresponding eigenvectors for a particular eigenvalue Λ_i can the be evaluated from Equation(3.5.5) by making the substitution of Λ_i and then determining the most general non-zero solution of the resulting system. The real parts of the eigenvalues $\Lambda_i(i = 1, 3, ...m)$ of the Jacobian matrix evaluated at the equilibrium point $\bar{x}$ of Equation (3.2.1) establish stability in the following way:

. $\mathrm{Re}(\Lambda_i) < 0$ for all i implies asymptotic stability, and

. $\mathrm{Re}(\Lambda_j) > 0$ for one or more j implies instability.

Example 3.8. Consider a state space system for a pendulum with damping force.

$$\begin{cases} \dot{x}_1 = x_2 \\ \dot{x}_2 = -\frac{g}{l} sin x_1 - \frac{k}{m} x_2 \end{cases} \tag{3.5.8}$$

Let $\frac{g}{l} = \varsigma > 0$ and $\frac{k}{m} = \nu > 0$. The equilibrium points for this system are 0 and π. The Jacobian matrix at the equilibrium point $\bar{x} = 0$ is $J = \begin{pmatrix} 0 & 1 \\ -\varsigma & -\nu \end{pmatrix}$. Evaluation of the determinant equation $|J - \Lambda I|$ gives the eigenvalues: $\Lambda = \frac{-\varsigma \pm \sqrt{(\varsigma^2 - 4\nu)}}{2}$. Since the real part of the eigenvalues is negative, $\bar{x} = 0$ is stable equilibrium point.

The Jacobian matrix at the equilibrium point $\bar{x} = \pi$ is $J = \begin{pmatrix} 0 & 1 \\ \varsigma & -\nu \end{pmatrix}$.

The solution of determinant equation $|J - \Lambda I|$ gives the eigenvalues: $\Lambda = \pm\varsigma$. Since one of the eigenvalues has a real positive value, $\bar{x} = \pi$ is unstable equilibrium point.

Example 3.9. Consider the differential equation dependent on one parameter ζ.

$$\begin{cases} \dot{a} = f_1(a, b) = -2b + a(\zeta - (a^2 + b^2) \\ \dot{b} = f_2(a, b) = 2a + b(\zeta - (a^2 + b^2) \end{cases} \tag{3.5.9}$$

The above system of differential equation has an equilibrium point at $(a, b) = (0, 0)$ for all $\zeta \in \mathbb{R}$. The Jacobian matrix is given by:

$$J = \begin{pmatrix} \frac{\partial f_1}{\partial a} & \frac{\partial f_1}{\partial b} \\ \frac{\partial f_2}{\partial a} & \frac{\partial f_2}{\partial b} \end{pmatrix} = \begin{pmatrix} \zeta - 3a^2 - b^2 & -2 - 2ab \\ 2 - 2ab & \zeta - a^2 - 3b^2 \end{pmatrix}$$

Evaluating the Jacobian matrix at the equilibrium point give: $\bar{J} = \begin{pmatrix} \zeta & -2 \\ 2 & \zeta \end{pmatrix}$
We now evaluate the determinant of the equation $|\bar{J} - \Lambda I| = 0$ to get the equation: $\Lambda^2 - 2\zeta\Lambda + (\zeta^2 + 4) = 0$. The corresponding eigenvalues are thus: $\Lambda_{1,2} = \zeta \pm 2i$, where $i = \sqrt{-1}$ is an imaginary value. Thus if $\zeta < 0$, the fixed point is asymptotically stable, while for $\zeta > 0$ yields an unstable point. For $\zeta = 0$, we are not able to establish the stability of the equilibrium point and thus we are compelled to utilize another class of functions referred to as Lyapunov functions.

3.6 Lyapunov Functions

Lyapunov function $\{V : \aleph \subseteq \mathbb{R}^n \to \mathbb{R}\}$ is a resemblance of an energy function that can be used to determine the stability condition of a given system of equations. This function is undoubtedly one of the most powerful tools for determining stability.
Consider a positive function $V(x)$ that is always decreasing along trajectories of the system ($\frac{dV}{dt}x(t) = \sum_{i=1}^{m} \frac{\partial V}{\partial x_i}\dot{x}_i = \sum_{i=1}^{m} \frac{\partial V}{\partial x_i} f_i(x_i(t)) \leq 0$), we can make a determination that the minimum value attainable is a locally stable equilibrium point, while for $\dot{V}(x) < 0$, we have asymptotically stable equilibrium.

Example 3.10. Establish the stability of the system given that the origin is an equilibrium of the above system:

$$\dot{x_1} = ax_2$$

$$\dot{x_2} = -bx_1 - x_2$$

Solution

We consider a Lyapunov candidate: $V(x_1, x_2) = {x_1}^2 + x_2^2$. Its worth noting that $V(x)$ is positive definite function. $\frac{\partial V}{\partial x} = 2x_1\dot{x}_1 + 2x_2\dot{x}_2$ which upon substitution yields: $\frac{\partial V}{\partial x} = 2(a-b)x_1x_2 - {x_2}^2$. To guarantee negative definiteness of $\frac{\partial V}{\partial x}$, and hence local stability of the above system $a = b$.

3.6.1 The variable method of determining Lyapunov function

This method involves working from the derivative function to the function itself. Generally, we investigate a general expression of $\dot{V}(x)$ and using the given system, we further chose the parameters of $V(x)$ in attempt to make $\dot{V}(x) < 0$.

Here, given the system $\dot{x} = f(x,t)$, we assume an arbitrary function:

$$\nabla V(x) = \begin{pmatrix} a_{11}(x)x_1 + a_{12}(x)x_2 + ... + a_{1m}(x)x_m \\ a_{21}(x)x_1 + a_{22}(x)x_2 + ... + a_{2m}(x)x_m \\ . \\ . \\ a_{m1}(x)x_1 + a_{m2}(x)x_2 + ... + a_{mm}(x)x_m \end{pmatrix} \tag{3.6.1}$$

Where $a_{11}(x), ..., a_{mm}(x)$ are arbitrary constants or functions to be determined. Let

$$\dot{V}(x) = \frac{dV}{dt} = \frac{\partial V}{\partial x_1}\dot{x}_1 + \frac{\partial V}{\partial x_2}\dot{x}_2 + ... + \frac{\partial V}{\partial x_m}\dot{x}_m \tag{3.6.2}$$

The above equation can be expressed as: $\dot{V}(x) = (\nabla V(x))^T \dot{x}$

We make constraints so that $\dot{V}(x) < 0$.

Using the curl requirements: $\frac{m(m-1)}{2}$ and $\frac{\partial \nabla V_i}{\partial x_j} = \frac{\partial \nabla V_j}{\partial x_i}$, we determine the remaining unknown coefficients in equation (3.6.1). Equation (3.6.2) above can be expressed as: $V(x) = \int_0^x (\nabla V)^T dx$, which upon evaluation gives the required Lyapunov function . Its worth noting that the integration is taken from zero(0) to an arbitrary value in the phase space $(x_1, x_2, ..., x_m)$.

3.6.2 LaSalle's Invariance Principle

LaSalle's theorem is of great importance since it enables us to conclude the asymptotic stability of an equilibrium point in situations where $\dot{V}(x)$ is negative semi-definite on Ω.

Definition 3.11. A positive invariant set: A set M is said to be a positive invariant set with respect to $\dot{x} = f(x)$ if all trajectories starting at M stays in M forever. *i.e* $x(0) \in M, \Rightarrow x(t) \in M, \forall t > 0$.

Theorem 3.12. Kawski [59],**LaSalle's Theorem**: Let f be a locally Lischitz function defined over a domain $D \in \mathbb{R}^n$ and $M \in D$ be a compact set that is positively invariant with respect to $\dot{x} = f(x)$. Let $V(x)$ be a C^1 function defined over D such that $V(x) \leq 0$ in M. Let S be the set of all points in M where $\dot{V}(x) = 0$ and Ψ is the largest invariant subset of S with respect to the system dynamics. Then every solution starting in M approaches Ψ as $t \to \infty$ means that $d(x(t, x), \Psi) \to 0$ as $t \to \infty$ $\forall x_0 \in M$.

3.6.3 Theorem on Center Manifold Theory

Here, we reproduce Theorem (4.1) of Chavez et al. [31].

Theorem 3.13. *(see Chavez et al. [31]). Consider the following general system of ordinary differential equations with parameter ϕ.*

$$\frac{dx}{dt} = f(x, \phi), f : \mathbb{R}^n \times \mathbb{R} \to \mathbb{R}, f \in \mathbb{C}^2(\mathbb{R}^n \times \mathbb{R}), \tag{3.6.3}$$

where 0 is an equilibrium of the system, that is, $f(0, \phi) = 0$ for all ϕ. Assume the following:
A1: $\mathcal{A} = D_x f(0,0) = ((\frac{\partial f_i}{\partial x_j})(0,0))$ is the liberalization of the system (3.6.3) around the equilibrium 0 with ϕ evaluated at 0. Zero is a simple eigenvalue of $\mathcal{A}$, and other eigenvalues have negative real parts.
A2:the matrix $\mathcal{A}$ has a right eigenvector w and a left eigenvector v corresponding to the zero eigenvalue.
Let f_k be the k^{th} component of f and

$$\begin{aligned} a &= \sum_{k,i,j=1}^{n} v_k w_i w_j \frac{\partial^2 f_k}{\partial x_i \partial \phi}(0,0) \\ b &= \sum_{k,i=1}^{n} v_k w_i \frac{\partial^2 f_k}{\partial x_i \partial \phi}(0,0). \end{aligned} \tag{3.6.4}$$

The local dynamics of systems (3.6.3) around 0 are completely determined by the signs of a and b:

(i) $a > 0, b > 0$. When $\phi < 0$ with $|\phi| \ll 1$, 0 is locally asymptotically stable and there exists a positive unstable equilibrium; when $0 < \phi \ll 1$, 0 is unstable and the exists a negative and locally asymptotically stable equilibrium;

(ii) $a < 0, b < 0$. *When* $\phi < 0$ *with* $|\phi| \ll 1$, *0 is unstable; when* $0 < \phi \ll 1$, *0 is locally asymptotically stable, and there exists a positive unstable equilibrium;*

(iii) $a > 0, b < 0$. *When* $\phi < 0$ *with* $|\phi| \ll 1$, *0 is unstable and there exists a locally asymptotically stable negative equilibrium; when* $0 < \phi \ll 1$, *0 is stable and a positive unstable equilibrium appears;*

(iv) $a < 0, b > 0$. *When* ϕ *changes from negative to positive, 0 changes its stability from stable to unstable. Correspondingly, a negative unstable equilibrium becomes positive and locally asymptotically stable.*

3.7 Model analysis

We examine the positivity and boundedness of the dynamical system's solutions in the models to be developed. In addition, we show the existence of the disease-free and endemic equilibrium points analytically. We also prove that these points are asymptotically stable both locally and globally and provide the prerequisites for backward bifurcation in our models. Additionally, we'll perform sensitivity analysis.

3.7.1 Positivity and boundedness of solutions

We are to examine the systems to formulated inside the biologically significant area Ω. It is crucial to demonstrate that the state variables and the associated parameters are non-negative for all time, $t \geq 0$, as the models track changes in the human population. One crucial technique

for confirming the presence of the given model's solution is its existence. We need to show that the closed set Ω for the models to be developed is positively invariant.

3.7.2 Disease-free equilibrium (DFE)

The steady-state solution of an epidemiological model in the absence of infection or sickness is known as the disease-free equilibrium (DFE) points. This is evaluated by setting the right side of the system's equation to zero and explicitly solving for the state variables.

3.7.3 Existence of endemic equilibrium(EE) point

When an illness in a certain geographic region is continuously maintained at a baseline level without the help of outside inputs like medicine or vaccination, among other control techniques, it is considered to have reached its endemic equilibrium in epidemiology. The steady states where the illness may continue to spread across the population are known as the model's endemic equilibria; these are the conditions under which at least one of the model's infected compartments is not empty. We first determine the basic reproduction number in order to demonstrate the presence of endemic equilibrium.

3.7.4 Basic reproduction number, R_0

According to Tulu et al. [107], the basic reproduction number is the average number of cases that one case produces over the infectious period in either a completely susceptible population or an uninfected population. When analyzing epidemiological models for disease control, the fundamental reproduction number is a crucial parameter that yields the following interpretations:

(i) When $R_0 < 0$, the illness eventually disappears from the population because the average number of secondary infections brought on by a single person who is predominantly affected is less than the unity value (Driessche et al. [39]).

(ii) $R_0 = 1$ denotes the threshold value, beyond which the sickness also ends since the number of secondary infections brought on by the initial infection remains constant.

(iii) When $R_0 > 1$, it indicates that a single infectious person is responsible for an average of many additional infections and that the illness will eventually spread across the community as a pandemic.

Without a doubt, the next-generation matrix approach (NGM) (Diekmann et al. [38] is the ideal basis for defining and figuring out R_0 in cases where people are categorised into discrete distinct finite states. The construction of NGM arises from the specifications of the model which is depended on epidemiological traits and interpretation. According to this technique, there are $m < n$ diseased compartments inside each of the n mutually exclusive compartments that make up the whole population.

The number of infected people in the i^{th} infected compartment at time t may be expressed as $x_i, i = 1, 2, 3, ...m$. The above model can also be written as:

$\frac{dx_i}{dt} = F_i(x) - V_i(x),$ where $V_i(x) = [V_i^-(x) - V_i^+(x)]$

From the above equations, we note that the rate of new infection appearance in compartment i is represented by $F_i(x)$, the rate of individual transfer into compartment i is represented by $V_i^+(x)$, and the rate of individual transfer out of compartment i is represented by $V_i^-(x)$. The matrix (FV^{-1}) is referred to as the next generation matrix (NGM). Diekman et al. [38] proved that the basic reproduction number R_0 corresponds to the most dominating non-zero eigenvalue or spectral radius of NGM.

3.7.5 The Local Stability of Disease Free Equilibrium (DFE)

We linearize the system of model equations to produce the Jacobian Matrix $J(B_0)$, which allows us to derive the local stability for the disease-free equilibrium point B_0. When $R_0 < 1$, DFE is locally asymptotically stable in epidemiological models; when $R_0 > 1$, it is unstable.

3.7.6 The Global Stability of Disease Free Equilibrium (DFE)

Using the Lyapunov function technique, we examine the global stability of the disease-free equilibrium point B_0 in this model.

3.7.7 Sensitivity analysis

Sensitivity analysis ascertains the impact of varying independent variable values on a certain dependent variable under a given set of presumptions. Two categories of sensitivity analysis are examined:

(i) Local sensitivity analysis: This type of study involves taking the derivative at a specific location in the model parameters' state space at the parameter baseline values. Since the net influence of a parameter on the outcome's attribute is determined while assuming that all other factors remain unchanged, it is also referred to as one-factor-at-a-time technique.

(ii) Global sensitivity analysis; This analysis focuses on a number of concurrently varying input parameter values.

3.8 Numerical Simulation

Analytical investigations are incomplete without numerical validation of the findings. From a practical standpoint, these numerical results are equally significant. In this study, we utilize PYTHON software to graphically illustrate the effects of change on different parameters to our model. The parameter values will be obtained from the secondary data that is in the existing research work.

Chapter 4

RESULTS AND DISCUSSION

4.1 Introduction

In this section, we formulate model 1 which assumes that COVID-19 vaccine confers permanent immunity to the disease infection. The existence and uniqueness of the solution, the positivity and boundedness of the state variables, the model's reproduction number,R_ν , the stability of endemic equilibrium and the local and global stability of DFE are examined. Sensitivity and numerical analysis are carried out to validate the analytical results and to ascertain the most significant parameters respectively.

4.2 Model 1 Formulation

The model descriptions, equations, flow diagram, and assumptions are all included in this subsection.

4.2.1 Assumptions made

The following assumptions are made in this study:

(i). There is homogeneous mixing of the population and individuals become exposed to COVID-19 infection after coming into contact with asymptomatic and symptomatic persons.

(ii). The vaccine acquired immunity prevents one from getting infected with COVID-19.

(iii). The vaccine immunity wanes after some period and this makes one to get back to the susceptible population.

(iv). The exposed persons become either symptomatic or asymptomatic depending on their innate immunity.

4.2.2 Model Description

In this study, the whole population $N_h(t)$ is stratified into (6) mutually exclusive compartments, S_h, V_h, E_h, I_{hA}, I_h and R_h which respectively represent the susceptible, vaccinated, exposed, asymptomatic, symptomatic and Recovered individuals.

Equation of the model are derived as follows: The growth of the susceptible population is as a result of immigration or birth at a rate π (Olumuyiwa et al. [86]) as well as the reinfection of recovered individuals at the rate τ. COVID-19 vaccine administered is to the susceptible population at the rate θ. This vaccine is assumed to wane at the rate φ.

Furthermore, the susceptible individuals progress to the exposed phase upon interaction with the asymptomatic and the symptomatic individuals. The force of infection λ is thus expressed as:

$$\lambda = \beta(\xi I_{hA} + I_h)$$

where parameter β is the transmission coefficient which accounts for contacts having the potential to cause infection, while $\xi \in (0, 1)$ is the modification parameter which accounts for presumed reduction in infectiousness of the asymptomatic individuals relative to the symptomatic individuals. All the population clusters are presumed to decrease at a constant value μ which accounts for natural death rate. The rate of progression of both susceptible and vaccinated individuals is thus given as:

$$\begin{aligned} \frac{dS_h}{dt} &= \pi + \varphi V_h + \tau R_h - (\lambda + \mu + \theta) S_h \\ \frac{dV_h}{dt} &= \theta S_h - (\mu + \varphi) V_h \end{aligned}$$

The growth of the exposed population is necessitated by the susceptible at the rate λ and it is diminished at a constant rate ω when a fraction ϵ of the individuals develop symptoms and the rest $(1 - \epsilon)$ progress to asymptomatic compartment. It is worth noting that the exposed individuals are those who are infected with COVID-19, do not manifest symptoms of the disease yet and they register negative when subjected to polymerase chain reaction (PCR) tests. Such patients are said to be in latency phase and are regarded as non-infectious. Between exposure and the onset of symptoms, COVID-19 is known to have an incubation period that ranges

from 2 to 14 days. [4]. Thus we obtain the expression;

$$\frac{dE_h}{dt} = \lambda S_h - (\mu + \omega)E_h$$

The asymptomatic class class I_{hA} consist of those who fail to develop clinical COVID-19 symptoms after the disease incubation. In this study we assume that a certain proportion of asymptomatic individuals become symptomatic if left untreated. This is because the adaptive immunity developed from infection by a given COVID-19 variant does not make one immune to infection from a different variant. A certain percentage of the asymptomatic patients is assumed to recover naturally from the disease at the rate κ. In fact κ is the measure of efficacy of identification and treatment of the asymptomatic individuals. The expression for asymptomatic thus becomes:

$$\frac{dI_{hA}}{dt} = (1 - \epsilon)\omega E_h - (\mu + \alpha)I_{hA}$$

Besides natural death rate μ, the symptomatic individuals are diminished by COVID-19 induced death rate at δ. The parameter γ accounts for the successful treatment and recovery rate of the symptomatic. The expressions for symptomatic is thus given as:

$$\frac{dI_h}{dt} = \epsilon\omega E_h + (1 - \kappa)\alpha I_{hA} - (\mu + \gamma + \delta)I_h$$

Lastly, the recovery of the asymptomatic and symptomatic leads to the expansion of the recovered people, which is then reduced by reinfection

at the rate τ. The rate of recovery equation is expressed as:

$$\frac{dR_h}{dt} = \gamma I_h + \alpha\kappa I_{hA} - (\mu + \tau)R_h$$

Thus it follows that our model consist of the following system of non-linear differential equations:

$$\begin{aligned}
\frac{dS_h}{dt} &= \pi + \tau R_h + \varphi V_h - (\lambda + \mu + \theta)S_h \\
\frac{dV_h}{dt} &= \theta S_h - (\varphi + \mu)V_h \\
\frac{dE_h}{dt} &= \lambda S_h - (\omega + \mu)E_h \\
\frac{dI_{hA}}{dt} &= \omega(1 - \epsilon)E_h - (\mu + \alpha)I_{hA} \\
\frac{dI_h}{dt} &= \omega\epsilon E_h + (1 - \kappa)\alpha I_{hA} - (\mu + \delta + \gamma)I_h \\
\frac{dR_h}{dt} &= \kappa\alpha I_{hA} + \gamma I_h - (\mu + \tau)R_h
\end{aligned} \tag{4.2.1}$$

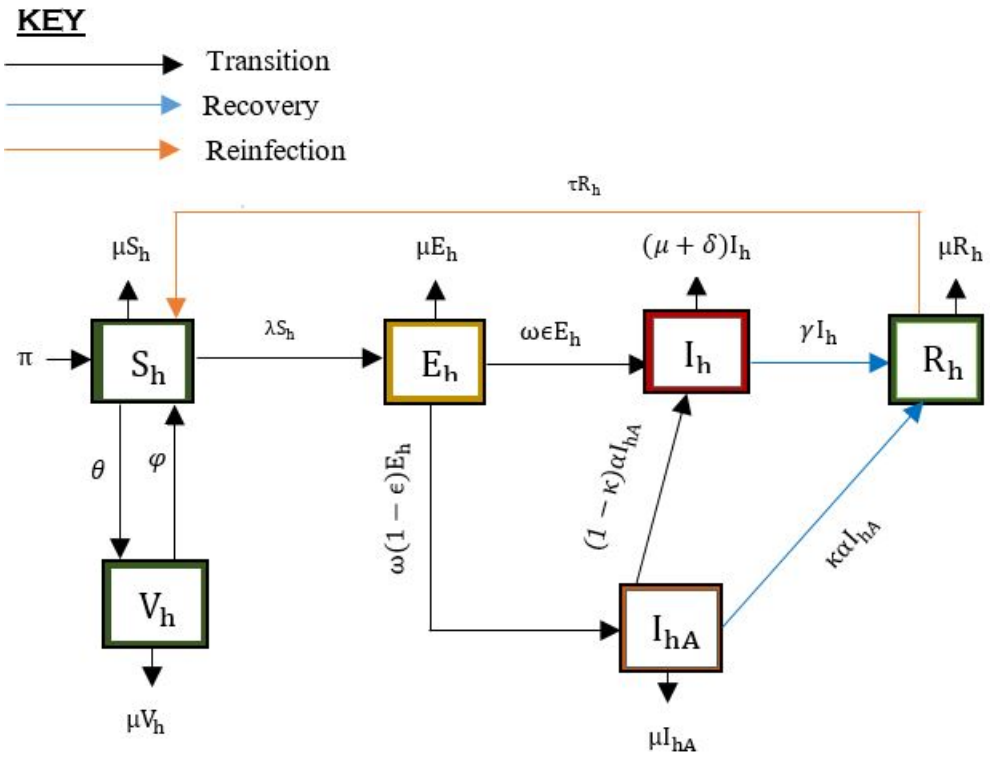

Fig. 4.2.1. General COVID-19 flow diagram for our model 1

Table 4.1: Definition of state variables

Variable	**Definition**
S_h	Human population susceptible to COVID-19 disease
V_h	Fully vaccinated population
E_h	Individuals in a latency period
I_{hA}	Infected population that do not show symptoms of COVID-19 disease.
I_h	A highly infectious individuals who are sick
R_h	Recovered population.

Descriptions of all the parameters are summarized in **Table 4.2** below.

Table 4.2: Definition of parameters

Variable	Definition
π	Recruitment rate of susceptible into the population
μ	Natural death rate
β	COVID-19 transmission rate.
ξ	Modification factor for asymptomatic persons.
ϵ	Rate at which the exposed persons who become symptomatic.
γ	Recovery rate of the symptomatic individuals.
δ	COVID-19 induced death rate for symptomatic individuals
ω	Rate at which exposed population become sick of COVID-19
φ	Rate of waning of COVID-19 vaccine induced immunity
α	Rate of movement from asymptomatic infected class
κ	Rate of identification and treatment of the asymptomatic persons.
θ	Rate of vaccination of susceptible population.
τ	Rate of susceptibility of a recovered individual

4.2.3 The basic properties of the model

Theorem 4.1. *If* $S_h(0) \geq 0, V_h(0) \geq 0, E_h(0) \geq 0, I_{hA}(0) \geq 0, I_h(0) \geq 0$ *and* $R_h(0) \geq 0$*, then the solution* $(S_h(t) \geq 0, V_h(t) \geq 0, E_h(t) \geq 0, I_{hA}(t) \geq 0, I_h(t) \geq 0$ *and* $R_h(t) \geq 0)$ *of model (4.2.1) of the model are non-negative* $\forall t > 0$*.*

Proof. According to Asha et al. [12], Kifle et al. [123] and Rabiu et.al.

[90], we prove the positivity of our system (4.2.1) by contradiction. Given the non-negative initial conditions for $S_h(0), V_h(0), E_h(0)$,
$I_{hA}(0), I_h(0)$ and $R_h(0)$, the positivity of the system can be determined as follows: We make an assumption that there exists time t_i such that, $S_h(0) > 0, S_h(t_i) = 0, S_h'(t_i) < 0, V_h(t) > 0, E_h(t) > 0, I_{hA}(t) > 0, I_h(t) > 0, R_h(t) > 0$, for all $0 \leq t < t_i$.
In relation to our case and considering the first equation of the system (4.2.1), we have:

$$\frac{dS_h}{dt}(t_i) = \pi + \varphi V_h(t_i) + \tau R_h(t_i) - (\lambda + \mu + \theta) S_h(t_i)$$

Based on our assumption, this equation implies that:

$$\frac{dS_h}{dt}(t_i) = \pi + \varphi V_h(t_i) + \tau R_h(t_i) > 0$$

which is a contradiction. This indicates that $S_h(t) > 0$ for all $t > 0$.
For the second equation, we have

$$\frac{dV_h}{dt} = \theta S_h - (\varphi + \mu) V_h \geq -(\varphi + \mu) V_h$$

Utilizing separation of variables and applying the initial conditions, solution to the above equation is: $V_h(t) \geq V_h(0) \exp(-(\mu + \varphi)t) \geq 0$ In the similar manner the equations three to equation six of the system (4.2.1) becomes

$$\frac{dE_h}{dt} = \lambda S_h - (\omega + \mu)E_h \geq -(\omega + \mu)E_h$$
$$\frac{dI_{hA}}{dt} = \omega(1-\epsilon)E_h - (\mu + \alpha)I_{hA} \geq -(\mu + \alpha)I_{hA}$$
$$\frac{dI_h}{dt} = \omega\epsilon E_h + (1-\kappa)\alpha I_{hA} - (\mu + \delta + \gamma)I_h \geq -(\mu + \delta + \gamma)I_h$$
$$\frac{dR_h}{dt} = \kappa\alpha I_{hA} + \gamma I_h - (\mu + \tau)R_h \geq -(\mu + \tau)R_h$$

whose solution are respectively given as:

$$E_h(t) = E_h(0)\exp(-(\mu + \omega)t) \geq 0 \quad \forall t > 0$$
$$I_{hA}(t) = I_{hA}(0)\exp(-(\mu + \alpha)t) \geq 0 \quad \forall t > 0$$
$$I_h(t) = I_h(0)\exp(-(\mu + \delta + \gamma)t) \geq 0 \quad \forall t > 0$$
$$R_h(t) = R_h(0)\exp(-(\mu + \tau)t) \geq 0 \quad \forall t > 0$$

This demonstrates that the solution of all the model system's state variables (4.2.1) are non-negative. □

4.2.4 Invariant region

A population is said to be biologically meaningful if its global solution is confined within an invariant region Ω (Asamoah et al. [11] and Ega et al. [41]).

Theorem 4.2. *The solution set* $\{S_h(t), V_h(t), E_h(t), I_{hA}(t), I_h(t), R_h(t)\}$ *of the model equation (4.2.1) is confined to non-negative feasible region*

Ω.

Proof. Consider the feasible region:
$\Omega = \{S_h(t), V_h(t), E_h(t), I_{hA}(t), I_h(t), R_h(t)\} \in \mathbb{R}^6_+ \ \ \forall t \geq 0$. At any given time, equation (4.2.1) gives the total population as:

$$N_h = S_h + V_h + E_h + I_{hA} + I_h + R_h \tag{4.2.2}$$

Differentiating equation (4.2.2) with respect to t gives:

$$\frac{dN_h}{dt} = \frac{dS_h}{dt} + \frac{dV_h}{dt} + \frac{dE_h}{dt} + \frac{dI_{hA}}{dt} + \frac{dI_h}{dt} + \frac{dR_h}{dt} \tag{4.2.3}$$

We now substitute equation (4.2.1) into (4.2.3)

$$\begin{aligned}\frac{dN_h}{dt} &= [\pi + \tau R_h + \varphi V_n - (\lambda + \mu + \theta)S_h] + [\theta S_h - (\varphi + \mu)V_h] \\ &+ [\lambda S_h - (\omega + \mu)E_h] + [\omega(1-\epsilon)E_h - (\mu + \alpha)I_{hA}] \\ &+ [\omega\epsilon E_h + (1-\kappa)\alpha I_{hA} - (\mu + \delta + \gamma)I_h] \\ &+ [\kappa\alpha I_{hA} + \gamma I_h - (\mu + \tau)R_h]\end{aligned} \tag{4.2.4}$$

Expansion and simplification of equation (4.2.4) yields:

$$\frac{dN_h}{dt} = \pi - [S_h(t) + V_h(t) + E_h(t) + I_{hA} + I_h(t) + R_h(t)]\mu - \delta I_h \tag{4.2.5}$$

Substituting equation (4.2.2) to (4.2.5) gives:

$$\frac{dN_h}{dt} = \pi - \mu N_h - \delta I_h \leq \pi - \mu N_h \tag{4.2.6}$$

Evaluation of the equation (4.2.6) yields $N_h(t) \leq A\exp(-\mu t) + \frac{\pi}{\mu}$ which

upon substituting the initial conditions, the above equation becomes:

$$N_h(t) \leq \frac{\pi}{\mu} + \left(\frac{\pi - \mu N_{h0}}{\mu}\right) \exp(-\mu t) \tag{4.2.7}$$

where $N_{h0} = N_h(0)$

This implies that:

$$\limsup_{t\to\infty} \quad N_h(t) \leq \frac{\pi}{\mu}$$

This shows that the positive solutions of the model (4.2.1) are bounded. Hence, the system under consideration is well posed mathematically and epidemiologically. □

4.2.5 Analysis of Disease-free equilibrium(DFE),B_0

The disease-free equilibrium (DFE) denoted as B_0 is a steady-state solution in which there is no COVID-19 infection in the community. Consequently, apart from the susceptible and the vaccinated, all other compartments are equated to zero. Thus $E_h = I_{hA} = I_h = R_h = 0$ and $\frac{dS_h^0}{dt} = \frac{dV_h^0}{dt} = 0$. Equation (4.2.1) reduces to:

$$\begin{cases} \pi + \varphi V_h^0 - (\mu + \theta) S_h^0 = 0 \\ \theta S_h^0 - (\mu + \varphi) V_h^0 = 0 \end{cases} \tag{4.2.8}$$

Solving equation (4.2.8) simultaneously yields:

$$S_h^0 = \frac{\pi(\varphi + \mu)}{\mu(\varphi + \mu + \theta)} \quad and \quad V_h^0 = \frac{\pi\theta}{\mu(\varphi + \mu + \theta)} \tag{4.2.9}$$

Thus the DFE state, B_0, is given by:

$$\left(S_h^0, V_h^0, E_h^0, I_{hA}^0, I_h^0, R_h^0\right) = \left\{\frac{\pi(\varphi+\mu)}{\mu(\varphi+\mu+\theta)}, \frac{\pi\theta}{\mu(\varphi+\mu+\theta)}, 0, 0, 0, 0\right\} \tag{4.2.10}$$

4.2.6 Basic Reproduction Number R_0

The number of cases that one COVID-19 case typically creates during the infectious period in a community that is fully susceptible is known as the basic reproduction number (Tulu et al. [107]). We derive R_0 for our dynamical system using the next generation matrix technique (Diekmann [37]). The infected compartments are split up into two matrices using this method: F is the matrix that contains the components of the new infection, and V is the matrix that contains the elements of the transmission terms. The model equations (4.2.1) can be re-expressed as:

$$\frac{d\chi}{dt} = F(\chi) - V(\chi) \tag{4.2.11}$$

where χ represents the COVID-19 infected classes, $F(\chi) = \begin{pmatrix} \beta(I_h + \xi I_{hA})S_h \\ 0 \\ 0 \end{pmatrix}$

and $V(\chi) = \begin{pmatrix} (\omega+\mu)E_h \\ -\omega(1-\varepsilon)E_h + (\mu+\alpha)I_{hA} \\ -\omega\varepsilon E_h - (1-\kappa)\alpha I_{hA} + (\mu+\gamma+\delta)I_h \end{pmatrix}$

More explicitly, the above equation can be written as:

$$\begin{pmatrix} \dot{E}_h \\ \dot{I}_{hA} \\ \dot{I}_h \end{pmatrix} = \begin{pmatrix} \beta(I_h + \xi I_{hA})S_h \\ 0 \\ 0 \end{pmatrix} - \begin{pmatrix} (\omega+\mu)E_h \\ -\omega(1-\varepsilon)E_h + (\mu+\alpha)I_{hA} \\ -\omega\varepsilon E_h - (1-\kappa)\alpha I_{hA} + (\mu+\gamma+\delta)I_h \end{pmatrix}$$

Evaluation of the Jacobian of matrices F and V at the solution set $B_0 = \left\{\frac{\pi(\varphi+\mu)}{\mu(\varphi+\mu+\theta)}, \frac{\pi\theta}{\mu(\varphi+\mu+\theta)}, 0, 0, 0, 0\right\}$ are given by:

$$\mathcal{F} = \left(\frac{\partial \Phi_i}{\partial \chi_j}\right)|_{1\leq i,j\leq 3} = \begin{pmatrix} 0 & \frac{\beta\xi\pi(\mu+\varphi)}{\mu(\mu+\theta+\varphi)} & \frac{\beta\pi(\mu+\varphi)}{\mu(\mu+\theta+\varphi)} \\ 0 & 0 & 0 \\ 0 & 0 & 0 \end{pmatrix}$$

and

$$\mathcal{V} = \left(\frac{\partial \Psi_i}{\partial \chi_j}\right)|_{1\leq i,j\leq 3} = \begin{pmatrix} (\mu+\omega) & 0 & 0 \\ -\omega(1-\varepsilon) & (\alpha+\mu) & 0 \\ -\varepsilon\omega & -\alpha(1-\kappa) & (\mu+\gamma+\delta) \end{pmatrix}$$

The basic reproduction number is the spectral radius (The largest eigenvalue) of the next generation matrix $\mathcal{F}\mathcal{V}^{-1}$[37]. It can be shown that:

$$\mathcal{V}^{-1} = \begin{pmatrix} \frac{1}{\mu+\omega} & 0 & 0 \\ \frac{\omega(1-\varepsilon)}{(\alpha+\mu)(\omega+\mu)} & \frac{1}{\alpha+\mu} & 0 \\ \frac{\alpha\kappa\omega(1-\varepsilon)+\omega(\alpha+\mu\varepsilon)}{(\mu+\omega)(\alpha+\mu)(\mu+\delta+\mu)} & \frac{\alpha(1-\kappa)}{(\alpha+\mu)(\mu+\delta+\gamma)} & \frac{1}{\mu+\delta+\gamma} \end{pmatrix} \tag{4.2.12}$$

$$\mathcal{F}\mathcal{V}^{-1} = \begin{pmatrix} a_{11} & a_{12} & a_{13} \\ 0 & 0 & 0 \\ 0 & 0 & 0 \end{pmatrix}$$

Where:

$a_{11} = \frac{\pi\beta\omega(\mu+\varphi)\{\xi(1-\varepsilon)(\mu+\delta+\gamma)+\alpha(1-\kappa)+\varepsilon(\alpha\kappa+\mu)\}}{\mu(\mu+\omega)(\mu+\alpha)(\mu+\theta+\varphi)(\mu+\gamma+\delta)}$

$a_{12} = \frac{\pi\beta(\mu+\varphi)[\xi(\mu+\gamma+\delta)+\alpha(1-\kappa)]}{\mu(\mu+\alpha)(\mu+\gamma+\delta)(\mu+\theta+\varphi)}$

$a_{13} = \frac{\pi\beta(\mu+\varphi)}{\mu(\mu+\theta+\varphi)(\mu+\gamma+\delta)}$

The basic reproduction number plays a pivotal role when analyzing any epidemiological model. The effective reproduction of our dynamical system is thus:

$$R_\nu = \frac{\pi\beta\omega(\mu+\varphi)\{\xi(1-\varepsilon)(\mu+\delta+\gamma)+\alpha(1-k)+\varepsilon(\alpha\kappa+\mu)\}}{\mu(\mu+\omega)(\mu+\alpha)(\mu+\theta+\varphi)(\mu+\gamma+\delta)} \tag{4.2.13}$$

The threshold quantity above is also referred to as the control reproduction number,R_ν . This number measures the estimate of new COVID-19 cases generated by an index case (a single infected individual in an entirely susceptible population) in a community where Non-pharmaceutical measures and vaccination programmes have been set up. The administered vaccine is assumed to be imperfect.

For clear interpretation of the above reproduction number, we can separate this expression of R_ν as follows:

$$R_\nu = R_A + R_S \tag{4.2.14}$$

Where

$$R_A = \frac{\pi\beta\omega(\mu+\varphi)\xi(1-\varepsilon)}{\mu(\mu+\omega)(\mu+\alpha)(\mu+\theta+\varphi)} \tag{4.2.15}$$

R_A is the likelihood that the entire population will become asymptomatic after infection multiplied by the average number of exposed, asymptomatic, and vaccinated individuals.

$$R_S = \frac{\pi\beta\omega(\mu+\varphi)\{\alpha(1-k)+\varepsilon(\alpha\kappa+\mu)\}}{\mu(\mu+\omega)(\mu+\alpha)(\mu+\theta+\varphi)(\mu+\gamma+\delta)} \tag{4.2.16}$$

R_S is the likelihood that the entire population will have symptoms after contracting COVID-19 multiplied by the average number of exposed,

asymptomatic, symptomatic, and immunised individuals.
The analytically generated R_ν from our model thus points to the fact that the prevalence of COVID-19 in the general population may be fueled by the coexistence of both symptomatic and asymptomatic individuals.
The basic reproduction number can be generated from the equation (4.2.13) above by setting the parameters $\theta = \varphi = 0$, giving:

$$R_0 = \frac{\pi\beta\omega\{\xi(1-\varepsilon)(\mu+\delta+\gamma)+\alpha(1-\kappa)+\varepsilon(\alpha\kappa+\mu)\}}{\mu(\mu+\omega)(\mu+\alpha)(\mu+\gamma+\delta)} \tag{4.2.17}$$

R_0 represents the number of secondary infections generated by infectious person over his infectious period in absence of vaccination as a COVID-19 control strategy.

4.2.7 Local Stability of Disease-Free Equilibrium Point

We now explore the local and global stability of the model (4.2.1) around the disease-free equilibrium. The local and global stability of DFE gives a significant insight in any dynamical system in that a small influx of COVID-19 infection to a susceptible population does not lead to COVID-19 outbreak if $R_\nu < 1$.

Theorem 4.3. *The disease-free state, B_0, of the model system (4.2.1) is locally asymptotically stable(LAS) when $R_\nu < 1$ and unstable if $R_\nu > 1$.*

Proof. Consider the model system (4.2.1) and let:

$$g_1 = \frac{dS_h}{dt},\ g_2 = \frac{dV_h}{dt},\ g_3 = \frac{dE_h}{dt},\ g_4 = \frac{dI_{hA}}{dt},\ g_5 = \frac{dI_h}{dt},\ g_6 = \frac{dR_h}{dt} \tag{4.2.18}$$

The Jacobian of the system (4.2.1) is given by:

$$J_{B_0} = \begin{pmatrix} \frac{\partial g_1}{\partial S_h} & \frac{\partial g_1}{\partial V_h} & \frac{\partial g_1}{\partial E_h} & \frac{\partial g_1}{\partial I_{hA}} & \frac{\partial g_1}{\partial I_h} & \frac{\partial g_1}{\partial R_h} \\ \frac{\partial g_2}{\partial S_h} & \frac{\partial g_2}{\partial V_h} & \frac{\partial g_2}{\partial E_h} & \frac{\partial g_2}{\partial I_{hA}} & \frac{\partial g_2}{\partial I_h} & \frac{\partial g_2}{\partial R_h} \\ \frac{\partial g_3}{\partial S_h} & \frac{\partial g_3}{\partial V_h} & \frac{\partial g_3}{\partial E_h} & \frac{\partial g_3}{\partial I_{hA}} & \frac{\partial g_3}{\partial I_h} & \frac{\partial g_3}{\partial R_h} \\ \frac{\partial g_4}{\partial S_h} & \frac{\partial g_4}{\partial V_h} & \frac{\partial g_4}{\partial E_h} & \frac{\partial g_4}{\partial I_{hA}} & \frac{\partial g_4}{\partial I_h} & \frac{\partial g_4}{\partial R_h} \\ \frac{\partial g_5}{\partial S_h} & \frac{\partial g_5}{\partial V_h} & \frac{\partial g_5}{\partial E_h} & \frac{\partial g_5}{\partial I_{hA}} & \frac{\partial g_5}{\partial I_h} & \frac{\partial g_5}{\partial R_h} \\ \frac{\partial g_6}{\partial S_h} & \frac{\partial g_6}{\partial V_h} & \frac{\partial g_6}{\partial E_h} & \frac{\partial g_6}{\partial I_{hA}} & \frac{\partial g_6}{\partial I_h} & \frac{\partial g_6}{\partial R_h} \end{pmatrix} \tag{4.2.19}$$

At DFE state the Jacobian above becomes:

$$J_{B_0} = \begin{pmatrix} -(\mu+\theta) & \varphi & 0 & -\frac{\beta\xi(\varphi+\mu)\pi}{\mu(\mu+\varphi+\theta)} & -\frac{\beta(\varphi+\mu)\pi}{\mu(\mu+\varphi+\theta)} & \tau \\ \theta & -(\mu+\varphi) & 0 & 0 & 0 & 0 \\ 0 & 0 & -(\mu+\omega) & \frac{\beta\xi\pi(\varphi+\mu)}{\mu(\mu+\varphi+\theta)} & \frac{\beta\pi(\varphi+\mu)}{\mu(\mu+\varphi+\theta)} & 0 \\ 0 & 0 & \omega(1-\epsilon) & -(\alpha+\mu) & 0 & 0 \\ 0 & 0 & \epsilon\omega & \alpha(1-\kappa) & -(\mu+\gamma+\delta) & 0 \\ 0 & 0 & 0 & \alpha\kappa & \gamma & -(\mu+\tau) \end{pmatrix} \tag{4.2.20}$$

From the Jacobian matrix equation (4.2.20), we make use of the trace-determinant method so as to prove the local stability of B_0. For local asymptotic stability, the following Routh-Hurwitz conditions have to be satisfied:

(i) $\mathrm{Tr}J_{B_0} < 0$

(ii) $\mathrm{Det}J_{B_0} > 0$

Thus:

$$\begin{cases} TrJ_{B_0} = -(\mu+\theta+\mu+\varphi+\mu+\omega+\mu+\alpha+\mu+\gamma+\delta+\mu+\tau) \\ \quad = -(6\mu+\theta+\varphi+\omega+\alpha+\gamma+\delta+\tau) < 0 \end{cases} \tag{4.2.21}$$

Due to the complexity of the matrix space involved, we utilize Python programming language to determine the determinant of $J(B_0)$. This gives:

$$\begin{cases} DetJ_{B_0} = -\mu(\mu+\tau)(\mu+\theta+\varphi)\{-(\mu+\omega)(\alpha+\mu)(\mu+\gamma+\delta) \\ +\frac{\beta\pi\omega(\varphi+\mu)}{\mu(\mu+\varphi+\theta)}[\xi(1-\varepsilon)(\mu+\gamma+\delta)+\alpha(1-\kappa)+\varepsilon(\alpha\kappa+\mu)]\} \end{cases} \tag{4.2.22}$$

Through further simplification and utilization of equation (4.2.13), equation (4.2.23) becomes:

$$DetJ_{B_0} = \mu(\mu+\tau)(\mu+\theta+\varphi)(\mu+\omega)(\mu+\alpha)(\mu+\gamma+\delta)(1-R_\nu) \tag{4.2.23}$$

Where R_ν is the effective reproduction number.
For determinant $DetJ(B_0) > 0$, it follows that:

$$DetJ_{B_0} = [\mu(\mu+\tau)(\mu+\theta+\varphi)(\mu+\omega)(\mu+\alpha)(\mu+\gamma+\delta)(1-R_\nu)] > 0 \tag{4.2.24}$$

If and only if $R_\nu < 1$. □

This proves theorem (4.3) as its clear that the DFE of COVID-19 model (4.2.1) is locally asymptotically stable if $R_\nu < 1$. The epidemiological implication of the above theorem is that, COVID-19 can be wiped out

from the community if $R_\nu < 1$ and if the initial size of the infected persons is in the region of attraction of DFE (4.2.10). DFE is unstable when $R_\nu > 1$ and the implication of this is that the possibility of COVID-19 invasion cannot be ruled out.

4.2.8 Global stability of DFE

Theorem 4.4. *The COVID-19-free equilibrium point B_0 of model (4.2.1) is globally asymptotically stable in the region Ω if $R_\nu \leq 1$ and unstable if $R_\nu > 1$.*

Proof. We determine the global stability of COVID-19 free equilibrium point B_0 by utilizing Lyapunov function approach [11] and [122]. Let L be a Lyapunov function with positive constants c_1, c_2, c_3 and c_4 such that:

$$\begin{cases} L = (S_h - S_h^0 - S_h^0 \ln \frac{S_h}{S_h^0}) + (V_h - V_h^0 - V_h^0 \ln \frac{V_h}{V_h^0}) + c_1 E_h \\ \quad + c_2 I_{hA} + c_3 I_h + c_4 R_h \end{cases} \tag{4.2.25}$$

Differentiating the above Lyapunov equation with respect to time gives:

$$\begin{cases} \frac{dL}{dt} = (1 - \frac{S_h^0}{S_h}) \frac{dS_h}{dt} + (1 - \frac{V_h^0}{V_h}) \frac{dV_h}{dt} + c_1 \frac{dE_h}{dt} \\ \quad + c_2 \frac{dI_{hA}}{dt} + c_3 \frac{dI_h}{dt} + c_4 \frac{dR_h}{dt} \end{cases} \tag{4.2.26}$$

Substituting equation (4.2.1) into (4.2.26) yields:

$$\begin{cases} \frac{dL}{dt} = (1 - \frac{S_h^0}{S_h})[\pi + \varphi V_h + \tau R_h - \lambda S_h - (\mu + \theta)S_h] \\ \quad +(1 - \frac{V_h^0}{V_h})[\theta S_h - (\mu + \varphi)V_h] + c_1[\lambda S_h - (\mu + \omega)E_h] \\ \quad +c_2[(1-\epsilon)\omega E_h - (\mu + \alpha)I_{hA}] \quad + c_3[\epsilon\omega E_h + (1-\kappa)\alpha I_{hA} - (\mu + \gamma + \delta)I_h] \\ \quad +c_4[\alpha\kappa I_{hA} + \gamma I_h - (\mu + \tau)R_h] \end{cases} \tag{4.2.27}$$

Suppose $S_h \leq S_h^0 = \frac{\pi(\mu+\varphi)}{\mu(\mu+\theta+\varphi)}$ and $V_h \leq V_h^0 = \frac{\pi\theta}{\mu(\mu+\theta+\varphi)}$, and upon substituting $\lambda = \beta(\xi I_{hA} + I_h)$ to equation (4.2.27) yields:

$$\begin{cases} \frac{dL}{dt} \leq c_1[\frac{\pi(\mu+\varphi)\beta(\xi I_{hA}+I_h)}{\mu(\mu+\theta+\varphi)} - (\mu + \omega)E_h] \\ \quad +c_2[(1-\epsilon)\omega E_h - (\mu + \alpha)I_{hA}] \\ \quad +c_3[\epsilon\omega E_h + (1-\kappa)\alpha I_{hA} - (\mu + \gamma + \delta)I_h] \\ \quad +c_4[\alpha\kappa I_{hA} + \gamma I_h - (\mu + \tau)R_h] \end{cases} \tag{4.2.28}$$

The above equation implies that:

$$\begin{cases} \frac{dL}{dt} \leq [-(\mu + \omega)c_1 + \omega(1-\epsilon)c_2 + \epsilon\omega c_3]E_h \\ \quad +[\frac{\pi\beta\xi(\mu+\varphi)}{\mu(\mu+\theta+\varphi)}c_1 - (\mu + \alpha)c_2 + \alpha(1-\kappa)c_3 + \alpha\kappa c_4]I_{hA} \\ \quad +[\frac{\pi\beta(\mu+\varphi)}{\mu(\mu+\theta+\varphi)}c_1 - (\mu + \gamma + \delta)c_3 + \gamma c_4]I_h - (\mu + \tau)c_5 R_h \end{cases} \tag{4.2.29}$$

Equating the coefficients of E_h, I_{hA}, I_h and R_h to zero gives:

$c_1 = (\mu + \gamma + \delta)$, $c_2 = \frac{\mu(\mu+\omega)(\mu+\theta+\varphi)(\mu+\gamma+\delta) - \pi\epsilon\omega\beta(\mu+\varphi)}{\mu\omega(1-\epsilon)(\mu+\theta+\varphi)}$

$c_3 = \frac{\beta\pi(\mu+\varphi)}{\mu(\mu+\theta+\varphi)}$, $c_4 = c_5 = 0$

We thus obtain:

$$\frac{dL}{dt} \leq \frac{(\mu + \omega)(\mu + \alpha)(\mu + \gamma + \delta)}{\omega(1-\epsilon)}(R_\nu - 1)I_{hA} \tag{4.2.30}$$

Its worth noting that: $\frac{dL}{dt} \leq 0$, if $R_\nu \leq 1$ and $\frac{dL}{dt} = 0$ iff $I_{hA} = 0$. Thus, plugging $E_h = I_{hA} = I_h = R_h = 0$ into equation (4.2.1) points to the fact that $S_h(t) \to \frac{\pi(\mu+\varphi)}{\mu(\mu+\theta+\varphi)}$ and $V_h(t) \to \frac{\pi\theta}{\mu(\mu+\theta+\varphi)}$ as $t \to \infty$. Thus, the biggest invariant set that is compact in $\{(S_h, V_h, E_h, I_{hA}, I_h, R_h) \in \Omega; \frac{dL}{dt} \leq 0\}$, is the singleton set B_0. Thus from LaSalle's invariance principle [78], we make the conclusion that the COVID-19 free equilibrium point is globally asymptotically stable in Ω if $R_\nu < 1$.

The explanation above points to the fact that an infection with COVID-19 can be abased if and only if $R_\nu < 1$.

□

4.2.9 COVID-19 Endemic Equilibrium Point(CEEP)

We endeavor to examine whether endemic equilibrium B_e exists in this subsection.

Theorem 4.5. *If $R_\nu > 1$, there exists a unique endemic equilibrium $B_e = (S_h^*, V_h^*, E_h^*, I_{hA}^*, I_h^*, R_h^*)$ of the model (4.2.1).The endemic equilibrium does not exist for $R_\nu < 1$.*

Proof. We set the right side of the system of equations (4.2.1) to zero in

order to determine the existence of endemic equilibrium.

$$\begin{cases} \pi + \tau R_h^* + \varphi V_h^* - \beta(I_h^* + \xi I_{hA}^*)S_h^* - (\mu+\theta)S_h^* = 0 \\ \theta S_h^* - (\varphi+\mu)V_h^* = 0 \\ \omega(1-\varepsilon)E_h^* - (\mu+\alpha)I_{hA}^* = 0 \\ \beta(I_h^* + \xi I_{hA}^*)S_h^* - (\omega+\mu)E_h^* = 0 \\ \omega\varepsilon E_h^* + (1-\kappa)\alpha I_{hA}^* - (\mu+\delta+\gamma)I_h^* = 0 \\ \kappa\alpha I_{hA}^* + \gamma I_h^* - (\mu+\delta+\gamma)R_h^* = 0 \end{cases} \tag{4.2.31}$$

Solution to the above system gives rise to the following:

$S_h^* = \frac{\pi(\mu+\varphi)}{\mu(\mu+\theta+\varphi)R_\nu}$

$V_h^* = \frac{\pi\theta}{\mu(\mu+\theta+\varphi)R_\nu}$

$E_h^* = \frac{\pi\Phi_1\Phi_2\Phi_3(R_\nu-1)}{\{(\mu+\omega)\Phi_1\Phi_2\Phi_3-\tau\omega(\Phi_3\Phi_5+\gamma\Phi_4)\}R_\nu}$

$I_{hA}^* = \frac{\pi\omega\Phi_2\Phi_3\Phi_5(R_\nu-1)}{\alpha\kappa\{(\mu+\omega)\Phi_1\Phi_2\Phi_3-\tau\omega(\Phi_3\Phi_5+\gamma\Phi_4)\}R_\nu}$

$I_h^* = \frac{\pi\omega\Phi_4\Phi_2(R_\nu-1)}{\{(\mu+\omega)\Phi_1\Phi_2\Phi_3-\tau\omega(\Phi_3\Phi_5+\gamma\Phi_4)\}R_\nu}$

$R_h^* = \frac{\pi\omega(R_\nu-1)(\Phi_3\Phi_5+\gamma\Phi_4)}{\{(\mu+\omega)\Phi_1\Phi_2\Phi_3-\tau\omega(\Phi_3\Phi_5+\gamma\Phi_4)\}R_\nu}$

where $\Phi_1 = (\mu+\alpha)$, $\Phi_2 = (\mu+\tau)$, $\Phi_3 = (\mu+\delta+\gamma)$, $\Phi_4 = \alpha(1-\kappa)+\varepsilon(\alpha\kappa+\mu)$ and $\Phi_5 = \alpha\kappa(1-\varepsilon)$.

Substitution of the values of $\Phi_1, \Phi_2.\Phi_3, \Phi_4$ and Φ_5 in $\{(\mu+\omega)\Phi_1\Phi_2\Phi_3 - \tau\omega(\Phi_3\Phi_5+\gamma\Phi_4)\}$ and then simplification yields:

$\{(\mu+\omega)\Phi_1\Phi_2\Phi_3-\tau\omega(\Phi_3\Phi_5+\gamma\Phi_4)\} = \mu^2\{\Phi_1(\omega+\tau+\Phi_3)+\omega\tau+(\delta+\gamma)(\omega+\tau)\} + \tau\omega\alpha(\mu+\delta)(\varepsilon\kappa+(1-\kappa)) + \mu\omega(\tau\gamma(1-\varepsilon)+\delta(\alpha+\tau)) + \mu\alpha\gamma(\omega+\tau)$.

Since $\varepsilon < 1$ and also $\kappa < 1$, $\{(\mu+\omega)\Phi_1\Phi_2\Phi_3 - \tau\omega(\Phi_3\Phi_5+\gamma\Phi_4)\} > 0$.

It can therefore be observed that if $R_\nu = 1$, we obtain the COVID-19 free equilibrium point. The unique endemic equilibrium in Ω exists if $E_h^* > 0$,

$I^*_{Ah} > 0$, $I^*_h > 0$ and $R^*_h > 0$. This is actualized if and only if $R_\nu > 1$ and no endemic equilibrium when $R_\nu < 1$. □

4.2.10 Bifurcation of the Model

Transcritical bifurcation is synonymous to most disease transmission dynamic models. However, backward bifurcation is known to occur in models with vaccination class, a scenario in which the DFE and stable endemic equilibrium coexist when the classical epidemiological dictate of bringing down R_ν below a unit so as to curtail disease propagation in the population has been met. In this subsection, we establish that the occurrence of several COVID-19 persistent equilibria for the case when $R_\nu < 1$ results from a backward bifurcation. We examine the characteristics of bifurcation by utilizing Theorem 4.1 from Castilo-Chavez et al. [26] which is based on the center manifold theory (Guckenheimer [47]). The dynamics of the system on the centre manifold are represented by two significant coefficients, let's say a and b. These coefficients provide us information about the bifurcation trend. The bifurcation is forward if $a < 0$ and $b > 0$; reverse if $a > 0$ and $b > 0$.

Theorem 4.6. *The endemic equilibrium point, based on the Theorem 4.1 by Castilo-Chavez et al. [26], is locally asymptotically stable for $R_\nu > 1$ (but near 1).*

Proof. For simplicity and ease in algebraic manipulations, we re-write the state variables of our model (4.2.1) as follows: $S_h = x_1, V_h = x_2, E_h =$

$x_3, I_{hA} = x_4, I_h = x_5$ and $R_h = x_6$. We further define equation $\frac{dX}{dt} = F(x)$ where $X = (x_1, x_2, x_3, x_4, x_5, x_6)$ and $F = (f_1, f_2, f_3, f_3, f_4, f_5, f_6)$.Thus:

$$\begin{cases} \frac{dx_1}{dt} = f_1 = \pi + \varphi x_2 + \tau x_6 - \beta(\xi x_4 + x_5)x_1 - (\mu + \theta)x_1 \\ \frac{dx_2}{dt} = f_2 = \theta x_1 - (\mu + \varphi)x_3 \\ \frac{dx_3}{dt} = f_3 = \beta(\xi x_4 + x_5)x_1 - (\mu + \omega)x_3 \\ \frac{dx_4}{dt} = f_4 = \omega(1 - \epsilon)x_3 - (\mu + \alpha)x_4 \\ \frac{dx_5}{dt} = f_5 = \omega\epsilon x_3 + (1 - k)\alpha x_4 - (\mu + \delta + \gamma)x_5 \\ \frac{dx_6}{dt} = f_6 = \kappa\alpha x_4 + \gamma x_5 - (\mu + \tau)x_6 \end{cases} \tag{4.2.32}$$

We choose the rate of transmission β as a bifurcation parameter when $R_\nu = 1$ thus:

$$\beta = \beta^* = \frac{\mu(\mu + \omega)(\mu + \alpha)(\mu + \theta + \varphi)(\mu + \delta + \gamma)}{\pi\omega(\mu + \varphi)\{\xi(1 - \epsilon) + \alpha(1 - \kappa) + \epsilon(\alpha\kappa + \mu)\}} \tag{4.2.33}$$

Let the Jacobian at B_0 when $\beta = \beta^*$ be denoted by B_0^*, then;

$$\begin{pmatrix} -(\mu + \theta) & \varphi & 0 & -\frac{\beta^*\xi(\varphi+\mu)\pi}{\mu(\mu+\varphi+\theta)} & -\frac{\beta^*(\varphi+\mu)\pi}{\mu(\mu+\varphi+\theta)} & \tau \\ \theta & -(\mu + \varphi) & 0 & 0 & 0 & 0 \\ 0 & 0 & -(\mu + \omega) & \frac{\beta^*\xi\pi(\mu+\varphi)}{\mu(\mu+\varphi+\theta)} & \frac{\beta^*\pi(\mu+\varphi)}{\mu(\mu+\varphi+\theta)} & 0 \\ 0 & 0 & \omega(1 - \epsilon) & -(\alpha + \mu) & 0 & 0 \\ 0 & 0 & \epsilon\omega & \alpha(1 - \kappa) & -(\mu + \gamma + \delta) & 0 \\ 0 & 0 & 0 & \alpha\kappa & \gamma & -(\mu + \tau) \end{pmatrix} \tag{4.2.34}$$

Some of the eigenvalues of the matrix B_0^* above are $\lambda_1 = 0, \lambda_2 = -\mu, \lambda_3 = -(\mu+\tau)$ and $\lambda_4 = -(\mu+\theta+\varphi)$. It can be proved that the two remaining eigenvalues have a non-positive real part. It is thus imperative that B_0^*

has a non-hyperbolic equilibrium when $\beta = \beta^*$. We can therefore utilize the center manifold theory Castilo-Chavez et al. [26] to establish the the local stability of endemic equilibrium. The presence of a simple (zero) eigenvalue is an indication that the Jacobian $J(B_0^*)$ has respectively a right eigenvector given by $\mathbf{W} = (w_1, w_2, w_3, w_4, w_5, w_6)^T$ and a left eigenvector $\mathbf{V} = (v_1, v_2, v_3, v_4, v_5, v_6)$.

$$(\mathbf{B}_0^* - \lambda \mathbf{I})(\mathbf{W}) = \mathbf{0} \tag{4.2.35}$$

Where $\mathbf{I}$ is a 6×6 identity matrix.

Evaluation of w_1, w_2, w_3, w_4, w_5 and w_6 for $\lambda = 0$ gives:
$w_1 = -\frac{(\mu+\varphi)w_6(\frac{A}{w_6}-\tau)}{\mu(\mu+\theta+\varphi)}, w_2 = -\frac{\theta w_6(\frac{A}{w_6}-\tau)}{\mu(\mu+\theta+\varphi)}$
where $A = \frac{(\mu+\omega)(\mu+\alpha)\{\xi(1-\varepsilon)(\mu+\gamma+\delta)+\alpha(1-\kappa)+\epsilon(\mu+\alpha\kappa)\}}{\xi(1-\epsilon)+\alpha(1-\kappa)+\epsilon(\mu+\alpha\kappa)}$
$w_3 = \mu + \alpha, w_4 = \omega(1-\epsilon), w_5 = \frac{\omega\{\epsilon(\mu+\alpha\kappa)+\alpha(1-\kappa)\}}{\mu+\gamma+\delta}, w_6 = \alpha\kappa(1-\epsilon)\omega + \gamma w_5$
Furthermore, the the components of the left eigenvector (corresponding to the eigenvalue $\lambda = 0$), $\mathbf{V} = (v_1, v_2, v_3, v_4, v_5, v_6)$, must satisfy the equations $\mathbf{V.J(B)} = 0$ and $\mathbf{V.W}=\mathbf{1}$. We consider:

$$(\mathbf{B}_0^{*T} - \lambda \mathbf{I})(\mathbf{V}) = \mathbf{0} \tag{4.2.36}$$

Where matrix $\mathbf{B}_0^{*T}$ is defined as:

$$\begin{pmatrix} -(\mu+\theta) & \theta & 0 & 0 & 0 & 0 \\ \varphi & -(\mu+\varphi) & 0 & 0 & 0 & 0 \\ 0 & 0 & -(\mu+\omega) & \omega(1-\epsilon) & \epsilon\omega & 0 \\ -\frac{\beta^*\xi(\varphi+\mu)\pi}{\mu(\mu+\varphi+\theta)} & 0 & \frac{\beta^*\xi(\mu+\varphi)\pi}{\mu(\mu+\varphi+\theta)} & -(\alpha+\mu) & \alpha(1-\epsilon) & \alpha\kappa \\ -\frac{\beta^*(\varphi+\mu)\pi}{\mu(\mu+\varphi+\theta)} & 0 & \frac{\beta^*(\mu+\varphi)\pi}{\mu(\mu+\varphi+\theta)} & 0 & -(\mu+\gamma+\delta) & \gamma \\ \tau & 0 & 0 & 0 & 0 & -(\mu+\tau) \end{pmatrix} \tag{4.2.37}$$

Evaluation for components of $\mathbf{V}$ yields:

$v_1 = v_2 = v_6 = 0$, $v_3 = \frac{\omega\{\xi(1-\epsilon)+\alpha(1-\kappa)+\epsilon(\mu+\alpha\kappa)\}v_5}{(\mu+\omega)(\alpha+\alpha)}$, $v_4 = \frac{\{\xi+\alpha(1-\kappa)\}v_5}{\mu+\alpha}$ and $v_5 = \frac{1}{c_1+c_2+w_5}$ where $c_1 = \frac{\omega\{\xi(1-\epsilon)+\alpha(1-\kappa)+\epsilon(\mu+\alpha\kappa)\}}{\mu+\omega}$ and $c_2 = \frac{\omega(1-\epsilon)\{\xi+\alpha(1-\kappa)\}}{\mu+\alpha}$

We now Utilize Theorem 4.1 of [26] to calculate the bifurcation constants a and b where:

$$a = \sum_{k,i,j=1}^{6} v_k w_i w_j \frac{\partial^2 f_k}{\partial x_i \partial x_j}(B_0, \beta^*)$$

$$b = \sum_{k,i,j=1}^{6} v_k w_i \frac{\partial^2 f_k}{\partial x_i \partial \beta}(B_0, \beta^*)$$

To evaluate a, we compute the non-zero second partial derivatives for the linearized system (4.2.32). It is evident that we do not have to compute the partial derivatives of f_1, f_2 and f_3 since $v_1 = v_2 = v_6 = 0$.

We thus consider the following:

$$\begin{cases} v_3 w_1 w_4 \frac{\partial^2 f_3}{\partial x_1 \partial x_4} = -v_3 \frac{(\mu+\varphi) w_6 \{\frac{A}{w_6} - \tau\}}{\mu(\mu+\theta+\varphi)} w_4 \beta^* \xi \\ v_3 w_4 w_1 \frac{\partial^2 f_3}{\partial x_4 \partial x_1} = -v_3 w_4 \frac{(\mu+\varphi) w_6 \{\frac{A}{w_6} - \tau\}}{\mu(\mu+\theta+\varphi)} \beta_1^* \xi \\ v_3 w_1 w_5 \frac{\partial^2 f_3}{\partial x_1 \partial x_5} = -v_3 \frac{(\mu+\varphi) w_6 \{\frac{A}{w_6} - \tau\}}{\mu(\mu+\theta+\varphi)} w_5 \beta_1^* \\ v_3 w_5 w_1 \frac{\partial^2 f_3}{\partial x_1 \partial x_5} = -v_3 w_5 \frac{(\mu+\varphi) w_6 \{\frac{A}{w_6} - \tau\}}{\mu(\mu+\theta+\varphi)} \beta_1^* \end{cases} \tag{4.2.38}$$

The sum of the equations in (4.2.38) gives the value of a as:

$$a = -2v_3 \frac{(\mu+\varphi) w_6 \{\frac{A}{w_6} - \tau\}}{\mu(\mu+\theta+\varphi)} \beta_1^* (\xi w_4 + w_5) \tag{4.2.39}$$

To determine b, we let $k = 3, i = 4, 5$. This because when $k = 1, 2, 4, 5, 6$ and $i = 1, 2, 3, 4, 5$, the second derivative of f_k with respect to x_i and β_1^* at DFE gives zero values. Thus we have:

$$\begin{cases} v_3 w_4 \frac{\partial^2 f_3}{\partial x_4 \partial \beta_1^*} = v_3 w_4 \frac{\pi(\mu+\varphi)}{\mu(\mu+\theta+\varphi)} \\ v_3 w_5 \frac{\partial^2 f_3}{\partial x_5 \partial \beta_1^*} = v_3 w_5 \xi \frac{\pi(\mu+\varphi)}{\mu(\mu+\theta+\varphi)} \end{cases} \tag{4.2.40}$$

The sum of the equations in (4.2.40) gives the value of b as:

$$b = v_3 \frac{\pi(\mu+\varphi)}{\mu(\mu+\theta+\varphi)} (w_4 \xi + w_5) > 0 \tag{4.2.41}$$

None negativity of b implies that direction of bifurcation at $R_\nu = 1$ is entirely determined by the sign of a which depends on the re-infection rate τ. For backward bifurcation,

$$\tau > \frac{(\mu+\gamma+\delta)(\mu+\omega)(\mu+\alpha)(\xi(1-\epsilon)\omega + w_5)}{(\xi(1-\epsilon)\omega + (\mu+\gamma+\delta)w_5)(\alpha\kappa(1-\epsilon)\omega + \gamma w_5)} \tag{4.2.42}$$

□

Theorem 4.7. *The system (4.2.1) undergoes backward bifurcation at* $R_\nu = 1$ *whenever inequality (4.2.42) holds.*

The above theorem is in conformity with study by Kassa et.al. [58] that suggested that backward bifurcation is possible if the recovered individuals do not gain permanent immunity to infections regardless of the COVID-19 variant. Moreover, it is note worthy that for the case where the recovered persons acquires permanent immunity to COVID-19 infection (i.e $\tau = 0$), the bifurcation coefficient a becomes:

$$a = -2v_3 \frac{(\mu+\omega)(\mu+\alpha)(\mu+\varphi)(\mu+\gamma+\delta)(\xi(1-\epsilon)\omega+w_5)}{\mu(\mu+\theta+\varphi)[\xi(1-\epsilon)\omega+(\mu+\gamma+\delta)w_5]}\beta^*(\xi w_4+w_5) < 0$$

This rules out the occurrence of backward bifurcation but instead, forward bifurcation sets in. Hence we obtain the following conclusion:

Theorem 4.8. *(Local stability of endemic equilibrium). The unique endemic equilibrium* B_e *of model 1 is locally asymptotically stable (LAS) if* $R_\nu > 1$.

4.2.11 Global stability of COVID-19 endemic equilibrium

Theorem 4.9. *The unique endemic equilibrium* B_e *of the model (4.2.1) is globally asymptotically stable in* Ω *whenever* $R_\nu > 1$.

Proof. Let c_1, c_2, c_3, c_4, c_5 and c_6 be non-negative constants and with no loss of generality, we consider a special case of our system where $\varphi = 0$

and $\tau = 0$. We consider a Lyapunov function defined as:

$$L = c_1L_1 + c_2L_2 + c_3L_3 + c_4L_4 + c_5L_5 + c_6L_6$$

where

$$\begin{cases} L_1 = S_h^*.g\left(\frac{S_h}{S_h^*}\right),\ L_2 = V_h^*.g\left(\frac{V_h}{V_h^*}\right),\ L_3 = E_h^*.g\left(\frac{E_h}{E_h^*}\right), \\ L_4 = I_{hA}^*.g\left(\frac{I_{hA}}{I_{hA}^*}\right),\ L_5 = I_h^*.g\left(\frac{I_h}{I_h^*}\right),\ L_6 = R_h^*.g\left(\frac{R_h}{R_h^*}\right). \end{cases} \tag{4.2.43}$$

and that $g(x) = x - 1 - lnx \geq g(1) = 0$ for any $x > 0$

Differentiating L with respect to t gives:

$$\begin{cases} \frac{dL}{dt} = c_1\left(1 - \frac{S_h^*}{S_h}\right)\left\{\pi - \beta(\xi I_{hA} + I_h)S_h - (\mu + \theta)S_h\right\} \\ \quad +c_2\left(1 - \frac{V_h^*}{V_h}\right)\left\{\theta S_h - \mu V_h\right\} \\ \quad +c_3\left(1 - \frac{E_h^*}{E_h}\right)\left\{\beta(\xi I_{hA} + I_h)S_h - (\mu + \omega)E_h\right\} \\ \quad +c_4\left(1 - \frac{I_{hA}^*}{I_{hA}}\right)\left\{\omega(1-\varepsilon)E_h - (\mu + \alpha)I_{hA}\right\} \\ \quad +c_5\left(1 - \frac{I_h^*}{I_h}\right)\left\{\omega\varepsilon E_h + (1-\kappa)\alpha)I_{hA} - (\mu + \delta + \gamma)I_h\right\} \\ \quad +c_6\left(1 - \frac{R_h^*}{R_h}\right)\left\{\kappa\alpha I_{hA} + \gamma I_h - \mu R_h\right\} \end{cases} \tag{4.2.44}$$

At steady endemic equilibrium,

$$\begin{cases} \pi = \beta(\xi I_{hA}^* + I_h^*)S_h^* + (\mu + \theta)S_h^*,\ \theta = \frac{\mu V_h^*}{S_h^*}, \\ (\mu + \omega) = \frac{\beta(\xi I_{hA}^* + I_h^*)S_h^*}{E_h^*},\ (\mu + \alpha) = \frac{\omega(1-\varepsilon)E_h^*}{I_{hA}^*}, \\ (\mu + \delta + \gamma) = \frac{\omega\varepsilon E_h^* + (1-\kappa)\alpha I_{hA}^*}{I_h^*},\ \mu = \frac{\kappa\alpha I_{hA}^* + \gamma I_h}{R_h^*}. \end{cases} \tag{4.2.45}$$

Substituting (4.2.45) into (4.2.44) gives

$$\begin{cases} \frac{dL}{dt} = c_1\left(1-\frac{S_h^*}{S_h}\right)\left\{\beta\xi S_h^* I_{hA}^*\left(1-\frac{S_h I_{hA}}{S_h^* I_{hA}^*}\right)+\beta S_h^* I_h^*\left(1-\frac{S_h I_h}{S_h^* I_h^*}\right)\right. \\ \quad \left.+(\mu+\theta)S_h^*\left(1-\frac{S_h}{S_h^*}\right)\right\}+c_2\left(1-\frac{V_h^*}{V_h}\right)\left\{\mu V_h^*\left(\frac{S_h}{S_h^*}-\frac{V_h}{V_h^*}\right)\right\} \\ \quad +c_3\left(1-\frac{E_h^*}{E_h}\right)\left\{\beta\xi S_h^* I_{hA}^*\left(\frac{S_h I_{hA}}{S_h^* I_{hA}^*}-\frac{E_h}{E_h^*}\right)+\beta S_h^* I_h^*\left(\frac{S_h I_h}{S_h^* I_h^*}-\frac{E_h}{E_h^*}\right)\right\} \\ \quad +c_4\left(1-\frac{I_{hA}^*}{I_{hA}}\right)\left\{\omega(1-\varepsilon)E_h^*\left(\frac{E_h}{E_h^*}-\frac{I_{hA}}{I_{hA}^*}\right)\right\} \\ \quad +c_5\left(1-\frac{I_h^*}{I_h}\right)\left\{\omega\varepsilon\left(\frac{E_h}{E_h^*}-\frac{I_h}{I_h^*}\right)+(1-\kappa)\alpha I_{hA}^*\left(\frac{I_{hA}}{I_h^*}-\frac{I_h}{I_h^*}\right)\right\} \\ \quad +c_6\left(1-\frac{R_h^*}{R_h}\right)\left\{\kappa\alpha I_{hA}^*\left(\frac{I_{hA}}{I_{hA}^*}-\frac{R_h}{R_h^*}\right)+\gamma I_h^*\left(\frac{I_h}{I_h^*}-\frac{R_h}{R_h^*}\right)\right\} \end{cases} \tag{4.2.46}$$

We introduce the notations: $a_1 = \frac{S_h}{S_h^*}$, $a_2 = \frac{V_h}{V_h^*}$, $a_3 = \frac{E_h}{E_h^*}$,
$a_4 = \frac{I_{hA}}{I_{hA}^*}$, $a_5 = \frac{I_h}{I_h^*}$, $a_6 = \frac{R_h}{R_h^*}$.
Equation (4.2.46) upon substitution and reorganization becomes:

$$\begin{cases} \frac{dL}{dt} = -\frac{c_1}{a_1}(\mu+\theta)(a_1-1)^2 + c_1\beta\xi S_h^* I_{hA}^*\left\{\left(1-\frac{1}{a_1}\right)(1-a_1a_4)\right. \\ \quad \left.+\frac{c_3}{c_1}\left(1-\frac{1}{a_3}\right)(a_1a_4-a_3)\right\}+c_1\beta S_h^* I_h^*\left\{\left(1-\frac{1}{a_1}\right)(1-a_1a_5)\right. \\ \quad \left.+\frac{c_3}{c_1}\left(1-\frac{1}{a_3}\right)(a_1a_5-a_3)\right\}+c_2\mu V_h^*\left\{\left(1-\frac{1}{a_2}\right)(a_1-a_2)\right\} \\ \quad +c_4\omega(1-\varepsilon)E_h^*\left\{\left(1-\frac{1}{a_4}\right)(a_3-a_4)\right\}+c_5\omega\varepsilon E_h^* \\ \quad +\left\{\left(1-\frac{1}{a_5}\right)(a_3-a_5)\right\}+c_5(1-\kappa)\alpha I_{hA}^*\left\{\left(1-\frac{1}{a_5}\right)(a_4-a_5)\right\} \\ \quad +c_6\kappa\alpha I_{hA}^*\left\{\left(1-\frac{1}{a_6}\right)(a_4-a_6)\right\}+c_6\gamma I_h^*\left\{\left(1-\frac{1}{a_6}\right)(a_5-a_6)\right\} \end{cases} \tag{4.2.47}$$

With further simplification and letting $c_1 = c_3$ (both being arbitrary non-negative constants), equation (4.2.47) becomes:

$$\begin{cases} \frac{dL}{dt} = -\frac{c_1}{a_1}(\mu+\theta)(a_1-1)^2 + c_1\beta\xi S_h^* I_{hA}^* \Big\{2 - \frac{1}{a_1} + a_4 - a_3 - \frac{a_1 a_4}{a_3}\Big\} \\ \quad + c_1\beta S_h^* I_h^* \Big\{2 - \frac{1}{a_1} + a_5 - a_3 - \frac{a_1 a_5}{a_3}\Big\} \\ \quad + c_2\mu V_h^* \Big\{1 + a_1 - \frac{a_1}{a_2} - a_2\Big\} + c_4\omega(1-\varepsilon)E_h^* \Big\{1 + a_3 - \frac{a_3}{a_4} - a_4\Big\} \\ \quad + c_5\omega\varepsilon E_h^* \Big\{1 + a_3 - \frac{a_3}{a_5} - a_5\Big\} + c_5(1-\kappa)\alpha I_{hA}^* \Big\{1 + a_4 - \frac{a_4}{a_5} - a_5\Big\} \\ \quad + c_6\kappa\alpha I_{hA}^* \Big\{1 + a_4 - \frac{a_4}{a_6} - a_6\Big\} + c_6\gamma I_h^* \Big\{1 + a_5 - \frac{a_5}{a_6} - a_6\Big\} \end{cases} \tag{4.2.48}$$

We let $c_4 = \frac{\beta\xi S_h^* I_{hA}^*}{\omega(1-\varepsilon)E_h^*} c_1$ and $c_5 = \frac{\beta S_h^* I_h^*}{\omega\varepsilon E_h^*} c_1$

This is because c_4 and c_5 are arbitrary positive constants. Equation (4.2.48) becomes:

$$\begin{cases} \frac{dL}{dt} = -\frac{c_1}{a_1}(\mu+\theta)(a_1-1)^2 + c_1\beta\xi S_h^* I_{hA}^* \Big\{3 - \frac{1}{a_1} - \frac{a_3}{a_4} - \frac{a_1 a_4}{a_3}\Big\} \\ \quad + c_1\beta S_h^* I_h^* \Big\{3 - \frac{1}{a_1} - \frac{a_3}{a_5} - \frac{a_1 a_5}{a_3}\Big\} \\ \quad + c_2\mu V_h^* \Big\{1 + a_1 - \frac{a_1}{a_2} - a_2\Big\} + c_5(1-\kappa)\alpha I_{hA}^* \Big\{1 + a_4 - \frac{a_4}{a_5} - a_5\Big\} \\ \quad + c_6\kappa\alpha I_{hA}^* \Big\{1 + a_4 - \frac{a_4}{a_6} - a_6\Big\} + c_6\gamma I_h^* \Big\{1 + a_5 - \frac{a_5}{a_6} - a_6\Big\} \end{cases} \tag{4.2.49}$$

Substituting back the values of a_i for $i = 1, 2, 3, 4, 5, 6$ to equation (4.2.49) gives:

$$\begin{cases} \frac{dL}{dt} = -\frac{c_1 S_h^*}{S_h}(\mu+\theta)\left(\frac{S_h}{S_h^*} - 1\right)^2 + c_1\beta\xi S_h^* I_{hA}^* \Big\{3 - \frac{S_h^*}{S_h} - \frac{E_h I_{hA}^*}{E_h^* I_{hA}} - \frac{S_h E_h^* I_{hA}}{S_h^* E_h I_{hA}^*}\Big\} \\ \quad + c_1\beta S_h^* I_h^* \Big\{3 - \frac{S_h^*}{S_h} - \frac{E_h I_h^*}{E_h^* I_h} - \frac{S_h E_h^* I_h}{S_h^* E_h I_h^*}\Big\} + c_2\mu V_h^* \Big\{1 - \frac{V_h}{V_h^*} - \frac{S_h}{S_h^*}\left(\frac{V_h^*}{V_h} - 1\right)\Big\} \\ \quad + c_5(1-\kappa)\alpha I_{hA}^* \Big\{1 - \frac{I_h}{I_h^*} - \frac{I_{hA}}{I_{hA}^*}\left(\frac{I_h^*}{I_h} - 1\right)\Big\} \\ \quad + c_6\kappa\alpha I_{hA}^* \Big\{1 - \frac{R_h}{R_h^*} - \frac{I_{hA}}{I_{hA}^*}\left(\frac{R_h^*}{R_h} - 1\right)\Big\} + c_6\gamma I_h^* \Big\{1 - \frac{R_h}{R_h^*} - \frac{I_h}{I_h^*}\left(\frac{R_h^*}{R_h} - 1\right)\Big\} \end{cases} \tag{4.2.50}$$

Finally, since the geometric mean equals or is less than the arithmetic

mean as applied by Nainggolan et al [79], NYamberi et al. [83] and Safi et al. [95], it follows that:

$$\left(3-\frac{S_h^*}{S_h}-\frac{E_hI_{hA}^*}{E_h^*I_{hA}}-\frac{S_hE_h^*I_{hA}}{S_h^*E_hI_{hA}^*}\right)\leq 0,\ \left(3-\frac{S_h^*}{S_h}-\frac{E_hI_h^*}{E_h^*I_h}-\frac{S_hE_h^*I_h}{S_h^*E_hI_h^*}\right)\leq 0$$
$$\left\{1-\frac{V_h}{V_h^*}-\frac{S_h}{S_h^*}\left(\frac{V_h^*}{V_h}-1\right)\right\}\leq 0,\ \left\{1-\frac{I_h}{I_h^*}-\frac{I_{hA}}{I_{hA}^*}\left(\frac{I_h^*}{I_h}-1\right)\right\}\leq 0$$
$$\left\{1-\frac{R_h}{R_h^*}-\frac{I_{hA}}{I_{hA}^*}\left(\frac{R_h^*}{R_h}-1\right)\right\}\leq 0,\ \left\{1-\frac{R_h}{R_h^*}-\frac{I_h}{I_h^*}\left(\frac{R_h^*}{R_h}-1\right)\right\}\leq 0$$

The non-negativity of the system parameters permits us to make conclusion that $\frac{dL}{dt}\leq 0$ for $R_\nu > 1$. Moreover, the set where $\frac{dL}{dt}=0$ is $\Omega=\{(S_h,V_h,E_h,I_{hA},I_h,R_h):S_h=S_h^*,V_h=V_h^*,E_h=E_h^*,I_{hA}=I_{hA}^*,I_h=I_h^*,R_h=R_h^*\}$, and by LaSalle's Invariance Principle (Hale [50]), the only compact invariant set of Ω is the singleton set B_e^*. Thus B_e^* is globally asymptotically stable. This completes the proof. □

4.2.12 Fitting the model to the real COVID-19 data for Kenya

In this section, we estimate parameters used in the model (4.2.1) based on monthly cumulative COVID-19 data for confirmed infective cases in Kenya from the 30th day of March, 2020 until March 31st March 2022 (see table 4.3) below. The data is obtained from the worldmeters and can be accessed via the link given in Worldometer [34]. This corresponds to the period when the corona cases in Kenya, just like the rest of the countries in the world, were growing at an alarming rate. It is worth noting that for the purpose of model fitting, the model system is reduced to a simpler version, but at the same time ensuring key population classes are maintained. We consider both θ and φ to be equal to zero which implies

that the vaccinated class is ignored during the curve fitting. The time unit considered in the model versus data fitting is a unit per month. The average life expectancy of Kenyans in 2022 is 67.21 years (Kenya population [61]). The estimate of the natural death rate is obtained by taking the reciprocal of the life expectancy per month, i.e $\frac{1}{67.12\times12}$, an approach utilized by Agusto [5].

Table 4.3: Monthly cumulative COVID-19 cases

Month	Confirmed cases	Month	Confirmed cases
Mar. 30, 2020	50	April 28, 2021	157492
April 29, 2020	374	May 30, 2021	170647
May 29, 2020	1618	June 29, 2021	182884
June 29, 2020	6070	July 30, 2021	201009
July 29, 2020	19125	Aug. 29, 2021	234589
Aug. 30, 2020	33794	Sep. 29, 2021	248770
Sep. 30, 2020	38378	Oct. 30, 2021	253151
Oct. 30, 2020	52612	Nov. 30, 2021	254979
Nov. 30, 2020	83316	Dec. 30, 2021	288951
Dec. 30, 2020	96251	Jan. 30, 2022	321234
Jan. 30, 2021	100675	Feb. 28, 2022	322930
Feb. 28, 2021	105648	Mar. 30, 2022	323402
Mar. 30, 2021	132646		

The recruitment rate into susceptible population for our mass action model is obtained by utilizing the approach employed by Buonomo [23]

and Tchoumi et al. [106] i.e, $\pi = \frac{1000}{67.21\times12}$. The latent period for COVID-19 ranges from five to seven days, thus $\omega = 1/7$ (Bugalia et al. [22]). To obtain the numerical values of the rest of the parameters, we fit the COVID-19 data using nonlinear least-square curve fitting method embedded in lmfit python package (Newville et al. [81]). According to Corona virus Pandemic in Kenya, WHO report (WHO [34]), there have been 50 COVID-19 reported cases as at March 30th 2020. We take the initial conditions for symptomatic patients to be $I_h(0) = 50$. Kenya, just like any other third world countries experienced some challenges in conducting tests to the general population due to the limited resources and trained personnel. We therefore make the assumption that the disease spread unabated and thus the number of active cases could be higher than those declared by the MOH. The presence of asymptomatic persons (infected persons who do not show any symptoms of COVID-19) cannot be ruled out. The initial conditions for the state variables utilized for this study are as follows: $V_h(0) = 600$, $E_h(0) = 5500$, $I_{hA}(0) = 550$ and $R_h(0) = 60$. The total population in Kenya considered in the simulation is N(0)=54,027,487 (Kenya population [61]), thus $S_h(0) = N(0) - V_h(0) - E_h(0) - I_{hA}(0) - I_h(0) - R_h(0)$. The curve fit for our model is depicted in the fig.(4.2.2) below and its evident that our model has the best fitting to the reported data displayed in the table (4.4).

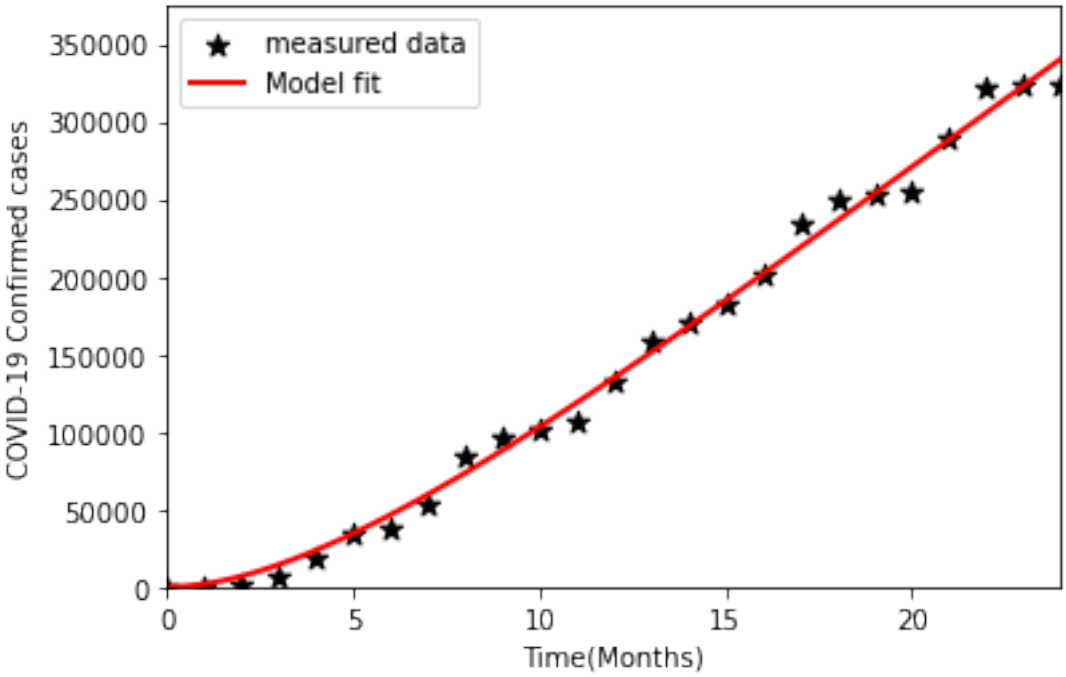

Fig. 4.2.2. The reported data versus model fitting for Kenya from March 30th, 2020 to March 30th, 2022

The estimated values of parameters for real COVID-19 cases in Kenya during the period under consideration (see table 4.4) produces the basic reproduction number $R_\nu = 1.0551339$, which is larger than the COVID-19 threshold value of one(1).

Table 4.4: The model parameter values and source

Parameters	values	References
π	$\frac{1000}{67.12\times12}$	[Buonomo [23], Tchoumi et al. [106]]
β	0.30000025	fitted
ω	$\frac{1}{7}$	Bugalia et al. [22]
μ	$\frac{1}{67.21\times12}$	Buonomo [23]
γ	0.00100	fitted
ξ	0.01075081	fitted
ϵ	0.18696757	fitted
α	1/15	[Okuonghae et al. [84], Olomuyiwa et al. [86]]
δ	0.58873049	fitted
κ	0.11032736	fitted
φ	0.000225	Assumed
θ	0.6785	Assumed
τ	0.00145	Assumed

4.2.13 Sensitivity Analysis

Sensitivity analysis is an important tool in mathematical modeling as it aids in unearthing the extend of influence various parameters have to the disease transmission and prevalence. Due to uncertainty of some of the model parameters, it is prudent to study the impact of perturbations in a variable with respect to changes in a parameter. With the analytical expression of the model's reproduction number, R_ν, its reasonable to utilize the normalized forward sensitivity index of R_ν that depends differentially

on a parameter $\hbar_i$, as defined by Chitnis et al. [32] and mathematically expressed as:

$$\Xi_{\hbar_i}^{R_\nu} = \frac{\partial R_\nu}{\partial \hbar_i} \times \frac{\hbar_i}{R_\nu}$$

, where $\hbar_i$ are the various model parameters whose sensitivity on R_ν is to be obtained.

Table 4.5: The normalized forward sensitivity indices of R_ν to model parameters evaluated at the baseline parameters as displayed in the table(4.4)

Parameters	Sensitivity indices	Values
β	$\Xi_{\beta}^{R_\nu}$	+1.0000000
φ	$\Xi_{\varphi}^{R_\nu}$	+0.1532637
ξ	$\Xi_{\xi}^{R_\nu}$	+0.0781661
ω	$\Xi_{\omega}^{R_\nu}$	+0.0086045
ϵ	$\Xi_{\epsilon}^{R_\nu}$	+0.0063422
θ	$\Xi_{\theta}^{R_\nu}$	-0.9978456
μ	$\Xi_{\mu}^{R_\nu}$	-0.1807076
κ	$\Xi_{\kappa}^{R_\nu}$	-0.0904906
α	$\Xi_{\alpha}^{R_\nu}$	-0.0634152
γ	$\Xi_{\gamma}^{R_\nu}$	-0.0015598

From table (4.5) above, it is evident that β, ω, ξ and φ have a positive effect on R_ν while the rest of the parameters have a negative impact. For instance, 10% increase(decrease) in ξ causes a corresponding increase(decrease) in R_ν by 0.781661% while 10% increase(decrease) in κ results in a corresponding decrease(increase) in R_ν by 0.904906%. It is

apparent that the greater in magnitude a parameter is, the more sensitive is that parameter to R_ν. It can be depicted from the table(4.5) that β, μ, ξ, κ, φ and θ are the most sensitive to R_ν since small perturbations to these parameters leads to a significant change in R_ν.

4.2.14 Numerical results and discussion

In this section, we endeavor to discuss the behavior derived from the numerical simulations. The model parameters utilized are those listed in table (4.4). Figure (4.2.3) shows the temporal variations of different population compartments. From the projection, it is apparent that the asymptomatic population is responsible for upsurge of COVID-19 infections in Kenya. Figure (4.2.4) effect of reinfection coefficient on the recovered population at different values are shown. The projection shows that the cumulative number of individuals becoming susceptible is great for large values of τ and decreases when τ assumes low values. Substituting the values in the table (4.4) to equation (4.2.42) gives $\tau > 1$ which is a contradiction since $\tau \in (0, 1)$. This rules out the existence of backward phenomenon for model (4.2.1) thus our vaccination model has unique disease free equilibrium at $R_\nu < 1$ and a unique Endemic equilibrium when $R_\nu > 1$ as per theorem (4.3).

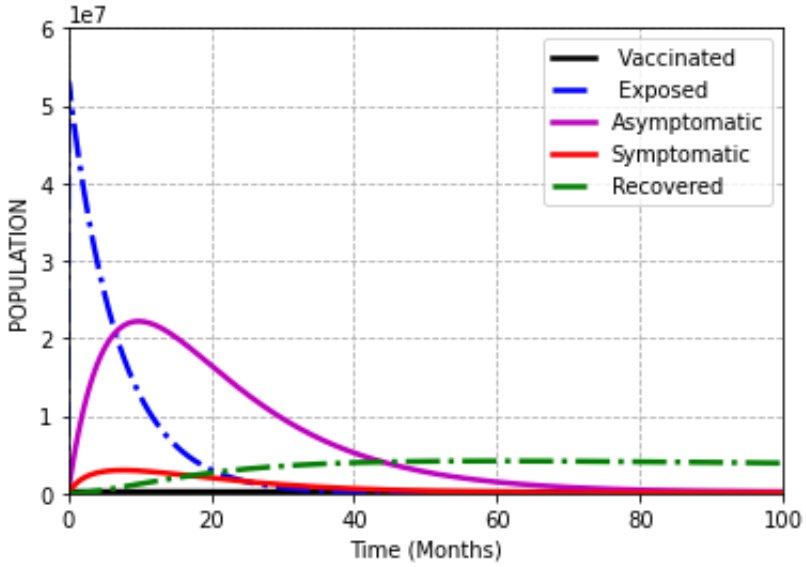

Fig. 4.2.3. The time dependent variation of different population classes

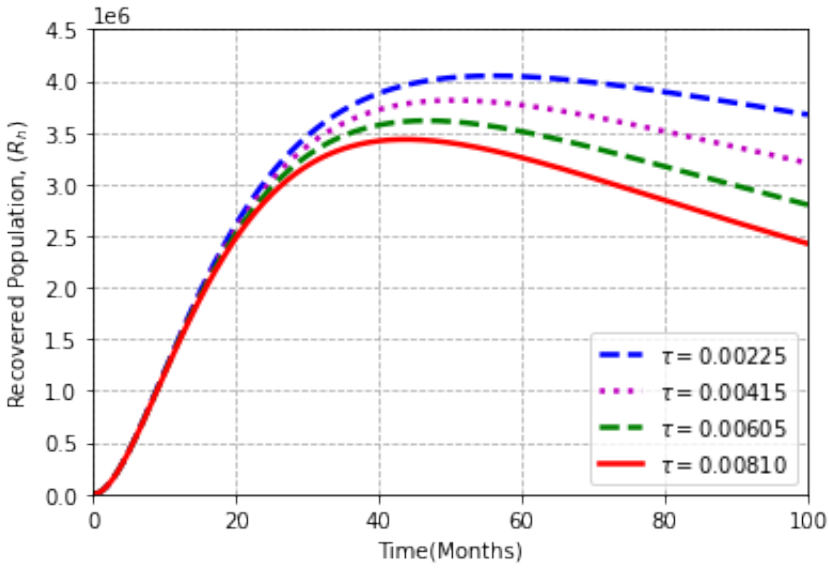

Fig. 4.2.4. Effect of reinfection on the recovered individuals

Figure (4.2.5) explores the variations of detection and treatment coefficient κ for the asymptomatic population. The projections points to the fact that increase in the value of κ leads to the decrease in the exposed population and increase in the recovered population, which ultimately leads to reduction in R_ν.

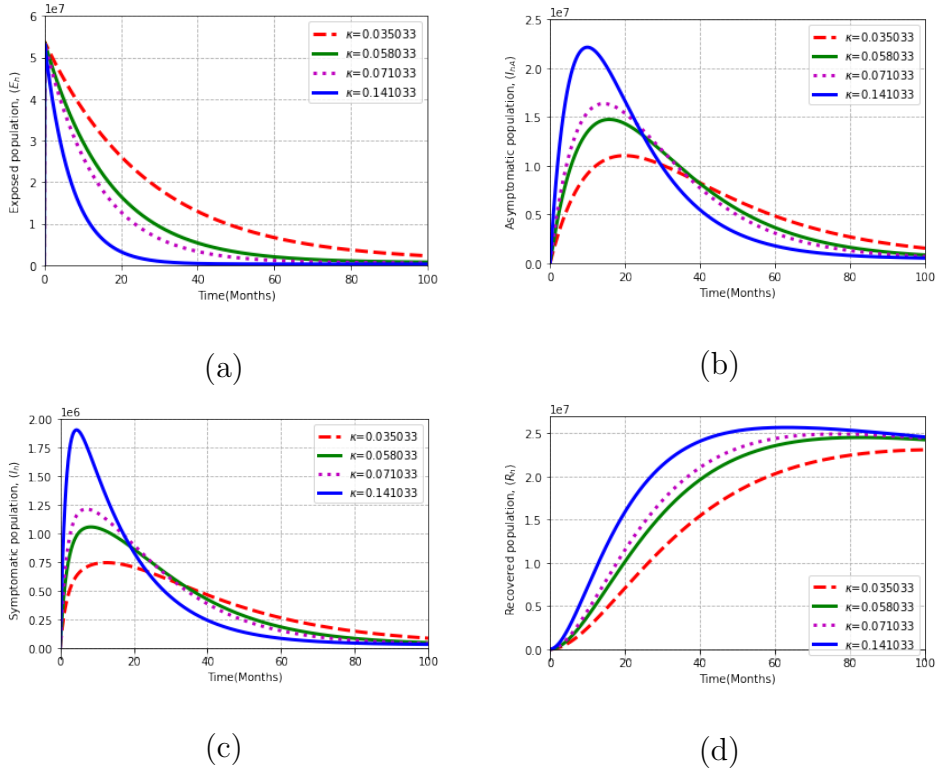

Fig. 4.2.5. Projections with varying effect of detection and treatment rate of asymptomatic to the exposed, asymptomatic, symptomatic and recovered population at values of $\kappa = 0.035033(R_\nu = 0.933579 < 1)$, $\kappa = 0.058033(R_\nu = 0.916991 < 1)$, $\kappa = 0.071033(R_\nu = 0.907616 < 1)$, $\kappa = 0.141033(R_\nu = 0.857133 < 1)$. All parameter values are given in table (4.4) except for $\beta = 0.250000025$ and the varied parameter.

Figure(4.2.6) shows the effect of various model parameters to reproduc-

tion number dynamics. These parameters have a positive impact on the value of R_ν in that increase(decrease) in these parameters causes a corresponding increase(decrease) in R_ν. It is visible that the waning of vaccine coefficient φ is the most prominent of these parameters as a small change in its value causes a significant change in R_ν. This underscores the importance of administration of booster vaccine to the vaccinated population so as to keep the reproduction number below the threshold value of one. It is also indisputable that the modification factor on asymptomatic persons ξ has a tremendous impact on the spread of COVID-19.

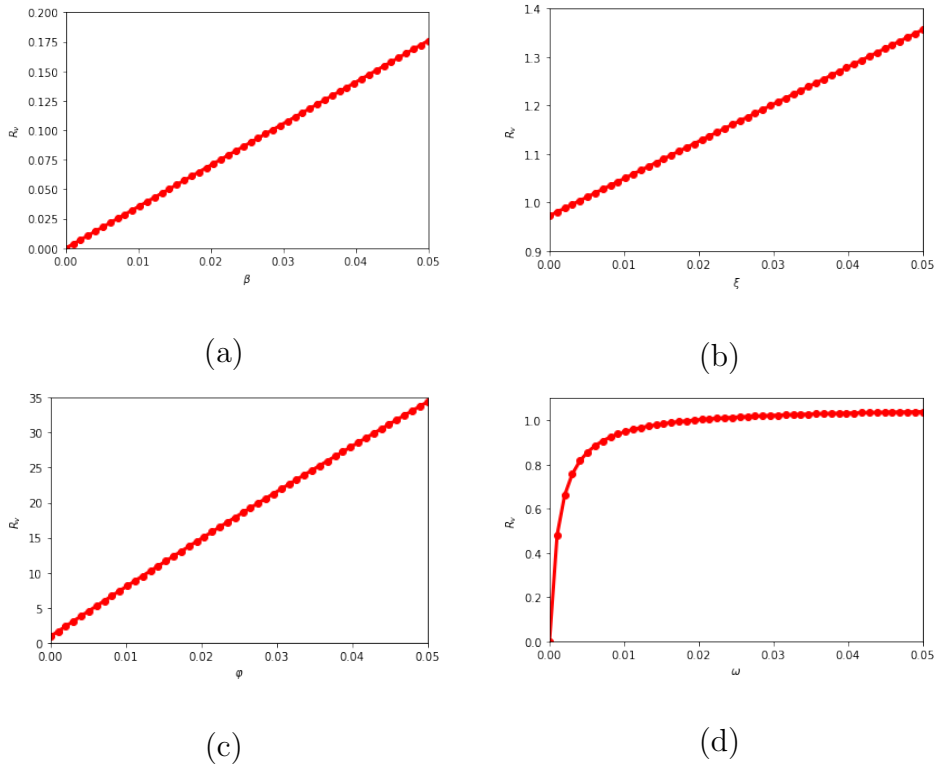

Fig. 4.2.6. Dynamics of R_ν for β, ξ, φ and ω. Dynamics of R_ν for κ, γ, θ and μ. All parameter values are given in table (4.2) except for the varied parameters.

Figure (4.2.7) shows the extend of influence various model parameters have on the spread of COVID-19. It is visible that these model coefficients have an inverse influence in that an increase(decrease) of a parameter causes a corresponding decrease(increase) in the reproduction number. Moreover, vaccination rate θ is the most significant of these parameters in abasing COVID-19 transmission. It is also evident that the treatment rate κ and γ of asymptomatic and symptomatic individuals respectively causes a substantial influence on R_ν.

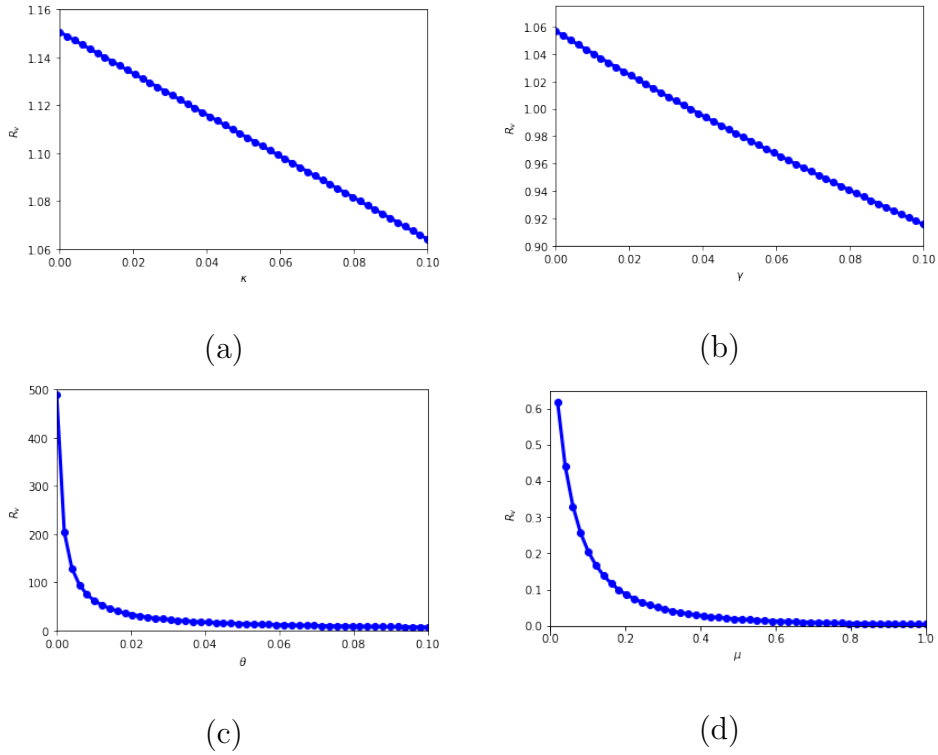

Fig. 4.2.7. Dynamics of R_ν for κ, γ, θ and μ. All parameter values are given in table (4.4) except for the varied parameters.

The fig.(4.2.8) shows the dynamics of R_ν against different parameters of the model. It is evident that the contribution of each parameter to the

COVID-19 transmission dynamic is indisputable as small perturbations on these parameters causes a notable change in the reproduction number. The fig.(a) shows that with increase in modification coefficient of asymptomatic at a given value of transmission coefficient leads to increase in the reproduction number. Fig.(b) reveals that reducing transmission rate as well as the waning of vaccine parameter leads to reduced R_ν.

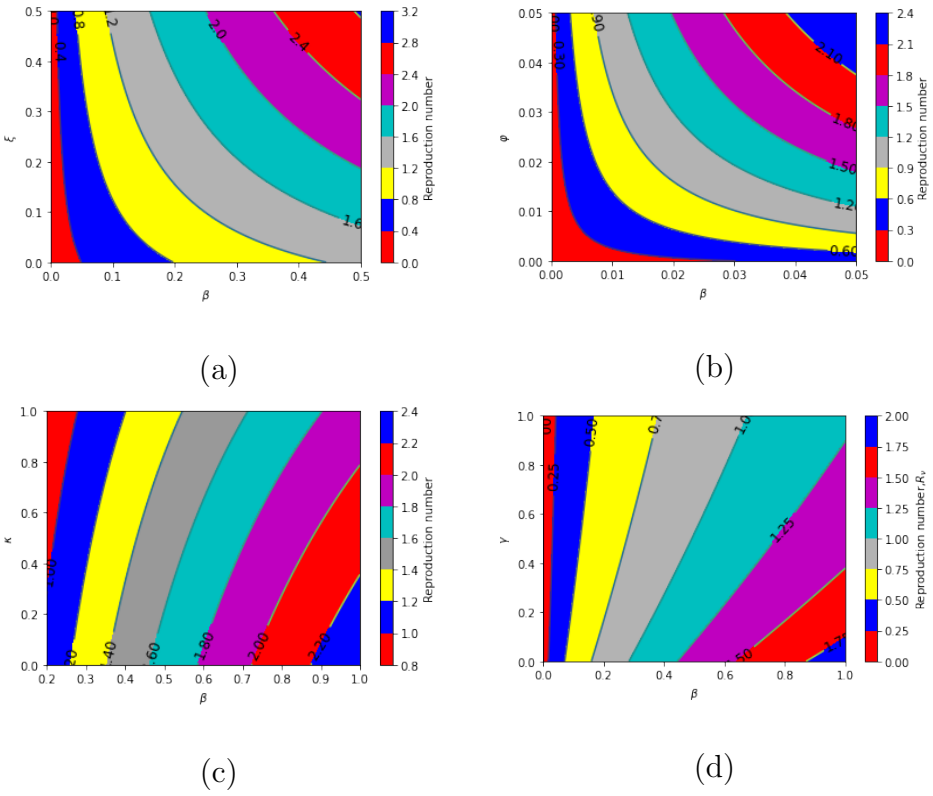

Fig. 4.2.8. Contour plots for R_ν versus: (a) transmission rate β and modification factor ξ (b) transmission rate β and rate of waning of vaccine induced immunity φ, (c) transmission rate β and rate of identification and treatment of asymptomatic patients κ and (d) transmission rate β and rate of treatment of symptomatic persons γ. All parameter values are given in table (4.2) except for the varied parameters.

In figure (c) and figure (d), the variation of R_ν with respect to COVID-19 transmission coefficient β and the the treatment rate κ of the asymptomatic and treatment rate γ of the symptomatic patients respectively are presented. In both scenarios, it is evident that increasing the rate of identifying and treating the symptomatic and asymptomatic individuals decreases the rate of infection from the ill individuals to the susceptible population which ultimately leads to the reduction in the value of the reproduction number.

4.3 Model 2

In this section, we consider model 2 which assumes that COVID-19 vaccine do not confer full protection against infection. The basic properties of the proposed model including existence and uniqueness of the solution, positivity and boundedness of the state variables, the model's reproduction number R_{0i} , Local and global stability of DFE as well as local and global stability of endemic equilibrium are discussed. Sensitivity analysis analysis as well as numerical analysis to validate analytical results are also carried out.

4.3.1 Model Formulation

This subsection involves the model assumptions, model descriptions, model flow chart and model equations.

4.3.2 Model Description

Our study involves seven determinist compartmental model that describes COVID-19 transmission dynamics at any time t. The whole population $N_h(t)$ is composed of seven (7) compartments, S_h, V_h, E_h, I_{hA}, I_h, J_h and R_h which respectively represent the susceptible, vaccinated,exposed, asymptomatic ,symptomatic, isolated and Recovered.

It is worth noting that the exposed individuals are those who are infected with COVID-19, do not manifest symptoms of the disease yet and they register negative when subjected to polymerase chain reaction (PCR) tests. Patients are said to be in latency phase and are regarded as non-infectious. Equation of the model are derived as follows: The individuals get into the susceptible population at rate π. COVID-19 vaccine whose efficacy is σ is administered to the susceptible population at the rate θ. This vaccine is assumed to wane at the rate φ in accordance to the study by Naaber et al. [88]. Furthermore, the susceptible individuals progress to the exposed phase upon interaction with the asymptomatic and the non-isolated symptomatic individuals. The force of infection λ is thus expressed as:

$$\lambda = \frac{\beta(\eta I_{hA} + I_h)}{N_h - J_h} \tag{4.3.1}$$

The parameter β in equation (4.3.1) is the transmission coefficient which accounts for contacts capable of leading to infection, while $\eta \in (0, 1)$ is the modification parameter which accounts for presumed reduction in infectiousness of the asymptomatic individuals relative to the symptomatic individuals. In the face of COVID-19 variants with larger number of mutations such as Omicron as compared to the Delta variant (the most

dominant variant according to WHO report (WHO [114]), it is apparent that breakthrough infections cannot be ruled out for the vaccinated population. In the light of this, a fraction of the those vaccinated progress to the exposed population at the rate $(1-\sigma)\lambda$ where $\sigma \in (0,1)$ is the efficacy of the vaccine administered. All the population clusters are presumed to decrease at a constant value μ which accounts for natural death rate. The rate of progression of both susceptible and vaccinated individuals is thus given as:

$$\frac{dS_h}{dt} = \pi + \varphi V_h - \lambda S_h - (\mu + \theta) S_h$$
$$\frac{dV_h}{dt} = \theta S_h - (1-\sigma)\lambda V_h - (\mu + \varphi) V_h$$

The growth of the exposed population is necessitated by the susceptible at the rate λ and the vaccinated cohort at the rate $(1-\sigma)\lambda$ and it is diminished at a constant rate ω when a fraction ϵ of the individuals develop symptoms and the rest $(1-\epsilon)$ progress to asymptomatic compartment. Thus we obtain the expression;

$$\frac{dE_h}{dt} = \lambda S_h + (1-\sigma)\lambda V_h - (\mu + \omega) E_h$$

The asymptomatic class exit this compartment at a rate α where a fraction κ progress to recovered compartment after having been identified and successfully treated while a fraction $(1-\kappa)$ become symptomatic since any infection compromises ones innate immune system rendering one vulnerable to infection from other COVID-19 variants. The expression for

asymptomatic thus becomes:

$$\frac{dI_{hA}}{dt} = (1-\epsilon)\omega E_h - (\mu+\alpha)I_{hA}$$

Besides natural death rate μ, the symptomatic and isolated individuals are diminished by COVID-19 induced death rate at δ_1 and δ_2 respectively. The parameter γ_1 accounts for the successful isolation rate of the symptomatic while γ_2 and γ_3 represent the rate at which the symptomatic and isolated persons respectively proceed to recovered class. We note that the isolated population are those who are hospitalized or self-isolated for treatment Olumuyiwa et al. [86]. The relative infectiousness of the isolated cohort to that of asymptomatic and symptomatic is assumed negligible in this study. The expressions for symptomatic and isolated individuals are thus:

$$\frac{dI_h}{dt} = \epsilon\omega E_h + (1-\kappa)\alpha I_{hA} - (\mu+\gamma_1+\gamma_2+\delta_1)I_h$$

$$\frac{dJ_h}{dt} = \gamma_1 I_h - (\mu+\delta_2+\gamma_3)J_h$$

Finally, the growth of the recovered individuals is generated by the recovery of the asymptomatic, symptomatic and isolated population. For mathematical tractability, it is assumed that the recovered acquire permanent immunity to re-infection and is given by the equation:

$$\frac{dR_h}{dt} = \gamma_2 I_h + \alpha\kappa I_{hA} + \gamma_3 J_h - \mu R_h$$

Thus it follows that our model consist of the following system of nonlinear differential equations:

$$
\begin{cases}
\frac{dS_h}{dt} = \pi + \varphi V_h - \lambda S_h - (\mu + \theta) S_h \\
\frac{dV_h}{dt} = \theta S_h - (1-\sigma)\lambda V_h - (\mu + \varphi) V_h \\
\frac{dE_h}{dt} = \lambda S_h + (1-\sigma)\lambda V_h - (\mu + \omega) E_h \\
\frac{dI_{hA}}{dt} = (1-\epsilon)\omega E_h - (\mu + \alpha) I_{hA} \\
\frac{dI_h}{dt} = \epsilon\omega E_h + (1-\kappa)\alpha I_{hA} - (\mu + \gamma_1 + \gamma_2 + \delta_1) I_h \\
\frac{dJ_h}{dt} = \gamma_1 I_h - (\mu + \delta_2 + \gamma_3) J_h \\
\frac{dR_h}{dt} = \gamma_2 I_h + \alpha\kappa I_{hA} + \gamma_3 J_h - \mu R_h
\end{cases} \tag{4.3.2}
$$

Where $\lambda = \frac{\beta(\eta I_{hA} + I_h)}{N_h - J_h}$, with initial conditions given by: $S_h(0) = S_{h0} \geq 0, V_h(0) = V_{h0} \geq 0, E_h(0) = E_{h0} \geq 0, I_{hA}(0) = I_{hA0} \geq 0, I_h(0) = I_{h0} \geq 0, J_h(0) = J_{h0} \geq 0, R_h(0) = R_{h0} \geq 0$

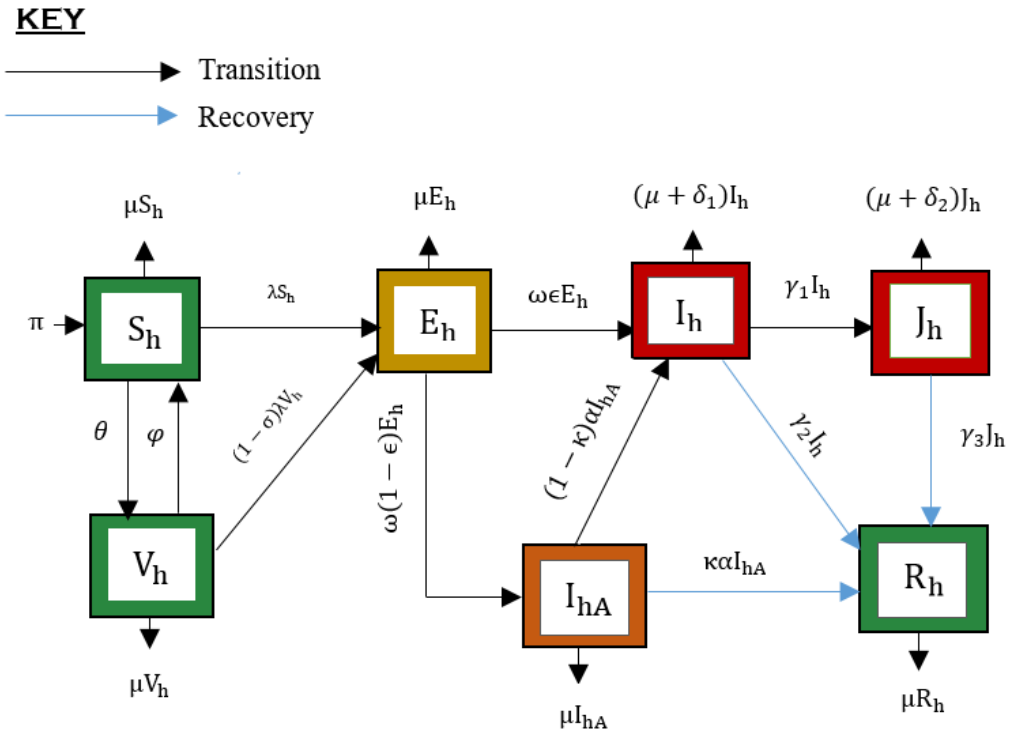

Fig. 4.3.1. General COVID-19 flow diagram for our model 2

Table 4.6: Definition of state variables

State	Description
S_h	Human population susceptible to COVID-19 disease
V_h	Fully vaccinated population
E_h	Individuals in a latency period
I_{hA}	Asymptomatic patients
I_h	Symptomatic patients
J_h	Isolated population
R_h	Recovered population

4.3.3 Positivity and boundedness

Since the model in consideration entails a human population, it is paramount for model equations (4.3.2) to be epidemiologically meaningful. We thus show that all state variables involved are nonnegative for all time $t > 0$ and that the region;

$$\Omega = \left\{(S_h, V_h, E_h, I_{hA}, I_h, J_h, R_h) \in \mathbb{R}^7_+ : S_h+V_h+E_h+I_{hA}+I_h+J_h+R_h \leq N_h(0)\right\} \tag{4.3.3}$$

is bounded. We thus state explicitly the following theorem.

Descriptions of all the parameters are summarized in **Table 4.4** below.

Table 4.7: Definition of Parameters

Parameter	Description
π	Recruitment rate of susceptible into the population
μ	Natural death rate
β	COVID-19 transmission rate.
η	Modification factor for asymptomatic persons.
ϵ	Rate at which the exposed persons who become symptomatic.
γ_1	Rate of the isolation symptomatic individuals.
γ_2	Recovery rate of the symptomatic individuals.
γ_3	Recovery rate of the isolated individuals.
δ_1	COVID-19 induced death rate for symptomatic individuals
δ_2	COVID-19 induced death rate for isolated individuals
σ	COVID-19 efficacy rate
ω	Rate at which exposed population become sick of COVID-19
φ	Rate of waning of COVID-19 vaccine induced immunity
α	Rate of movement from asymptomatic infected class
κ	Rate of identification and treatment of the asymptomatic persons.
θ	Rate of vaccination of susceptible population.

Table 4.8: The model parameter values and source

Parameters	values	References
π	66988	[Sun et al.[104],Kifle et al. [123]]
β	0.3000003	fitted
ω	$\frac{1}{7}$	Bugalia et al. [22]
μ	0.0012399	[Sun et al.[104], Kifle et al. [123]]
γ_1	0.0125	fitted
γ_2	0.05	Deressa et al. [35]
γ_3	0.001	fitted
η	0.01075081	fitted
ϵ	0.18696757	fitted
α	1/15	[Okuonghae et al. [84], Olumuyiwa et al.[86]]
δ_1	0.018	Diagne et bal. [36]
δ_2	0.0107	fitted
κ	0.11032736	fitted
φ	0.00225	Assumed
θ	0.6785	Assumed
σ	0.70	Assumed

Theorem 4.10. *If* $S_h(0) \geq 0, V_h(0) \geq 0, E_h(0) \geq 0, I_{hA}(0) \geq 0, I_h(0) \geq 0, J_h(0) \geq 0$ *and* $R_h(0) \geq 0$*, then the solution* $S_h(t) \geq 0, V_h(t) \geq 0, E_h(t) \geq 0, I_{hA}(t) \geq 0, I_h(t) \geq 0, J_h(0) \geq 0$ *and* $R_h(t) \geq 0$ *of model (4.3.2) are positive for all* $t > 0$.

Proof. According to Asha et al. [12] and Kifle et al. [123], we proof the positivity of our system (4.3.2) by contradiction. Given the non-

negative initial conditions for $S_h(0), V_h(0), E_h(0), I_{hA}(0), I_h(0), J_h(0)$ and $R_h(0)$, the positivity of the system can be determined as follows: We make an assumption that there exists time t_i such that, $S_h(0) > 0, S_h(t_i) = 0, S_h'(t_i) < 0, V_h(t) > 0, E_h(t) > 0, I_{hA}(t) > 0, I_h(t) > 0, J_h(t) > 0, R_h(t) > 0$, for all $0 \leq t < t_i$.

In relation to our case and considering the first equation of the system (4.3.2), we have:

$$\frac{dS_h}{dt}(t_i) = \pi + \varphi V_h(t_i) - (\lambda + \mu + \theta)S_h(t_i)$$

Based on our assumption, this equation implies that:

$$\frac{dS_h}{dt}(t_i) = \pi + \varphi V_h(t_i) > 0$$

which is a contradiction. This indicates that $S_h(t) > 0$ for all $t > 0$.

Moreover to prove the positivity of V_h, we make an assumption that there exists time t_f such that, $S_h(t) > 0, V_h(t) > 0, V_h(t_f) = 0, V_h'(t_f) < 0, E_h(t) > 0, I_{hA}(t) > 0, I_h(t) > 0, J_h(t) > 0, R_h(t) > 0$, for all $0 \leq t < t_f$. The second equation of our system thus becomes:

$$\frac{dV_h}{dt} = \theta S_h(t_f) - ((1-\sigma)\lambda + \mu + \varphi)V_h(t_f)$$

This implies that:

$$\frac{dV_h}{dt} = \theta S_h(t_f) > 0$$

which is also a contradiction, thus $V_h(t) > 0$ for all $t > 0$.

Based on the third equation of model (4.3.2),

$$\frac{dE_h}{dt} = \lambda S_h + (1-\sigma)\lambda V_h - (\mu+\omega)E_h \geq -(\mu+\omega)E_h$$

owing to the fact that both $S_h(t)$ and $V_h(t)$ are non-negative for all $t > 0$. Solving this equation gives:

$$E_h(t) = E_h(0)\exp(-(\mu+\omega)t) \geq 0 \quad \forall t > 0$$

In the similar manner, from the fourth equation of the model (4.3.2), we get,

$$\frac{dI_{hA}}{dt} = (1-\epsilon)\omega E_h - (\mu+\alpha)I_{hA} \geq -(\mu+\alpha)I_{hA}$$

which on solving yields,

$$I_{hA}(t) = I_{hA}(0)\exp(-(\mu+\alpha)t) \geq 0 \quad \forall t > 0$$

Handling the last three equations in the similar way and using the fact that $S_h(t) \geq 0, V_h(t) \geq 0, E_h(t) \geq 0$ and $I_{hA}(t)$, we obtain:

$$\begin{cases} \frac{dI_h}{dt} = \epsilon\omega E_h + (1-\kappa)\alpha I_{hA} - (\mu+\gamma_1+\gamma_2+\delta_1)I_h \geq -(\mu+\gamma_1+\gamma_2+\delta_1)I_h \\ \frac{dJ_h}{dt} = \gamma_1 I_h - (\mu+\delta_2+\gamma_3)J_h \geq -(\mu+\delta_2+\gamma_3)J_h \\ \frac{dR_h}{dt} = \gamma_2 I_h + \alpha\kappa I_{hA} + \gamma_3 J_h - \mu R_h \geq -\mu R_h \end{cases}$$

whose solution are respectively given as:

$$\begin{cases} I_h(t) = I_h(0)\exp(-(\mu+\gamma_1+\gamma_2+\delta_1)t) \geq 0 \quad \forall t > 0 \\ J_h(t) = J_h(0)\exp(-(\mu+\delta_2+\gamma_3)t) \geq 0 \quad \forall t > 0 \\ R_h(t) = R_h(0)\exp(-\mu R_h t) \geq 0 \quad \forall t > 0 \end{cases}$$

This demonstrates that the solution of all state variables of the model system (3) are non-negative. □

4.3.4 Invariant region

A population is said to be meaningful in biological sense if its global solution lies within an invariant region Ω (Asamoah et al. [11] and Ega et al. [41]).

Theorem 4.11. *The solution set* $\{S_h(t), V_h(t), E_h(t), I_{hA}(t), I_h(t), J_h, R_h(t)\}$ *of the model equation (4.3.2) is confined to non-negative feasible region* Ω.

Proof. Consider the feasible region:
$\Omega = \{S_h(t), V_h(t), E_h(t), I_{hA}(t), I_h(t), J_h(t), R_h(t)\} \in \mathbb{R}^7_+ \ \ \forall t \geq 0$. At any given time, equation(4.3.1) gives the total population as:

$$N_h(t) = S_h(t) + V_h(t) + E_h(t) + I_{hA} + I_h(t) + J_h(t) + R_h(t) \qquad (4.3.4)$$

Differentiating equation (4.3.4) with respect to t gives:

$$\frac{dN_h}{dt} = \frac{dS_h}{dt} + \frac{dV_h}{dt} + \frac{dE_h}{dt} + \frac{dI_{hA}}{dt} + \frac{dI_h}{dt} + \frac{dJ_h}{dt} + \frac{dR_h}{dt} \qquad (4.3.5)$$

We now substitute equation (4.3.2) into (4.3.5)

$$\frac{dN_h}{dt} = [\pi + \varphi V_h - \lambda S_h - (\mu + \theta)S_h] + [\theta S_h - (1-\sigma)\lambda V_h - (\mu + \varphi)V_h]$$
$$+ [\lambda S_h + (1-\sigma)\lambda V_h - (\mu + \omega)E_h] + [(1-\epsilon)\omega E_h - (\mu + \alpha)I_{hA}]$$
$$+ [\epsilon\omega E_h + (1-\kappa)\alpha I_{hA} - (\mu + \gamma_1 + \gamma_2 + \delta_1)I_h]$$
$$+ [\gamma_1 I_h - (\mu + \delta_2 + \gamma_3)J_h] + [\kappa\alpha I_{hA} + \gamma I_h - (\mu + \tau)R_h] \tag{4.3.6}$$

Expansion and simplification of equation (4.3.6) yields:

$$\frac{dN_h}{dt} = \pi - \mu[S_h(t) + V_h(t) + E_h(t) + I_{hA} + I_h(t) + J_h(t) + R_h(t)] - (\delta_1 I_h + \delta_2 J_h) \tag{4.3.7}$$

Substituting equation (4.3.4) to (4.3.7) gives:

$$\frac{dN_h}{dt} = \pi - \mu N_h - (\delta_1 I_h + \delta_2 J_h) \leq \pi - \mu N_h \tag{4.3.8}$$

Evaluation of the equation (4.3.8) yields $N_h(t) \leq A\exp(-\mu t) + \frac{\pi}{\mu}$ which upon application of initial conditions, the above equation becomes:

$$N_h(t) \leq \frac{\pi}{\mu} + \left(\frac{\pi - \mu N_{h0}}{\mu}\right)\exp(-\mu t) \tag{4.3.9}$$

where $N_{h0} = N_h(0)$

This implies that:

$$\limsup_{t\to\infty} \quad N_h(t) \leq \frac{\pi}{\mu}$$

This shows that the positive solutions of the model (4.3.2) are bounded. Hence, the system under consideration is well posed mathematically and epidemiologically. □

4.3.5 Basic Reproduction Number R_{0i}

We determine the basic reproduction number for our model with vaccine efficacy $\sigma \in (0, 1)$

We rewrite the model as:

$$\frac{d\chi}{dt} = F(\chi) - V(\chi) \tag{4.3.10}$$

Which can be expressed as:

$$\begin{pmatrix} \dot{E}_h \\ \dot{I}_{hA} \\ \dot{I}_h \\ \dot{J}_h \end{pmatrix} = \begin{pmatrix} \chi_1 \\ 0 \\ 0 \\ 0 \end{pmatrix} - \begin{pmatrix} (\omega+\mu)E_h \\ -\omega(1-\epsilon)E_h + (\mu+\alpha)I_h A \\ -\omega\epsilon E_h - (1-\kappa)\alpha I_h A + (\mu+\gamma_1+\gamma_2+\delta_1)I_h \\ -\gamma_1 I_h + (\mu+\gamma_3+\delta_2)J_h \end{pmatrix}$$

Where F and V represents the transmission and and transition matrices respectively. $\chi_1 = \frac{\beta(I_h+\eta I_{hA})S_h}{N_h - J_h} + \frac{(1-\sigma)\beta(\eta I_{hA}+I_h)V_h}{N_h-J_h}$

We evaluate the Jacobian of the matrices F and V at DFE. This becomes:

$$\mathcal{F} = \begin{pmatrix} 0 & \frac{\beta\eta\{\theta(1-\sigma)+\mu+\varphi\}}{(\mu+\theta+\varphi)} & \frac{\beta\{(\theta(1-\sigma)+\mu+\varphi)\}}{(\mu+\theta+\varphi)} & 0 \\ 0 & 0 & 0 & 0 \\ 0 & 0 & 0 & 0 \\ 0 & 0 & 0 & 0 \end{pmatrix}$$

and

$$\mathcal{V} = \begin{pmatrix} (\mu+\omega) & 0 & 0 & 0 \\ -\omega(1-\varepsilon) & (\alpha+\mu) & 0 & 0 \\ -\varepsilon\omega & -\alpha(1-\kappa) & (\mu+\gamma_1+\gamma_2+\delta_1) & 0 \\ 0 & 0 & -\gamma_1 & \mu+\gamma_3+\delta_2 \end{pmatrix}$$

The basic reproduction number is the spectral radius (The largest eigenvalue) of the next generation matrix $\mathcal{F}\mathcal{V}^{-1}$(Diekmann et al. [37]). By simple calculations, we can show that:

$$\mathcal{V}^{-1} = \begin{pmatrix} \frac{1}{\Phi_1} & 0 & 0 & 0 \\ \frac{\omega\{(1-\varepsilon)}{\Phi_1\Phi_2} & \frac{1}{\Phi_2} & 0 & 0 \\ \frac{\omega\{\alpha(1-\kappa)+\varepsilon(\mu+\alpha\kappa)\}}{\Phi_1\Phi_2\Phi_3} & \frac{\alpha(1-\kappa)}{\Phi_2\Phi_3} & \frac{1}{\Phi_3} & 0 \\ \frac{\omega\gamma_1\{\alpha(1-\kappa)+\varepsilon(\mu+\alpha\kappa)\}}{\Phi_1\Phi_2\Phi_3\Phi_4} & \frac{\alpha\gamma_1(1-\kappa)}{\Phi_2\Phi_3\Phi_4} & \frac{\gamma_1}{\Phi_3\Phi_4} & \frac{1}{\Phi_4} \end{pmatrix} \tag{4.3.11}$$

Where $\Phi_1 = (\mu+\omega), \Phi_2 = (\mu+\alpha), \Phi_3 = (\mu+\gamma_1+\gamma_2+\delta_1)$ and $\Phi_4 = (\mu+\gamma_3+\delta_2)$.

We determine the next generation matrix as:

$$\mathcal{F}\mathcal{V}^{-1} = \begin{pmatrix} a_{11} & a_{12} & a_{13} & 0 \\ 0 & 0 & 0 & 0 \\ 0 & 0 & 0 & 0 \\ 0 & 0 & 0 & 0 \end{pmatrix}$$

Where:

$a_{11} = \frac{\omega\beta[\theta(1-\sigma)+\mu+\varphi]\{\eta(1-\epsilon)\Phi_3+\alpha(1-\kappa)+\epsilon(\mu+\alpha\kappa)\}}{\Phi_1\Phi_2\Phi_3(\mu+\theta+\varphi)}$

$a_{12} = \frac{\beta[\theta(1-\sigma)+\mu+\varphi]\{\eta\Phi_3+\alpha(1-\kappa)\}}{\Phi_2\Phi_3(\mu+\theta+\varphi)}$

$a_{13} = \frac{\beta[\theta(1-\sigma)+\mu+\varphi]}{\Phi_3\mu(\mu+\theta+\varphi)}$

The most dominant eigenvalue of the next generation matrix, $\mathcal{F}\mathcal{V}^{-1}$ gives

the basic reproduction for the imperfect vaccine COVID-19 model as:

$$R_{0i} = \frac{\omega\beta[\theta(1-\sigma)+\mu+\varphi]\{\eta(1-\epsilon)\Phi_3+\alpha(1-\kappa)+\epsilon(\mu+\alpha\kappa)\}}{\Phi_1\Phi_2\Phi_3(\mu+\theta+\varphi)} \tag{4.3.12}$$

This number is an indicator of the potential for COVID-19 to spread in a population. It can be taken as a mathematical expression for the stability of a DFE and that it can be used as a pointer for disease control.

4.3.6 Local Stability of DFE

Theorem 4.12. *The DFE point* (B_i^0) *is locally asymptotically stable if* $R_{0i} < 1$ *and unstable if* $R_{0i} > 1$.

Proof. To proof the theorem (4.12), we evaluate the Jacobian of the system (4.3.2) at (B_i^0).

$$\begin{pmatrix} -(\mu+\theta) & \varphi & 0 & -\frac{(\mu+\varphi)\beta\eta}{(\mu+\theta+\varphi)} & -\frac{\beta\theta(\mu+\varphi)}{(\mu+\theta+\varphi)} & 0 & 0 \\ \theta & -(\mu+\varphi) & 0 & -\frac{(1-\sigma)\beta\eta\theta}{(\mu+\theta+\varphi)} & -\frac{(1-\sigma)\beta\theta}{(\mu+\theta+\varphi)} & 0 & 0 \\ 0 & 0 & -(\mu+\omega) & \frac{\beta\eta[\mu+\varphi+(1-\sigma)\theta]}{(\mu+\theta+\varphi)} & \frac{\beta[\mu+\varphi+(1-\sigma)\theta]}{(\mu+\theta+\varphi)} & 0 & 0 \\ 0 & 0 & \omega(1-\epsilon) & -(\alpha+\mu) & 0 & 0 & 0 \\ 0 & 0 & \epsilon\omega & \alpha(1-\kappa) & -\Phi_3 & 0 & 0 \\ 0 & 0 & 0 & 0 & \gamma_1 & -\Phi_4 & 0 \\ 0 & 0 & 0 & \alpha\kappa & \gamma_2 & \gamma_3 & -\mu) \end{pmatrix} \tag{4.3.13}$$

From the Jacobian matrix (B_i^0), the it is evident that the first four eigenvalues are; $\lambda_1 = -\mu, \lambda_2 = -\mu, \lambda_3 = -(\mu+\theta+\varphi)$ and $\lambda_4 = -(\mu+\delta_2+\gamma_3)$. We can determine the other three eigenvalues from the reduced matrix

(B^0_{iR}):

$$\begin{pmatrix} -(\mu+\omega) & \frac{\beta\eta[\mu+\varphi+(1-\sigma)\theta]}{(\mu+\theta+\varphi)} & \frac{\beta\eta[\mu+\varphi+(1-\sigma)\theta]}{(\mu+\theta+\varphi)} \\ \omega(1-\epsilon) & -(\alpha+\mu) & 0 \\ \epsilon\omega & \alpha(1-\kappa) & -(\mu+\gamma_1+\gamma_2+\delta_1) \end{pmatrix}$$

Using the above reduced form of matrix B^0_i, we utilize $det|B^0_{iR} - \mathbf{I}\lambda| = 0$ to obtain the following characteristic equation.

$$\lambda^3 + \zeta_1\lambda^2 + \zeta_2\lambda + \zeta_3 = 0 \tag{4.3.14}$$

where $\mathbf{I}$ is a 3×3 identity matrix.

Utilizing Liénard-Chirpart, which is a special case of Routh-Hurwitz stability criterion, as discussed in (3.3.1), we need to determine the values of ζ_1 and ζ_3.

$$\begin{cases} \zeta_1 = (3\mu + \omega + \alpha + \gamma_1 + \gamma_2 + \delta_1) > 0 \\ \zeta_3 = (\mu+\omega)(\mu+\alpha)(\mu+\gamma_1+\gamma_2+\delta_1)(1-R_{0i}) > 0 \end{cases}$$

Thus it is evident that for ζ_3 to be greater than zero R_{0i} should be less than one(1) thus the system above is locally asymptotically stable when $R_{0i} < 1$ and unstable when $R_{0i} > 1$. □

4.3.7 Global Stability of DFE

For global stability of DFE of the model (4.3.2), we utilize the technique implemented by Castillo-Chavez et al. [26].

To do this we first rewrite the model (4.3.2) as:

$$\begin{cases} \frac{dX}{dt} = F(X,Y), \\ \frac{dY}{dt} = G(X,Y), G(X,0) = 0 \end{cases} \tag{4.3.15}$$

where $X = (S_h, V_h, R_h) \in \mathbb{R}^3$ represents COVID-19 free compartments, while $Y = (E_h, I_{hA}, I_h, J_h) \in \mathbb{R}^4_+$ represents the infected as well as infectious compartments. For global asymptomatic stability of DFE of model (4.3.2), the following conditions (C1) and (C2) hold, where:
(C1):$\frac{dX}{dt} = F(X,0), X^0 = B^0$ is globally asymptotically stable.
(C2):$G(X,Y) = AY - \tilde{G}(X,Y), \tilde{G}(X,Y) \geq 0$, for $(X,Y) \in \mathbb{R}^7_+$, where $A = D_Y G(X^0, 0)$ and $\Omega \in \mathbb{R}^7_+$ is the invariant region of the model.

Theorem 4.13. *The disease-free equilibrium point,*
$B_0 = \left\{ \frac{\pi(\varphi+\mu)}{\mu(\varphi+\mu+\theta)}, \frac{\pi\theta}{\mu(\varphi+\mu+\theta)}, 0, 0, 0, 0, 0 \right\} \in \Omega$ *is GAS for the system equation (4.3.2) provided that* $R_{0i} < 1$ *and conditions* $(C1)$ *and* $(C2)$ *both apply.*

Proof. We consider the the system equation (4.3.2) and that:

$$F(X,0) = \begin{pmatrix} \pi + \varphi V_n - (\mu+\theta)S_h \\ \theta S_h - (\mu+\varphi)V_h \\ -\mu R_h \end{pmatrix} \tag{4.3.16}$$

First, we consider the limit of $F(X,0)$ as $t \to \infty$ and show that this limit leads to $X \to B^0$

$$\frac{dR_h}{dt} = -\mu R_h$$

$$R_h(t) = C_1 exp\{-\mu t\}$$

$$\lim_{t\to\infty} R_h(t) = 0 \tag{4.3.17}$$

We also have

$$\frac{dS_h}{dt} = \frac{\pi(\mu+\theta)(\varphi+\mu)}{\mu(\varphi+\mu+\theta)} - (\mu+\theta)S_h$$

$$S_h(t) = C_2 exp\{-(\mu+\theta)t\} + \frac{\mu(\varphi+\mu)}{\mu(\varphi+\theta+\mu)}$$

$$\lim_{t\to\infty} S_h(t) = \frac{\mu(\varphi+\mu)}{\mu(\varphi+\theta+\mu)} \tag{4.3.18}$$

$$\frac{dV_h}{dt} = \frac{\theta\pi(\varphi+\mu)}{\mu(\varphi+\mu+\theta)} - (\mu+\varphi)S_h$$

$$V_h(t) = C_3 exp\{-(\mu+\varphi)t\} + \frac{\theta\pi}{\mu(\varphi+\theta+\mu)}$$

$$\lim_{t\to\infty} V_h(t) = \frac{\theta\pi}{\mu(\varphi+\theta+\mu)} \tag{4.3.19}$$

Thus, we have shown that all points all points as $t \to \infty$ converge at:

$$B^0 = \left\{ \frac{\pi(\varphi+\mu)}{\mu(\varphi+\mu+\theta)}, \frac{\pi\theta}{\mu(\varphi+\mu+\theta)}, 0, 0, 0, 0 \right\} \in \Omega \tag{4.3.20}$$

We now consider the condition:

$$\tilde{G}(X,Y) = AY - G(X,Y) \tag{4.3.21}$$

where

$$A = \begin{pmatrix} -\Phi_1 & \frac{\beta\eta(S^0+V^0(1-\sigma))}{S^0+V^0} & \frac{\beta(S^0+V^0(1-\sigma))}{S^0+V^0} & 0 \\ \omega(1-\epsilon) & -\Phi_2 & 0 & 0 \\ \epsilon\omega & \alpha(1-\kappa) & -\Phi_3 & 0 \\ 0 & 0 & \gamma_1 & -\Phi_4 \end{pmatrix} \tag{4.3.22}$$

Thus A is M-matrix since all diagonal entries are negative and that all

other non-diagonal elements are non-negative [31].

$$AY = \begin{pmatrix} -\Phi_1 E_h + \frac{\beta\eta(S^0+V^0(1-\sigma))}{S^0+V^0} I_{hA} + \frac{\beta(S^0+V^0(1-\sigma))}{S^0+V^0} I_h \\ \omega(1-\epsilon)E_h - \Phi_2 I_{hA} \\ \epsilon\omega E_h + \alpha(1-\kappa)I_{hA} - \Phi_3 I_h \\ \gamma_1 I_h - \Phi_4 J_h \end{pmatrix} \tag{4.3.23}$$

and

$$G(X,Y) = \begin{pmatrix} \lambda S_h + (1-\sigma)\lambda V_h - \Phi_1 E_h \\ \omega(1-\epsilon)E_h - \Phi_2 I_{hA} \\ \epsilon\omega E_h + \alpha(1-\kappa)I_{hA} - \Phi_3 I_h \\ \gamma_1 I_h - \Phi_4 J_h \end{pmatrix} \tag{4.3.24}$$

Substituting equations (4.3.23) and (4.3.24) to equation (4.3.21) and performing some algebraic manipulation gives:

$$\tilde{G}(X,Y) = \begin{pmatrix} \lambda S^0 \left(\frac{\mathcal{X}_h}{S^0+V^0} - \frac{S_h}{S^0}\right) + \lambda(1-\sigma)V^0 \left(\frac{\mathcal{X}_h}{S^0+V^0} - \frac{V_h}{V^0}\right) \\ 0 \\ 0 \\ 0 \end{pmatrix} \tag{4.3.25}$$

From equation (4.3.25) it is evident that $\tilde{G}(X,Y) \geq 0$ for all $(X,Y) \in \Omega$. Both conditions $(C1)$ and $(C2)$ are satisfied thus the DFE, denoted as B^{0i}, is globally asymptotically stable provided that $R_{0i} < 1$. □

4.3.8 Endemic Equilibrium Point(EEP)

Endemic equilibrium for our model is caused by COVID-19 persistence in the community. We denote this equilibrium by $B^*_{0i} = (S^*_h, V^*_h, E^*_h, I^*_{hA}, I^*_h, J^*_h, R^*_h)$.

We denote the force of infection as

$$\lambda_f^* = \frac{\beta(\eta I_{hA}^* + I_h^*)}{N_h^* - J_h^*} \tag{4.3.26}$$

To obtain the value of B_{0i}^*, we equate equation (4.3.1) to zero. i.e

$$\begin{cases} \pi + \varphi V_h^* - \lambda_f^* S_h^* - (\mu + \theta) S_h^* = 0 \\ \theta S_h^* - (1-\sigma)\lambda_f^* V_h^* - (\mu + \varphi) V_h^* = 0 \\ \lambda_f^* S_h^* + (1-\sigma)\lambda_f^* V_h^* - (\mu + \omega) E_h^* = 0 \\ (1-\epsilon)\omega E_h^* - (\mu + \alpha) I_h^* = 0 \\ \epsilon\omega E_h^* + (1-\kappa) I_{hA}^* - (\mu + \gamma_1 + \gamma_2 + \delta_1) I_h^* = 0 \\ \gamma_1 I_h^* - (\mu + \delta_2 + \gamma_3) J_h^* = 0 \\ \gamma_2 I_h^* + \alpha\kappa I_{hA}^* + \gamma_3 J_h^* - \mu R_h^* = 0 \end{cases} \tag{4.3.27}$$

We solve the above system to obtain:

$$\begin{cases} S_h^* = \frac{((1-\sigma)\lambda_f^* + \Phi_5)\pi}{((1-\sigma)\lambda_f^* + \Phi_5)(\lambda_f^* + \Phi_0) - \theta\varphi} \\ V_h^* = \frac{\theta\pi}{((1-\sigma)\lambda_f^* + \Phi_5)(\lambda_f^* + \Phi_0) - \theta\varphi} \\ E_h^* = \frac{\lambda_f^* * S_h^*((1-\sigma)(\lambda_f^* + \theta)\Phi_5)}{\Phi_1((1-\sigma)\lambda_f^* + \Phi_5)} \\ I_{hA}^* = \frac{\omega(1-\epsilon)\lambda_f^* S_h^*((1-\sigma)(\lambda_f^* + \theta) + \Phi_5)}{\Phi_1\Phi_2((1-\sigma)\lambda_f^* + \Phi_5)} \\ I_h^* = \frac{\omega\lambda_f^* S_h^*((1-\sigma)(\lambda_f^* + \theta) + \Phi_5)(\epsilon\Phi_2 + \alpha(1-\kappa)(1-\epsilon))}{\Phi_1\Phi_2\Phi_3((1-\sigma)\lambda_f^* + \Phi_5)} \\ J_h^* = \frac{\omega\lambda_f^* S_h^*\gamma_1((1-\sigma)(\lambda_f^* + \theta) + \Phi_5)(\epsilon\Phi_2 + \alpha(1-\kappa)(1-\epsilon))}{\Phi_1\Phi_2\Phi_3\Phi_4((1-\sigma)\lambda_f^* + \Phi_5)} \\ R_h^* = \frac{\omega\lambda_f^* S_h^*((1-\sigma)(\lambda_f^* + \theta) + \Phi_5)(\alpha\kappa\Phi_3\Phi_4 + (\epsilon\Phi_2 + (1-\kappa)(1-\epsilon)(\gamma_2\Phi_4 + \gamma_1\gamma_3)))}{\mu K_1\Phi_2\Phi_3\Phi_4((1-\sigma)\lambda_f^* + \Phi_5)} \end{cases} \tag{4.3.28}$$

Substituting equation (4.3.28) to (4.3.26) gives:

$$P_2\lambda_f^{*2} + P_1\lambda_f^* + P_0 = 0 \tag{4.3.29}$$

Where

$P_2 = \Phi_2\Phi_3\Phi_4\mu\sigma_1+\Phi_2\Phi_4\epsilon\gamma_2\omega\sigma_1+\Phi_2\Phi_4\epsilon\mu\omega\sigma_1+\Phi_2\epsilon\gamma_1\gamma_3\omega\sigma_1+\Phi_3\Phi_4\alpha\kappa\omega\sigma_1+$
$\Phi_3\Phi_4\epsilon_1\mu\omega\sigma_1 + \Phi_4\alpha\epsilon_1\gamma_2\kappa_1\omega\sigma_1 + \Phi_4\alpha\epsilon_1\kappa_1\mu\omega\sigma_1 + \alpha\epsilon_1\gamma_1\gamma_3\kappa_1\omega\sigma_1$

$P_1 = \Phi_1\Phi_2\Phi_3\Phi_4\mu\sigma_1+\Phi_2\Phi_3\Phi_4\Phi_5\mu+\Phi_2\Phi_3\Phi_4\mu\sigma_1\theta+\Phi_2\Phi_4\Phi_5\epsilon\gamma_2\omega+\Phi_2\Phi_4\Phi_5\epsilon\mu\omega+$
$\Phi_2\Phi_4\epsilon\gamma_2\omega\sigma_1\theta+\Phi_2\Phi_4\epsilon\mu\omega\sigma_1\theta+\Phi_2\Phi_5\epsilon\gamma_1\gamma_3\omega+\Phi_2\epsilon\gamma_1\gamma_3\omega\sigma_1\theta+\Phi_3\Phi_4\Phi_5\alpha\kappa\omega+$
$\Phi_3\Phi_4\Phi_5\epsilon_1\mu\omega+\Phi_3\Phi_4\alpha\kappa\omega\sigma_1\theta+\Phi_3\Phi_4\epsilon_1\mu\omega\sigma_1\theta+\Phi_4\Phi_5\alpha\epsilon_1\gamma_2\kappa_1\omega+\Phi_4\Phi_5\alpha\epsilon_1\kappa_1\kappa_1\mu\omega+$
$\Phi_4\alpha\epsilon_1\gamma_2\kappa_1\omega\sigma_1\theta+\Phi_4\alpha\epsilon_1\kappa_1\mu\omega\sigma_1\theta+\Phi_5\alpha\epsilon_1\gamma_1\gamma_3\kappa_1\omega+\alpha\epsilon_1\gamma_3\kappa_1\omega\sigma_1\theta-\Phi_4\beta\mu\omega\sigma_1(\Phi_2\epsilon+$
$\Phi_3\epsilon_1\eta + \alpha\epsilon_1\kappa_1)$

$P_0 = \mu\Phi_1\Phi_2\Phi_3\Phi_4(\Phi_5 + \theta)(1 - R_{0i})$

Where $\sigma_1 = (1 - \sigma)$, $\kappa_1 = (1 - \kappa)$ and $\epsilon_1 = (1 - \epsilon)$.

We note that P_2, the coefficient of λ_f^{*2} is positive. It is explicitly clear that λ_f^* is given by the positive real roots of the polynomial (4.3.29). The number of all possible positive real roots of the quadratic polynomial (4.3.29) depends on the sign of P_0 and P_1. We establish this by utilizing Descarte's rule of sign. We illustrate the number of probabilities in the table below:

Table 4.9: Number of possible positive roots of the quadratic equation.

Case	P_2	P_1	P_0	R_{0i}	Changes in Sign	Positive Roots
1	+	-	-	$R_{0i} > 1$	1	1
2	+	+	-	$R_{0i} > 1$	1	1
3	+	-	+	$R_{0i} < 1$	2	2
4	+	+	+	$R_{0i} < 1$	0	0

From the table above, we can deduce the following:

(i) A unique endemic equilibrium exists if $P_0 < 0$ (i.e. if $R_{0i} > 1$), regardless the sign of P_1;

(ii) A unique endemic equilibrium exists if $P_1 < 0$; and $P_0 = 0$; or $P_1^2 - 4P_0P_2 = 0$;

(iii) Two endemic equilibria exist if $P_0 > 0$; $P_1 < 0$ and $P_1^2 - 4P_0P_2 > 0$;

(iv) There are no endemic equilibria if $P_0 > 0$ and $P_1 > 0$.

It is worth noting that case (iii) points to the fact that backward bifurcation in this model cannot be ruled out. The implication of this condition is the possibility of coexistence of stable DFE with a stable endemic equilibrium when the reproduction number R_{0i} is less than one(1). Epidemiologically, case (iii) indicates that $R_{0i} < 1$, is a necessary, but not sufficient condition for COVID-19 eradication in the community. Backward bifurcation thus frustrates the government efforts to compact the epidemic. For us to abase COVID-19 transmission, we have to scale down R_{0i} below

the critical value R_{0i}^c. To obtain R_{0i}^c, we equate the discriminant of the equation (4.3.29) to zero. Thus we get:

$$R_{0i}^c = 1 - \frac{P_1^2}{4P_2\mu\Phi_1\Phi_2\Phi_3\Phi_4(\Phi_5+\theta)}$$

Backward bifurcation thus occurs for values of $R_{0i}^c < R_{0i} < 1$. The results of this subsection can be summarized in the theorem below:

Theorem 4.14. *If $R_{0i} < 1$, then B_i^0 is an equilibrium of the system (4.3.1) and it is locally asymptotically stable. Furthermore, there exists an endemic equilibrium if conditions in item (ii) are satisfied, or two endemic equilibria if conditions in item (iii) are met. If $R_{0i} > 1$, then B_i^0 is unstable and there exists a unique endemic equilibrium.*

4.3.9 Bifurcation analysis of the Model

We utilize the center manifold theorem (Castillo-Chavez et al. [26]) to determine the local asymptotic stability of endemic equilibrium. The signs of two coefficients, a and b that represents the dynamics on the center manifold are investigated. If $a < 0$ and $b > 0$, then the bifurcation is forward; if $a > 0$ and $b > 0$, then the bifurcation is backward. We note that backward bifurcation has an implication that $R_{0i} < 1$ is no longer tenable condition for COVID-19 eradication in the community.

Theorem 4.15. *The endemic equilibrium point, based on the Theorem 4.1 by Castillo-Chavez et al. [26] is locally asymptotically stable for $R_{0i} > 1$ (but near 1).*

Proof. We first rewrite our model (4.3.2) by expressing $S_h = x_1$, $V_h =$

x_2, $E_h = x_3$, $I_{hA} = x_4$, $I_h = x_5$, $J_h = x_6$ and $R_h = x_7$. We further define equation $\frac{dX}{dt} = F(x)$ where $X = (x_1, x_2, x_3, x_4, x_5, x_6, x_7)$ and $F = (f_1, f_2, f_3, f_4, f_5, f_6, f_7)$.Thus:

$$\begin{cases} \frac{dx_1}{dt} = f_1 = \pi + \varphi x_2 - \frac{\beta(\eta x_4 + x_5)x_1}{x_1+x_2+x_3+x_4+x_5+x_7} - (\mu + \theta)x_1 \\ \frac{dx_2}{dt} = f_2 = \theta x_1 - \frac{\beta(1-\sigma)(\eta x_4 + x_5)x_2}{x_1+x_2+x_3+x_4+x_5+x_7} - (\mu + \varphi)x_2 \\ \frac{dx_3}{dt} = f_3 = \frac{\beta(\eta x_4 + x_5)x_1}{x_1+x_2+x_3+x_4+x_5+x_7} + \frac{\beta(1-\sigma)(\eta x_4 + x_5)x_2}{x_1+x_2+x_3+x_4+x_5+x_7} - (\mu + \omega)x_3 \\ \frac{dx_4}{dt} = f_4 = \omega(1-\epsilon)x_3 - (\mu + \alpha)x_4 \\ \frac{dx_5}{dt} = f_5 = \omega\epsilon x_3 + (1-k)\alpha x_4 - (\mu + \gamma_1 + \gamma_2 + \delta_1)x_5 \\ \frac{dx_6}{dt} = f_6 = \gamma_1 x_5 - (\mu + \delta_2 + \gamma_3)x_6 \\ \frac{dx_7}{dt} = f_7 = \gamma_2 x_5 + \kappa\alpha x_4 + \gamma_3 x_6 - \mu x_7 \end{cases} \tag{4.3.30}$$

We choose the rate of transmission $\beta = \beta^*$ as the bifurcation parameter. This is done by equating R_{0i} to one(1) and making it the subject of the formula.

$$\beta^* = \frac{\Phi_1\Phi_2\Phi_3(\theta + \Phi_5)}{\omega(\Phi_8 + \Phi_5)(\Phi_7\Phi_3 + \Phi_6)}$$

where as previously defined, $\Phi_1 = (\mu + \omega)$, $\Phi_2 = (\mu + \alpha)$, $\Phi_3 = (\mu + \gamma_1 + \gamma_2 + \delta_1)$, $\Phi_4 = (\mu + \gamma_3 + \delta_2)$ and $\Phi_5 = (\mu + \varphi)$

In order to make the analysis mathematically more tractable and convenient, we have introduced an additional symbols: $\Phi_6 = \alpha(1-\kappa) + \epsilon(\mu + \alpha\kappa)$, $\Phi_7 = \eta(1-\epsilon)$ and $\Phi_8 = \theta(1-\sigma)$.

We substitute the value of β^* in the DFE matrix (4.3.13) to give the matrix B^*_{0i} as:

$$\begin{pmatrix} -\Phi_0 & \varphi & 0 & -\frac{\eta\Phi_1\Phi_2\Phi_3\Phi_5}{\omega(\Phi_5+\Phi_8)(\Phi_6+\Phi_3\Phi_7)} & -\frac{\Phi_1\Phi_2\Phi_3\Phi_5}{\omega(\Phi_5+\Phi_8)(\Phi_6+\Phi_3\Phi_7)} & 0 & 0 \\ \theta & -\Phi_5 & 0 & -\frac{\eta\Phi_1\Phi_2\Phi_3\Phi_8}{\omega(\Phi_5+\Phi_8)(\Phi_6+\Phi_3\Phi_7)} & -\frac{\Phi_1\Phi_2\Phi_3\Phi_8}{\omega(\Phi_5+\Phi_8)(\Phi_6+\Phi_3\Phi_7)} & 0 & 0 \\ 0 & 0 & -\Phi_1 & \frac{\eta\Phi_1\Phi_2\Phi_3}{\omega(\Phi_6+\Phi_3\Phi_7)} & \frac{\Phi_1\Phi_2\Phi_3}{\omega(\Phi_6+\Phi_3\Phi_7)} & 0 & 0 \\ 0 & 0 & \omega(1-\epsilon) & -\Phi_2 & 0 & 0 & 0 \\ 0 & 0 & \epsilon\omega & \alpha(1-\kappa) & -\Phi_3 & 0 & 0 \\ 0 & 0 & 0 & 0 & \gamma_1 & -\Phi_4 & 0 \\ 0 & 0 & 0 & \alpha\kappa & \gamma_2 & \gamma_3 & -\mu) \end{pmatrix} \tag{4.3.31}$$

The eigenvalues of the above matrix are:$\lambda_1 = 0$, $\lambda_2 = -\mu$, $\lambda_3 = -\mu$, $\lambda_4 = -(\mu + \theta + \varphi)$ and $\lambda_5 = -(\mu + \delta_2 + \gamma_3) = -\Phi_4$. The two other eigenvalues have negative real parts. The presence of the simple zero(0) eigenvalue of the Jacobian matrix $J_{(B_{0i},\beta^*)}$ permits us to utilize the center manifold theory in order to determine the local stability of the endemic equilibrium B^*_{0i}. We first evaluate the right eigenvector $W = (w_1, w_2, w_3, w_4, w_5, w_6, w_7)^T$ by utilizing the matrix equation:

$$(\mathbf{B}^*_{0i} - \lambda\mathbf{I})(\mathbf{W}) = 0 \tag{4.3.32}$$

where $\lambda = 0$ and $\mathbf{I}$ is a 7×7 identity matrix. This gives:

$$\begin{cases} w_1 = -\frac{\Phi_1\Phi_2(\Phi_5^2+\varphi\Phi_8)}{\mu(\theta+\Phi_5)(\Phi_5+\Phi_8)}, \\ w_2 = -\frac{\Phi_1\Phi_2(\theta\Phi_5+\Phi_0\Phi_8)}{\mu(\theta+\Phi_5)(\Phi_5+\Phi_8)}, \\ w_3 = \Phi_2, \quad w_4 = \omega(1-\epsilon), \quad w_5 = \frac{\omega\Phi_6}{\Phi_3}, \quad w_6 = \frac{\omega\gamma_1\Phi_6}{\Phi_3\Phi_4}, \\ w_7 = \frac{\omega(\alpha\kappa(1-\epsilon)\Phi_3\Phi_4+(\gamma_2\Phi_4+\gamma_1\gamma_3)\Phi_6)}{\mu\Phi_3\Phi_4} \end{cases}$$

We now compute the left eigenvectors associated with the zero(0) eigenvalue, (i.e $(\mathbf{B}^{*T}_{0i} - \lambda\mathbf{I})(\mathbf{V}) = 0$, for $\lambda = 0$ and considering the fact that $\mathbf{V}.\mathbf{W} = 1$. This gives:

$$v_1 = v_2 = v_6 = v_7 = 0, v_3 = 1, v_4 = \frac{\Phi_1(\eta\Phi_3 + \alpha(1-\kappa))}{\omega(\Phi_6 + \Phi_3\Phi_7)}, v_5 = \frac{\Phi_1\Phi_2}{\omega(\Phi_6 + \Phi_3\Phi_7)}$$

The local stability of the endemic equilibrium is determined by utilizing the method implemented by Castilo-Chavez and Song [26] where we have the bifurcation constants a and b defined as:

$$a = \sum_{k,i,j=1}^{7} v_k w_i w_j \frac{\partial^2 f_k}{\partial x_i \partial x_j}(B_{0i}, \beta^*)$$

and

$$b = \sum_{k,i,j=1}^{7} v_k w_i \frac{\partial^2 f_k}{\partial x_i \partial \beta}(B_{0i}, \beta^*)$$

We note that we do not need to compute the derivatives of f_1, f_2, f_6 and f_7 since $v_1 = v_2 = v_6 = v_7 = 0$. Furthermore, from the second order partial derivatives of f_3, f_4 and f_5, the non-zero derivatives are:
$\frac{\partial^2 f_3}{\partial x_4 \partial \beta^*}(B_{0i}, \beta^*) = \frac{\eta(\mu+\varphi+\theta(1-\sigma))}{(\mu+\theta+\varphi)}$ and $\frac{\partial^2 f_3}{\partial x_5 \partial \beta^*}(B_{0i}, \beta^*) = \frac{\eta(\mu+\varphi+\theta(1-\sigma))}{(\mu+\theta+\varphi)}$
Thus $b = v_3 \left(w_4 \frac{\partial^2 f_3}{\partial x_4 \partial \beta}(B_{0i}, \beta) + w_5 \frac{\partial^2 f_3}{\partial x_5 \partial \beta}(B_{0i}, \beta) \right)$
Upon substitution and simplification, we obtain the value of b as:

$$b = (\eta w_4 + w_5)\frac{(\mu + \varphi + \theta(1-\sigma))}{(\mu + \theta + \varphi)} > 0$$

Since b is positive, the direction of bifurcation is determined by the sign of constant a. The non-zero derivatives of equation (4.3.30) for determining

the value of a are:

$$\begin{cases} \frac{\partial^2 f_3}{\partial x_4 \partial x_1}(B_{0i},\beta^*) = \frac{\partial^2 f_3}{\partial x_1 \partial x_4}(B_{0i},\beta^*) = \frac{\beta^*\eta\mu\theta\sigma}{\pi(\mu+\theta+\varphi)} \\ \frac{\partial^2 f_3}{\partial x_4 \partial x_2}(B_{0i},\beta^*) = \frac{\partial^2 f_3}{\partial x_2 \partial x_4}(B_{0i},\beta^*) = -\frac{\beta^*\eta\mu\sigma(\mu+\varphi)}{\pi(\mu+\theta+\varphi)} \\ \frac{\partial^2 f_3}{\partial x_4 \partial x_3}(B_{0i},\beta^*) = \frac{\partial^2 f_3}{\partial x_3 \partial x_4}(B_{0i},\beta^*) = -\frac{\beta^*\eta\mu(\mu+\varphi+\theta(1-\sigma))}{\pi(\mu+\theta+\varphi)} \\ \frac{\partial^2 f_3}{\partial x_4 \partial x_4}(B_{0i},\beta^*) = -\frac{2\beta^*\eta\mu(\mu+\varphi+\theta(1-\sigma))}{\pi(\mu+\theta+\varphi)} \\ \frac{\partial^2 f_3}{\partial x_4 \partial x_5}(B_{0i},\beta^*) = \frac{\partial^2 f_3}{\partial x_5 \partial x_4}(B_{0i},\beta^*) = -\frac{\beta^*(\eta+1)\mu(\mu+\varphi+\theta(1-\sigma))}{\pi(\mu+\theta+\varphi)} \\ \frac{\partial^2 f_3}{\partial x_4 \partial x_7}(B_{0i},\beta^*) = \frac{\partial^2 f_3}{\partial x_7 \partial x_4}(B_{0i},\beta^*) = -\frac{\beta^*\eta\mu(\mu+\varphi+\theta(1-\sigma))}{\pi(\mu+\theta+\varphi)} \\ \frac{\partial^2 f_3}{\partial x_1 \partial x_5}(B_{0i},\beta^*) = \frac{\partial^2 f_3}{\partial x_5 \partial x_1}(B_{0i},\beta^*) = \frac{\beta^*\mu\theta\sigma}{\pi(\mu+\theta+\varphi)} \\ \frac{\partial^2 f_3}{\partial x_2 \partial x_5}(B_{0i},\beta^*) = \frac{\partial^2 f_3}{\partial x_5 \partial x_2}(B_{0i},\beta^*) = -\frac{\beta^*\mu\sigma(\mu+\varphi)}{\pi(\mu+\theta+\varphi)} \\ \frac{\partial^2 f_3}{\partial x_3 \partial x_5}(B_{0i},\beta^*) = \frac{\partial^2 f_3}{\partial x_5 \partial x_3}(B_{0i},\beta^*) = -\frac{\beta^*\mu(\mu+\varphi+\theta(1-\sigma))}{\pi(\mu+\theta+\varphi)} \\ \frac{\partial^2 f_3}{\partial x_5 \partial x_5}(B_{0i},\beta^*) = -\frac{2\beta^*\mu(\mu+\varphi+\theta(1-\sigma))}{\pi(\mu+\theta+\varphi)} \\ \frac{\partial^2 f_3}{\partial x_7 \partial x_5}(B_{0i},\beta^*) = \frac{\partial^2 f_3}{\partial x_5 \partial x_7}(B_{0i},\beta^*) = -\frac{\beta^*\mu(\mu+\varphi+\theta(1-\sigma))}{\pi(\mu+\theta+\varphi)} \end{cases} \tag{4.3.33}$$

Thus:

$$\begin{cases} a = 2\Big\{ w_1 w_4 \frac{\partial^2 f_3}{\partial x_1 \partial x_4}(B_{0i},\beta^*) + w_2 w_4 \frac{\partial^2 f_3}{\partial x_2 \partial x_4}(B_{0i},\beta^*) + w_3 w_4 \frac{\partial^2 f_3}{\partial x_3 \partial x_4}(B_{0i},\beta^*) \\ + {w_4}^2 \frac{\partial^2 f_3}{\partial {x_4}^2}(B_{0i},\beta^*) + w_5 w_4 \frac{\partial^2 f_3}{\partial x_5 \partial x_4}(B_{0i},\beta^*) + w_7 w_4 \frac{\partial^2 f_3}{\partial x_7 \partial x_4}(B_{0i},\beta^*) \\ + w_1 w_5 \frac{\partial^2 f_3}{\partial x_1 \partial x_5}(B_{0i},\beta^*) + w_2 w_5 \frac{\partial^2 f_3}{\partial x_2 \partial x_5}(B_{0i},\beta^*) + w_3 w_5 \frac{\partial^2 f_3}{\partial x_3 \partial x_5}(B_{0i},\beta^*) \\ + {w_5}^2 \frac{\partial^2 f_3}{\partial {x_5}^2}(B_{0i},\beta^*) + w_7 w_5 \frac{\partial^2 f_3}{\partial x_7 \partial x_5}(B_{0i},\beta^*) \Big\} \end{cases} \tag{4.3.34}$$

Substituting equation (4.3.33) into (4.3.34) and further simplification gives the value of a as:

$$a = \frac{2\beta^*\mu(\eta w_4 + w_5)}{\pi(\mu+\theta+\varphi)}\left\{\sigma((\mu+\varphi)w_2 - \theta w_1) - (w_3+w_4+w_5+w_7)(\mu+\varphi+\theta(1-\sigma))\right\} \tag{4.3.35}$$

Assuming a situation where vaccine confers permanent immunity to infection, then $\sigma = 1$. Substituting the values of parameters as displayed in table (4.8) except for $\sigma = 1$, the terms in parentheses in equation (4.3.35) gives the value of -0.04013582. This gives $a < 0$ which implies that backward bifurcation is precluded when the vaccine administered offers 100% determent to infection. This is in conformity to research by Gummel[48]. We make an assumption that $a > 0$. This implies that:

$\sigma((\mu+\varphi)w_2 - \theta w_1) - (w_3+w_4+w_5+w_7)(\mu+\varphi+\theta(1-\sigma)) > 0$

This gives:

$$\sigma > \frac{(w_3+w_4+w_5+w_7)(\mu+\varphi+\theta)}{(\mu+\varphi)w_2 - \theta w_1 + (w_3+w_4+w_5+w_7)\theta} \tag{4.3.36}$$

Theorem 4.16. *The system (4.3.2) undergoes backward bifurcation at $R_{0i} = 1$ whenever inequality (4.3.36) holds.*

Substituting parameter values as given in table (4.8), gives:

$\frac{(w_3+w_4+w_5+w_7)(\mu+\varphi+\theta)}{(\mu+\varphi)w_2-\theta w_1+(w_3+w_4+w_5+w_7)\theta} = 1.006564 > 1$

This is a contradiction since σ ranges from zero to one exclusive, thus $a < 0$. This rules out the possibility of backward bifurcation for model (4.3.2) at $R_{0i} = 1$.

Since $a < 0$ and $b > 0$ at $\beta = \beta^*$, as per Castilo-Chavez and Song theorem, the model (4.3.2) undergoes forward/transcritical bifurcation.

The forward bifurcation has an an implication that as the basic reproduction number crosses the critical value $R_{0i} = 1$, the system transits

from one equilibrium point, a typically stable point, to two non-negative equilibrium points, with one of them stable and the other one being unstable. This means that covid-19 fizzles out from the general population for $R_{0i} < 1$. On the contrary, for $R_{0i} > 1$, the persistence of the disease in the community is assured. □

4.3.10 Global Stability of COVID-19 Endemic Equilibrium

Theorem 4.17. *The unique endemic equilibrium B^*_{0i} of the model (4.3.2) is globally asymptotically stable in Ω whenever $R_{0i} > 1$.*

Proof. We let $\alpha_1, \alpha_2, \alpha_3, \alpha_4, \alpha_5$ and α_6 be positive constants and with no loss of generality, we consider a special case of our system where $\varphi = 0$ and $\kappa = 1$ and also bilinear incident rate as utilized by Rabiu et al. [90], Safi et al. [95] and Sun et al.[104]. The reduced system under consideration is thus:

$$\begin{cases} \frac{dS_h}{dt} = \pi - \lambda S_h - (\mu + \theta)S_h \\ \frac{dV_h}{dt} = \theta S_h - (1-\sigma)\lambda V_h - \mu V_h \\ \frac{dE_h}{dt} = \lambda S_h + (1-\sigma)\lambda V_h - (\mu + \omega)E_h \\ \frac{dI_{hA}}{dt} = (1-\epsilon)\omega E_h - (\mu + \alpha)I_{hA} \\ \frac{dI_h}{dt} = \epsilon\omega E_h - (\mu + \gamma_1 + \gamma_2 + \delta_1)I_h \\ \frac{dJ_h}{dt} = \gamma_1 I_h - (\mu + \delta_2 + \gamma_3)J_h \end{cases} \tag{4.3.37}$$

where $\lambda = \beta(\eta I_{hA} + I_h)$

We define a non-linear Lyapunov function for our reduced system as,

$$V = \alpha_1 V_1 + \alpha_2 V_2 + \alpha_3 V_3 + \alpha_4 V_4 + \alpha_5 V_5 + \alpha_6 V_6$$

where

$$\begin{cases} V_1 = S_h^* . \chi\left(\frac{S_h}{S_h^*}\right), V_2 = V_h^* . \chi\left(\frac{V_h}{V_h^*}\right), V_3 = E_h^* . \chi\left(\frac{E_h}{E_h^*}\right), \\ V_4 = I_{hA}^* . \chi\left(\frac{I_{hA}}{I_{hA}^*}\right), V_5 = I_h^* . \chi\left(\frac{I_h}{I_h^*}\right), V_6 = J_h^* . \chi\left(\frac{J_h}{J_h^*}\right) \end{cases} \tag{4.3.38}$$

and that $\chi(y) = y - 1 - \ln y \geq \chi(1) = 0$, for any $y > 0$

Differentiating the function V gives:

$$\begin{cases} \frac{dV}{dt} = \alpha_1 \left(1 - \frac{S_h^*}{S_h}\right) \frac{dS_h}{dt} + \alpha_2 \left(1 - \frac{V_h^*}{V_h}\right) \frac{dV_h}{dt} + \alpha_3 \left(1 - \frac{E_h^*}{E_h}\right) \frac{dE_h}{dt} \\ \quad + \alpha_4 \left(1 - \frac{I_{hA}^*}{I_{hA}}\right) \frac{dI_{hA}}{dt} + \alpha_5 \left(1 - \frac{I_h^*}{I_h}\right) \frac{dI_h}{dt} + \alpha_6 \left(1 - \frac{J_h^*}{J_h}\right) \frac{dJ_h}{dt} \end{cases} \tag{4.3.39}$$

We can rewrite the above equation as:

$$\begin{cases} \frac{dV}{dt} = \alpha_1 \left(1 - \frac{S_h^*}{S_h}\right) [\pi - \beta(\eta I_{hA} + I_h) S_h - (\mu + \theta) S_h] \\ \quad + \alpha_2 \left(1 - \frac{V_h^*}{V_h}\right) [\theta S_h - (1 - \sigma)\beta(\eta I_{hA} + I_h) V_h - \mu V_h] \\ \quad + \alpha_3 \left(1 - \frac{E_h^*}{E_h}\right) [\beta(\eta I_{hA} + I_h) S_h + (1 - \sigma)\beta(\eta I_{hA} + I_h) V_h - (\mu + \omega) E_h] \\ \quad + \alpha_4 \left(1 - \frac{I_{hA}^*}{I_{hA}}\right) [(1 - \varepsilon)\omega E_h - (\mu + \alpha) I_{hA}] \\ \quad + \alpha_5 \left(1 - \frac{I_h^*}{I_h}\right) [\varepsilon\omega - (\mu + \gamma_1 + \gamma_2 + \delta_1) I_h] \\ \quad + \alpha_6 \left(1 - \frac{J_h^*}{J_h}\right) [\gamma_1 I_h - (\mu + \delta_2 + \gamma_3) J_h] \end{cases} \tag{4.3.40}$$

It's worth noting that at endemic steady-state B_{0i}^*,

$$\begin{cases} \pi = \beta(\eta I_{hA}^* + I_h)S_h^* + (\mu+\theta)S_h^*, \theta = \frac{(1-\sigma)\beta(\eta I_{hA}^* + I_h^*)V_h^* + \mu V_h^*}{S_h^*} \\ (\mu+\omega) = \frac{\beta(\eta I_{hA}^* + I_h)S_h^* + (1-\sigma)\beta(\eta I_{hA}^* + I_h^*)V_h^*}{E_h^*}, (\mu+\alpha) = \frac{(1-\varepsilon)E_h^*}{I_{hA}^*}, \\ (\mu+\gamma_1+\gamma_2+\delta_1) = \frac{\varepsilon\omega E_h^*}{I_h^*}, (\mu+\delta_2+\gamma_3) = \frac{\gamma_1 I_h^*}{J_h^*} \end{cases} \tag{4.3.41}$$

Substituting (4.3.41) into (4.3.40) yields;

$$\begin{cases} \frac{dV}{dt} = \alpha_1\left(1-\frac{S_h^*}{S_h}\right)\left\{\beta\eta I_{hA}^* S_h^*\left(1-\frac{I_{hA}S_h}{I_{hA}^*S_h^*}\right) + \beta I_h^* S_h^*\left(1-\frac{I_h S_h}{I_h^* S_h^*}\right)\right. \\ \left. +(\mu+\theta)S_h^*\left(1-\frac{S_h}{S_h^*}\right)\right\} + \alpha_2\left(1-\frac{V_h^*}{V_h}\right)\left\{(1-\sigma)\beta\eta I_{hA}^* V_h^*\left(\frac{S_h}{S_h^*}-\frac{I_{hA}V_h}{I_{hA}^*V_h^{**}}\right)\right. \\ \left. +(1-\sigma)\beta I_h^* V_h^*\left(\frac{S_h}{S_h^*}-\frac{I_h V_h}{I_h^* V_h^*}\right) + \mu V_h^*\left(\frac{S_h}{S_h^*}-\frac{V_h}{V_h^*}\right)\right\} \\ +\alpha_3\left(1-\frac{E_h^*}{E_h}\right)\left\{\beta\eta I_{hA}^* S_h^*\left(\frac{S_h I_{hA}}{S_h^* I_{hA}^*}-\frac{E_h}{E_h^*}\right) + \beta I_h^* S_h^*\left(\frac{S_h I_h}{S_h^* I_h^*}-\frac{E_h}{E_h^*}\right)\right. \\ \left. +(1-\sigma)\beta\eta I_{hA}^* V_h^*\left(\frac{V_h I_{hA}}{V_h^* I_{hA}^*}-\frac{E_h}{E_h^*}\right) + (1-\sigma)\beta I_h^* V_h^*\left(\frac{V_h I_h}{V_h^* I_h^*}-\frac{E_h}{E_h^*}\right)\right\} \\ +\alpha_4\left(1-\frac{I_{hA}^*}{I_{hA}}\right)(1-\varepsilon)\omega E_h^*\left\{\frac{E_h}{E_h^*}-\frac{I_{hA}}{I_{hA}^*}\right\} + \alpha_5\left(1-\frac{I_h^*}{I_h}\right)\varepsilon\omega E_h^*\left\{\frac{E_h}{E_h^*}-\frac{I_h}{I_h^*}\right\} \\ +\alpha_6\left(1-\frac{J_h^*}{J_h}\right)\gamma_1 I_h^*\left\{\frac{I_h}{I_h^*}-\frac{J_h}{J_h^*}\right\} \end{cases} \tag{4.3.42}$$

We introduce the notation: $m_1 = \frac{S_h}{S_h^*}$, $m_2 = \frac{V_h}{V_h^*}$, $m_3 = \frac{E_h}{E_h^*}$, $m_4 = \frac{I_{hA}}{I_{hA}^*}$, $m_5 = \frac{I_h}{I_h^*}$, $m_6 = \frac{J_h}{J_h^*}$.

Equation (4.3.42) becomes:

$$\begin{cases} \frac{dV}{dt} = -\frac{\alpha_1}{m_1}(m_1-1)^2(\mu+\theta)S_h^* \\ \quad +\alpha_1\beta\eta I_{hA}^* S_h^*\left\{\left(1-\frac{1}{m_1}\right)(1-m_1m_4)+\frac{\alpha_3}{\alpha_1}\left(1-\frac{1}{m_3}\right)(m_1m_4-m_3)\right\} \\ \quad +\alpha_1\beta I_h^* S_h^*\left\{\left(1-\frac{1}{m_1}\right)(1-m_1m_5)+\frac{\alpha_3}{\alpha_1}\left(1-\frac{1}{m_3}\right)(m_1m_5-m_3)\right\} \\ \quad +\alpha_2(1-\sigma)\beta\eta I_{hA}^* V_h^*\left\{\left(1-\frac{1}{m_2}\right)(1-m_2m_4)+\frac{\alpha_3}{\alpha_2}\left(1-\frac{1}{m_3}\right)(m_2m_4-m_3)\right\} \\ \quad +\alpha_2(1-\sigma)\beta I_h^* V_h^*\left\{\left(1-\frac{1}{m_2}\right)(1-m_2m_5)+\frac{\alpha_3}{\alpha_2}\left(1-\frac{1}{m_3}\right)(m_2m_5-m_3)\right\} \\ \quad +\alpha_2\mu V_h^*\left(1-\frac{1}{m_2}\right)(m_1-m_2)+\alpha_4(1-\varepsilon)\omega E_h^*\left(1-\frac{1}{m_4}\right)(m_3-m_4) \\ \quad +\alpha_5\varepsilon\omega E_h^*\left(1-\frac{1}{m_5}\right)(m_3-m_5)+\alpha_6\gamma_1 I_h^*\left(1-\frac{1}{m_6}\right)(m_5-m_6) \end{cases} \tag{4.3.43}$$

We let $\alpha_1 = \alpha_2 = \alpha_3$. The equation (4.3.43) becomes:

$$\begin{cases} \frac{dV}{dt} = -\frac{\alpha_1}{m_1}(m_1-1)^2(\mu+\theta)S_h^* \\ \quad +\alpha_1\beta\eta I_{hA}^* S_h^*\left\{2+m_4-\frac{1}{m_1}-m_3-\frac{m_1m_4}{m_3}\right\} \\ \quad +\alpha_1\beta I_h^* S_h^*\left\{2+m_5-\frac{1}{m_1}-m_3-\frac{m_1m_5}{m_3}\right\} \\ \quad +\alpha_2(1-\sigma)\beta\eta I_{hA}^* V_h^*\left\{1+m_1+m_4-\frac{m_1}{m_2}-m_3-\frac{m_2m_4}{m_3}\right\} \\ \quad +\alpha_2(1-\sigma)\beta I_h^* V_h^*\left\{1+m_1+m_5-\frac{m_1}{m_2}-m_3-\frac{m_2m_5}{m_3}\right\} \\ \quad +\alpha_2\mu V_h^*\left\{1+m_1-m_2-\frac{m_1}{m_2}\right\}+c_4(1-\varepsilon)\omega E_h^*\left\{1+m_3-m_4-\frac{m_3}{m_4}\right\} \\ \quad +\alpha_5\epsilon\omega E_h^*\left\{1+m_3-m_5-\frac{m_5}{m_6}\right\}+c_6\gamma_1 I_h^*\left\{1+m_5-m_6-\frac{m_5}{m_6}\right\} \end{cases} \tag{4.3.44}$$

We let $\alpha_4 = \frac{(1-\sigma)\beta\eta I_{hA}^* V_h^*}{(1-\epsilon)\omega E_h^*}\alpha_2$ and $\alpha_5 = \frac{(1-\sigma)\beta I_h^* V_h^*}{\varepsilon\omega E_h^*}\alpha_2$. Equation (4.3.44) reduces to:

$$\begin{cases} \frac{dV}{dt} = -\frac{\alpha_1}{m_1}(m_1-1)^2(\mu+\theta)S_h^* \\ \quad +\alpha_1\beta\eta I_{hA}^* S_h^*\left\{2+m_4-\frac{1}{m_1}-m_3-\frac{m_1m_4}{m_3}\right\} \\ \quad +\alpha_1\beta I_h^* S_h^*\left\{2+m_5-\frac{1}{m_1}-m_3-\frac{m_1m_5}{m_3}\right\} \\ \quad +\alpha_2(1-\sigma)\beta\eta I_{hA}^* V_h^*\left\{2+m_1-\frac{m_1}{m_2}-\frac{m_3}{m_4}-\frac{m_2m_4}{m_3}\right\} \\ \quad +\alpha_2(1-\sigma)\beta I_h^* V_h^*\left\{2+m_1-\frac{m_1}{m_2}-\frac{m_5}{m_6}-\frac{m_2m_5}{m_3}\right\} \\ \quad +\alpha_2\mu V_h^*\left\{1+m_1-m_2-\frac{m_1}{m_2}\right\} \\ \quad +\alpha_6\gamma_1 I_h^*\left\{1+m_5-m_6-\frac{m_5}{m_6}\right\} \end{cases} \tag{4.3.45}$$

Substituting back the values of m_i for $i = 1, 2, 3, 4, 5, 6$ to (4.3.45) and further reorganization of the equation gives:

$$\begin{cases} \frac{dV}{dt} = -(\mu+\theta)\frac{\alpha_1}{S_h}\left(\frac{S_h}{S_h^*}-1\right)^2 S_h^{*2} \\ \quad +\alpha_1\beta\eta I_{hA}^* S_h^*\left\{2-\frac{S_h^*}{S_h}-\frac{E_h}{E_h^*}-\frac{I_{hA}}{I_{hA}^*}\left(\frac{S_h}{S_h^*}\frac{E_h^*}{E_h}-1\right)\right\} \\ \quad +\alpha_1\beta\eta I_h^* S_h^*\left\{2-\frac{S_h^*}{S_h}-\frac{E_h}{E_h^*}-\frac{I_h}{I_h^*}\left(\frac{S_h}{S_h^*}\frac{E_h^*}{E_h}-1\right)\right\} \\ \quad +\alpha_2(1-\sigma)\beta\eta I_{hA}^* V_h^*\left\{2-\frac{E_h}{E_h^*}\frac{I_{hA}^*}{I_{hA}}-\frac{V_h}{V_h^*}\frac{E_h^*}{E_h}\frac{I_{hA}}{I_{hA}^*}-\frac{S_h}{S_h^*}\left(\frac{V_h^*}{V_h}-1\right)\right\} \\ \quad +\alpha_2(1-\sigma)\beta I_h^* V_h^*\left\{2-\frac{I_h}{I_h^*}\frac{J_h^*}{J_h}-\frac{V_h}{V_h^*}\frac{E_h^*}{E_h}\frac{I_h}{I_h^*}-\frac{S_h}{S_h^*}\left(\frac{V_h^*}{V_h}-1\right)\right\} \\ \quad +\alpha_2\mu V_h^*\left\{1-\frac{V_h}{V_h^*}-\frac{S_h}{S_h^*}\left(\frac{V_h^*}{V_h}-1\right)\right\} \\ \quad +\alpha_6\gamma_1 I_h^*\left\{1-\frac{J_h}{J_h^*}-\frac{I_h}{I_h^*}\left(\frac{J_h^*}{J_h}-1\right)\right\} \end{cases} \tag{4.3.46}$$

Finally, utilizing the same concept advanced by Nainggolan et al. [79], Nyaberi et al. [83] and Safi et al. [95], it is evident that:

$$\left\{2-\frac{S_h^*}{S_h}-\frac{E_h}{E_h^*}-\frac{I_{hA}}{I_{hA}^*}\left(\frac{S_h}{S_h^*}\frac{E_h^*}{E_h}-1\right)\right\}\leq 0$$
$$\left\{2-\frac{S_h^*}{S_h}-\frac{E_h}{E_h^*}-\frac{I_h}{I_h^*}\left(\frac{S_h}{S_h^*}\frac{E_h^*}{E_h}-1\right)\right\}\leq 0$$
$$\left\{2-\frac{E_h}{E_h^*}\frac{I_{hA}^*}{I_{hA}}-\frac{V_h}{V_h^*}\frac{E_h^*}{E_h}\frac{I_{hA}}{I_{hA}^*}-\frac{S_h}{S_h^*}\left(\frac{V_h^*}{V_h}-1\right)\right\}\leq 0$$

$$\left\{2-\frac{I_h}{I_h^*}\frac{J_h^*}{J_h}-\frac{V_h}{V_h^*}\frac{E_h^*}{E_h}\frac{I_h}{I_h^*}-\frac{S_h}{S_h^*}\left(\frac{V_h^*}{V_h}-1\right)\right\}\leq 0$$
$$\left\{1-\frac{V_h}{V_h^*}-\frac{S_h}{S_h^*}\left(\frac{V_h^*}{V_h}-1\right)\right\}\leq 0$$
$$\left\{1-\frac{J_h}{J_h^*}-\frac{I_h}{I_h^*}\left(\frac{J_h^*}{J_h}-1\right)\right\}\leq 0$$

It is worth noting that since all the model parameters are non-negative, $\frac{dV}{dt} \leq 0$ for $R_{0i} > 1$. Further, $\frac{dV}{dt} = 0$ if and only if $S_h = S_h^*$, $V_h = V_h^*$, $E_h = E_h^*$, $I_{hA} = I_{hA}^*$, $I_h = I_h^*$, $J_h = J_h^*$. Thus by LaSalle's invariance principle (Hale [50] and LaSalle [69]), it follows that every solution of the system (4.3.1) with initial conditions in the region $\Omega = \{(S_h, V_h, E_h, I_{hA}, I_h, J_h, R_h) \in \mathbb{R}_+^7; S_h > 0; V_h, E_h, I_{hA}, I_h, J_h, R_h \geq 0; N \leq \frac{\pi}{\mu}\}$ approach the endemic equilibrium point B_{0i}^*. Thus B_{0i}^* is globally asymptotically stable. □

4.3.11 Sensitivity Analysis of Model 2

In this section, we determine the most influential parameters by carrying out the sensitivity of model parameters with respect to the basic reproduction number R_{0i}. Implementation of sensitivity analysis entails computation of the sensitivity indices of the reproduction number R_{0i} subsequently to each parameter in the model. This permits us to quantify the effects of relative perturbation of a parameter to the COVID-19 infection and transmission dynamics. To investigate the most influential parameters we utilize the normalized forward sensitivity index.

Definition 4.18. The normalized forward index of a parameter $\mathcal{H}$ which

depends differentially on a parameter ϑ, is defined by:

$$\Xi_{\vartheta}^{\mathcal{H}} = \frac{\partial \mathcal{H}}{\partial \vartheta} \times \frac{\vartheta}{\mathcal{H}}$$

From the explicit equation of R_{0i},

$$R_{0i} = \frac{\omega\beta(\theta(1-\sigma)+\mu+\varphi)(\eta(1-\epsilon)(\mu+\gamma_1+\gamma_2+\delta_1)+\alpha(1-\kappa)+\epsilon(\mu+\alpha\kappa))}{(\mu+\omega)(\mu+\alpha)(\mu+\theta+\varphi)(\mu+\gamma_1+\gamma_2+\delta_1)}$$

the analytical expression for the sensitivity of parameter φ with respect to R_{0i} is derived as:

$$\Xi_{\varphi}^{R_{0i}} = \frac{\partial R_{0i}}{\partial \varphi} \times \frac{\varphi}{R_{0i}} = 0.007568$$

In the similar manner we obtain the sensitivity indices of the remaining parameters by utilizing baseline values as tabulated in table (4.8). The parameter and the corresponding sensitivity indices are written in the table (4.10). From the table (4.10), we note that the parameters with positive indices have a significant influence in accelerating the growth of disease. For instance, from $\frac{\partial R_{0i}}{\partial \varphi} \times \frac{\varphi}{R_{0i}} = 0.007568$, we deduce that increasing (or decreasing) the waning of vaccine factor by 10% causes a corresponding increase (or decrease) of reproduction number R_{0i} by 0.07568%. Furthermore, the parameters with negative indices implies that an increase of these parameters would be very paramount if the efforts against the spread of COVID-19 are going to bear fruits. For instance, increasing(or decreasing) γ_1 (the rate at which the symptomatic patients are isolated) by 10% would leading to the corresponding decrease(or increase) in the reproduction number by 1.51151%.

Table 4.10: The normalized forward sensitivity indices of R_ν to model parameters evaluated at the baseline parameters as displayed in the table(4.5)

Parameters	Sensitivity indices	Values
β	$\Xi_\beta^{R_{0i}}$	+1.000000
ϵ	$\Xi_\epsilon^{R_{0i}}$	+0.023408
η	$\Xi_\eta^{R_{0i}}$	+0.011593
ω	$\Xi_\omega^{R_{0i}}$	+0.008605
φ	$\Xi_\varphi^{R_{0i}}$	+0.007568
γ_2	$\Xi_{\gamma_2}^{R_{0i}}$	-0.604605
δ_1	$\Xi_{\delta_1}^{R_{0i}}$	-0.217658
γ_1	$\Xi_{\gamma_1}^{R_{0i}}$	-0.151151
κ	$\Xi_\kappa^{R_{0i}}$	-0.097026
μ	$\Xi_\mu^{R_{0i}}$	-0.0339244
θ	$\Xi_\theta^{R_{0i}}$	-0.011739

In figure (4.3.2): (a) the contours shows increasing the rate at which the symptomatic individuals are isolated γ_1 at a given value of disease transmission coefficient β leads to corresponding decrease in the reproduction number R_{0i} while increase in β at a particular value of γ_1 leads to increase in R_{0i}. In (b), it can be deduced that increasing the rate of detection and treatment coefficient κ of asymptomatic individuals at a specified value of transmission coefficient β leads to decrease in the R_{0i}. The contours displayed in (c) depicts that increasing the vaccine efficacy σ at a given value of β leads to reduction in the reproduction number. Furthermore, in

figure (d) the impact of simultaneous variation of modification parameter η and the rate of detection and treatment coefficient κ of asymptomatic individuals on reproduction numberR_{0i} is assessed. It is observed that at a given value of κ, increase in η leads to a corresponding increase in R_{0i}.

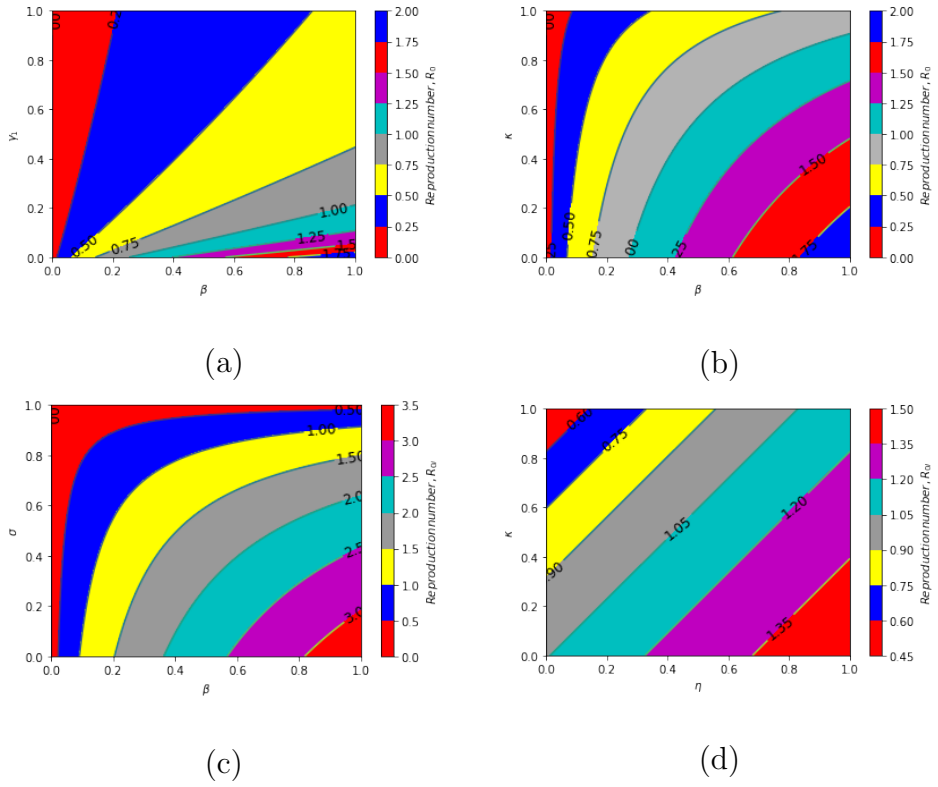

Fig. 4.3.2. Contour plots for R_{0i} versus: (a) transmission rate β and rate of isolation of symptomatic persons γ_1, (b) transmission rate β and detection rate of asymptomatic persons κ, (c) transmission rate β and vaccine efficacy coefficient σ and (d) modification factor of asymptomatic η and detection rate of asymptomatic persons κ.

In figure (4.3.3), panels (a) and (b) illustrates some of the parameters that leads to the growth of reproduction number. In (a) the reproduc-

tion number R_{0i} is directly proportional to the transmission coefficient β while (b) demonstrates a nonlinear relationship between waning of vaccine coefficient φ and R_{0i}. Moreover, panels (c) and (d) shows some of the parameters that cause decrease in reproduction number. In (c), the reproduction number is inversely proportional to the vaccine efficacy coefficient σ while (d) illustrates an exponential decrease in R_{0i} as the rate at which the infectious individuals are isolated γ_1 is increased.

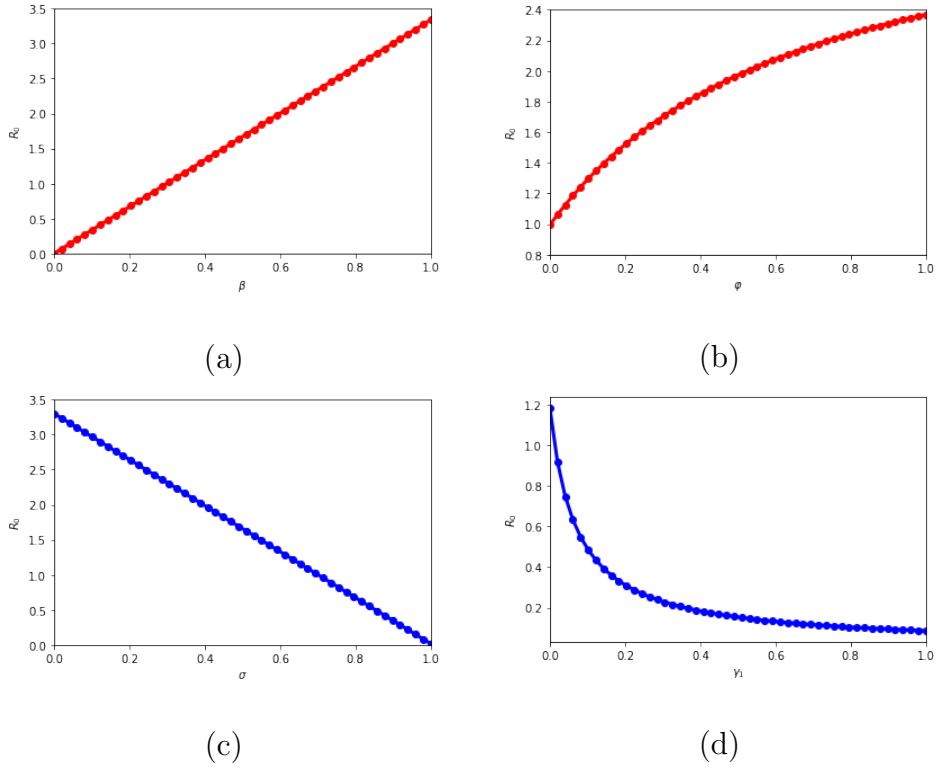

Fig. 4.3.3. Variation of R_{0i} with respect to: (a) coefficient of transmission β, (b) vaccine waning coefficient φ, (c) vaccine efficacy coefficient σ and (d) the rate of isolation of symptomatic individuals γ_1.

4.3.12 Effects of vaccination on COVID-19 control strategy

In this subsection we qualitatively explore the impact of vaccination of susceptible population on COVID-19 transmission dynamics. This is implemented by performing partial derivatives of the basic reproduction number R_0 with respect to the rate of vaccination θ. This gives:

$$\frac{\partial R_0}{\partial \theta} = -\frac{\sigma\Phi_5\beta\omega\{\alpha(1-\kappa)+\epsilon(\alpha\kappa+\mu)+\eta(1-\epsilon)\Phi_4\}}{\Phi_1\Phi_2\Phi_4(\theta+\Phi_5)^2}$$

so that $\frac{\partial R_0}{\partial \theta} < 0$ for all $0 < \sigma < 1$. From the above analysis, it is apparent that the vaccine efficacy always have a positive population-level impact. This implies that for every value of vaccine efficacy, the vaccination of susceptible population causes substantial reduction in the basic reproduction number R_0 leading to reduced COVID-19 infections. We summarise this result in the lemma below:

Lemma 1. For model (4.3.2), the impact of vaccination of the susceptible population always have positive population-level impact for every $0 < \sigma < 1$.

It is evident that the basic reproduction number R_0 is a decreasing function with respect to vaccination rate regardless of the value of σ.

4.3.13 Numerical results and discussion

In this section, we perform numerical simulation in order to verify the analytical results. In order to validate the local stability of DFE of model

(4.3.2), we choose the initial state variables as follows: $V_h = 500$, $E_h = 6500$, $I_{hA} = 560$, $I_h = 50$, $J_h = 20$ and $R_h = 60$. We now establish the initial size of the susceptible population by utilizing equation $S_h = N_h - (V_h + E_h + I_{hA} + I_h + J_h + R_h)$, where $N_h = 54027487$. Furthermore, we choose $\beta = 0.150000025$ and the other parametric values remain the same as displayed in table (4.8). At this value of $\beta = 0.150000025$, the reproduction number assumes the value $R_{0i} = 0.501281 < 1$. We note that the COVID-19 DFE is given by $E^0 = (54027487, 0, 0, 0, 0, 0, 0)$. The local stability of DFE for the model(4.3.2) is illustrated in figure (4.3.4). From this figure, it is apparent that the infective population gradually tends to disease free-equilibrium.

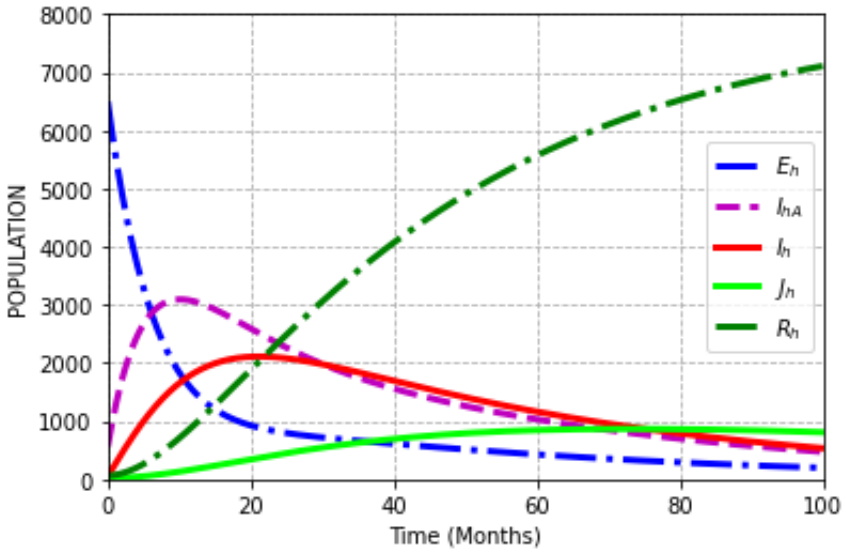

Fig. 4.3.4. The local stability of DFE for model (4.3.1). Parameter values used are those displayed in table (4.5) except for $\beta = 0.150000025$, so that $R_{0i} = 0.501281 < 1$.

For COVID-19 endemic equilibrium, we assume the following values for state variables: $B*_{0i} = (5.4001377\times10^{+7}, 5000, 8560, 4000, 500, 2000, 6050)$ and the reproduction number $R_{0i} = 1.0025636 > 1$. The local stability of EE for the model (4.3.2) is illustrated in figure(4.3.5). In this figure, all the infective compartments coexist in the population and tend to endemic equilibrium.

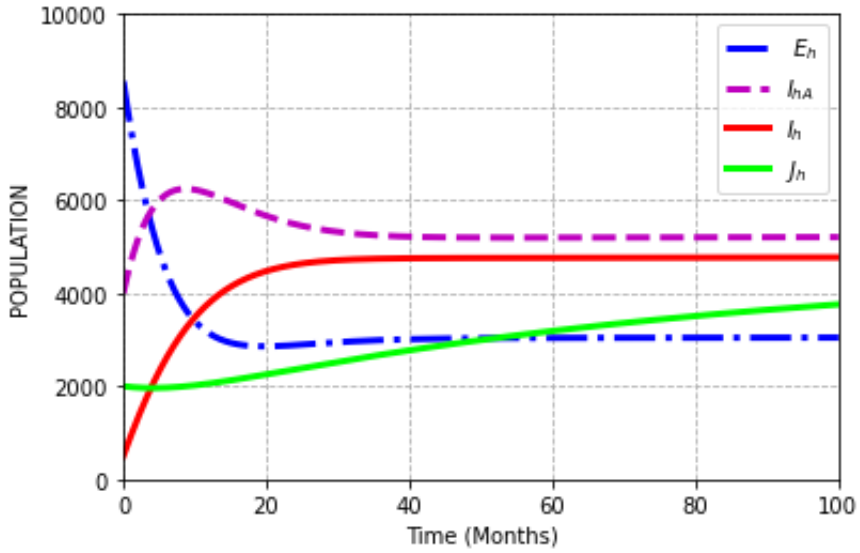

Fig. 4.3.5. The local stability of EE for model (4.3.2). Parameter values used are those displayed in table (4.8) so that $R_{0i} = 1.0025636 > 1$.

The global stability of COVID-19 free-equilibrium(CFE) state in tandem with theorem(4.12) is encapsulated in figure (4.3.6). From this figure we can deduce that for distinct initial values of the infective populace i.e (exposed, asymptomatic, symptomatic and isolated), all solution trajectories ultimately converge to CFE.

Figure (4.3.7) is a display panels for cases in which different values of

vaccine efficacy are simulated for the infective population. It is observed that COVID-19 transmission can be tamed if the vaccine used is of comparatively higher effectiveness. In figure (4.3.8) the effects of transmission coefficients at different values are presented. It apparent that at a particular value of this coefficient the infective population grows and this may stretch the available health care facilities beyond limit. This graphical illustrations underscores the importance of NPIs as one of the concerted effort to curtail contact rate. In figure (4.3.9) projections of various values of waning of vaccine coefficients φ for the vaccinated population are displayed. From the panels, it is evident that the fight against COVID-19 growth may be hampered for higher values of φ since rapid growth of infectious population is witnessed especially for values of φ when $R_{0i} > 1$. These illustrations underscores the importance of administration of COVID-19 booster vaccine to the vaccinated population. Figure (4.3.10) gives illustrations of projections using various values of vaccination coefficient. From the panels, it is evident that increasing the rate at which COVID-19 vaccine is administered to the susceptible individuals significantly lessens COVID-19 escalation.

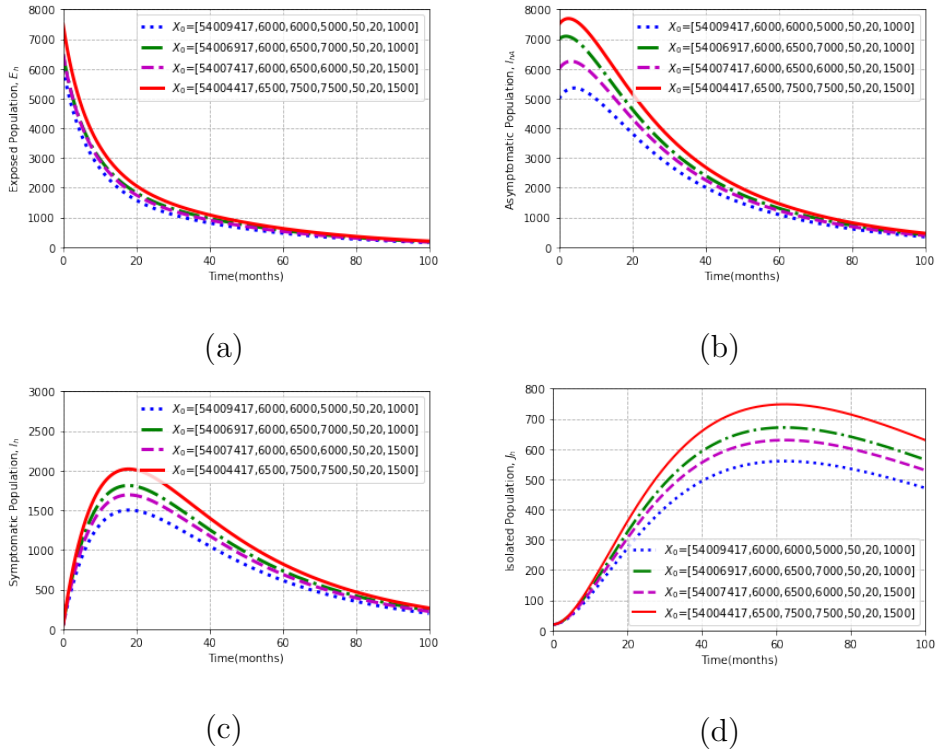

Fig. 4.3.6. Global convergence of solution trajectories for (a) Exposed, E_h (b) Asymptomatic, I_{hA} (c) Symptomatic, I_h and (d) Isolated, J_h individuals at distinct initial values in concurrence with theorem (4.12) by using parameter values as given in table (4.8) except for $\beta = 0.20000025$, so that $R_{0i} = 0.668376 < 1$.

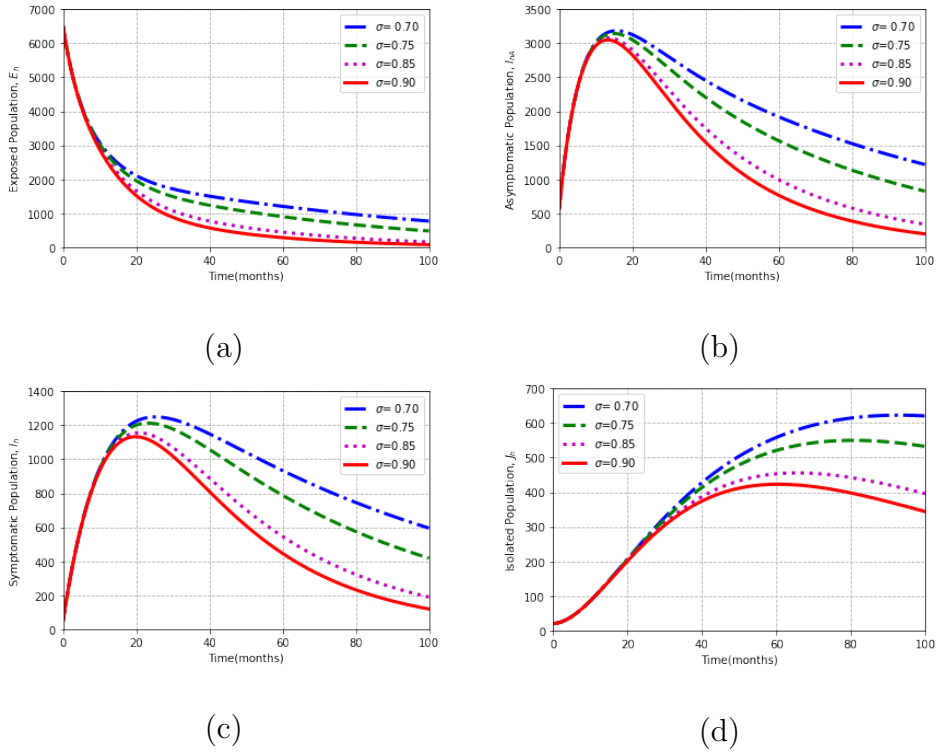

Fig. 4.3.7. Projections with varying effect of vaccine efficacy at values of $\sigma = 0.70(R_{0i} = 1.33675 > 1)$, $\sigma = 0.75(R_{0i} = 1.11771 > 1)$, $\sigma = 0.85(R_{0i} = 0.67964 < 1)$ and $\sigma = 0.90(R_{0i} = 0.46060 < 1)$ by using the parameters in table (4.8) except for $\beta = 0.40000025$ and the varied parameter.

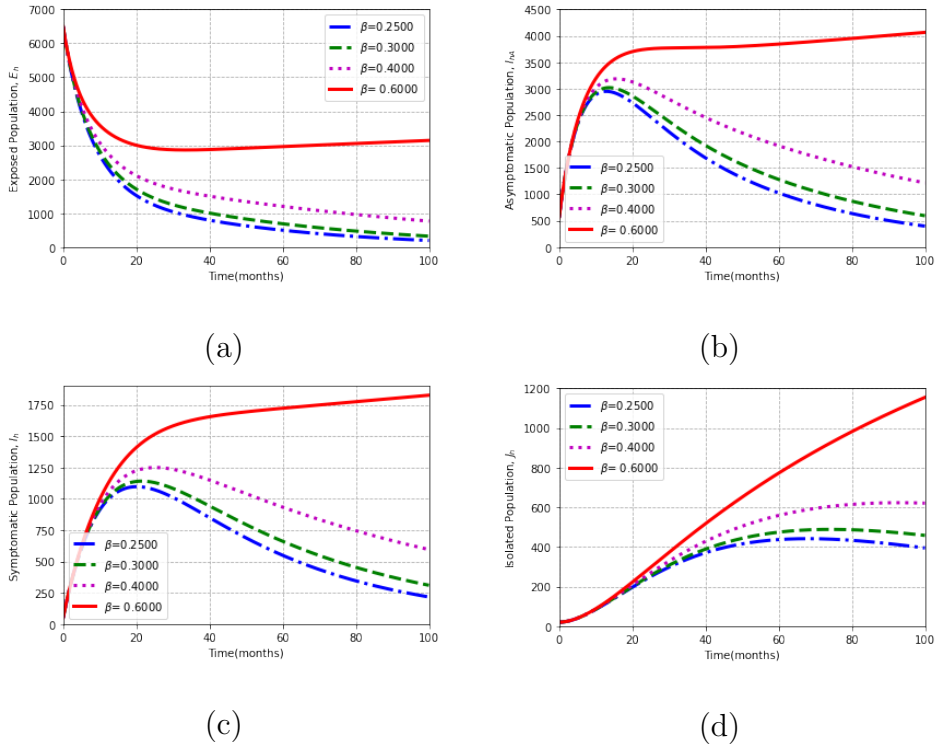

Fig. 4.3.8. Projections with varying effect of coefficient of transmission at values of $\beta = 0.25(R_{0i} = 0.83546 < 1)$, $\beta = 0.30(R_{0i} = 1.00256 > 1)$, $\beta = 0.40(R_{0i} = 1.33675 > 1)$ and $\beta = 0.60(R_{0i} = 2.00512 > 1)$ by using the parameters in table (4.8).

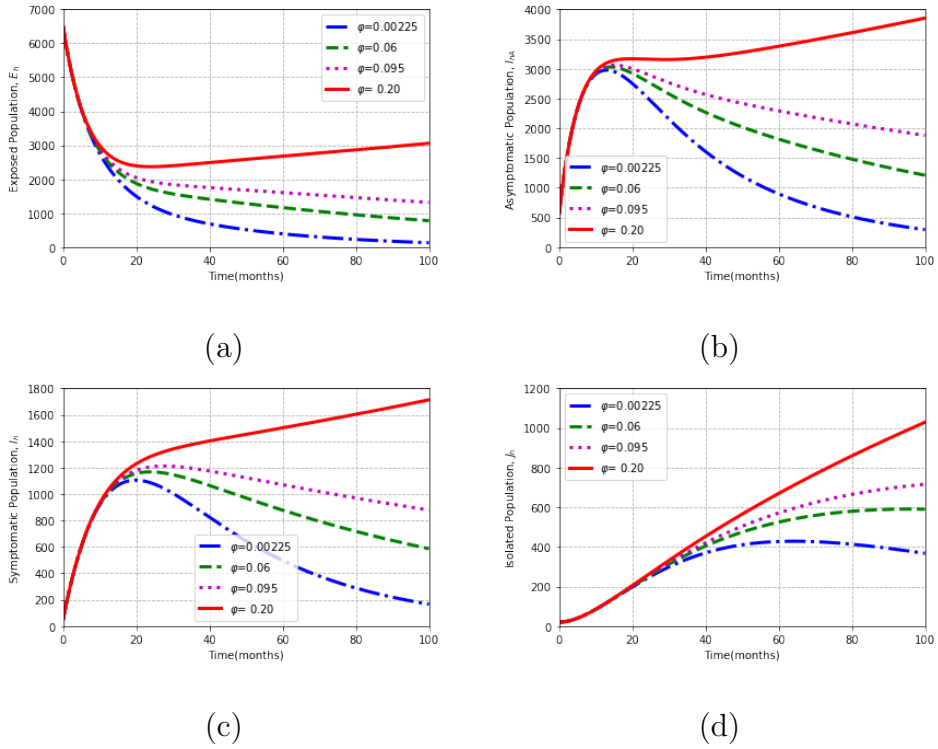

Fig. 4.3.9. Projections with varying effect of vaccine waning coefficients at values of $\varphi = 0.00225(R_{0i} = 0.67400 < 1)$, $\varphi = 0.06(R_{0i} = 0.87920 < 1)$, $\varphi = 0.095(R_{0i} = 0.98868 < 1)$ and $\varphi = 0.20(R_{0i} = 1.26483 > 1)$ by using the parameters in table (4.8) except the varied parameter.

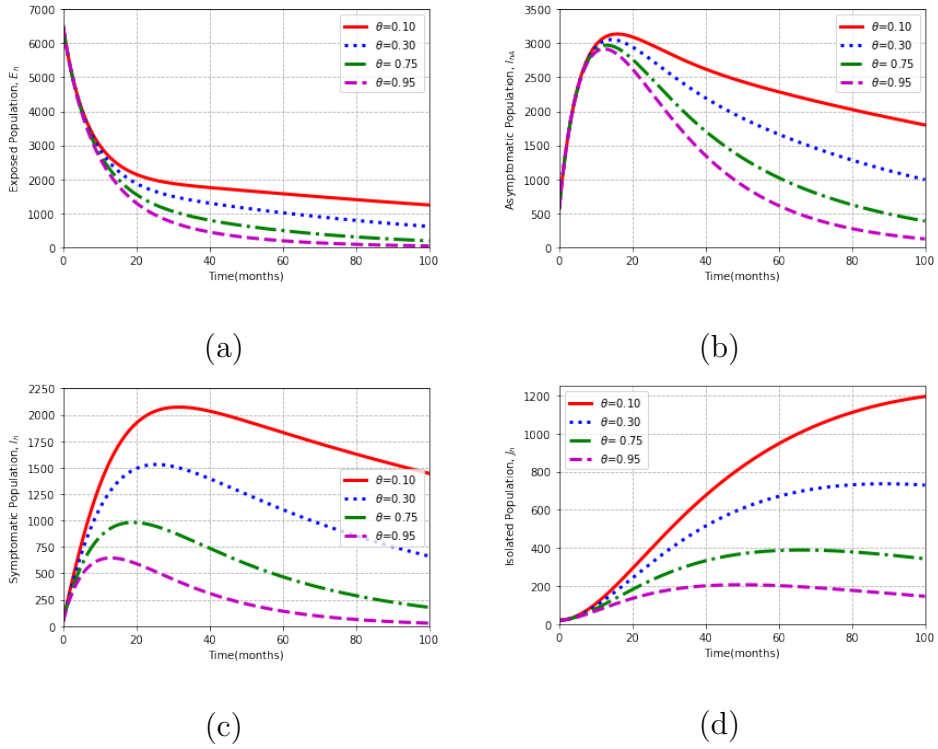

Fig. 4.3.10. Projections with varying effect of vaccination coefficients at values of $\theta = 0.10(R_{0i} = 1.00813 > 1)$, $\theta = 0.30(R_{0i} = 0.95966 < 1)$, $\theta = 0.75(R_{0i} = 0.94469 < 1)$ and $\theta = 0.95(R_{0i} = 0.94257 < 1)$ by using the parameters in table (4.8) except for $\beta = 0.2830000025$ and the varied parameter.

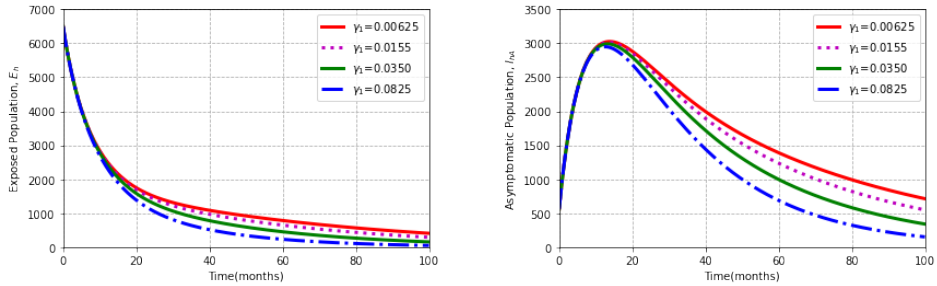

(a)

(b)

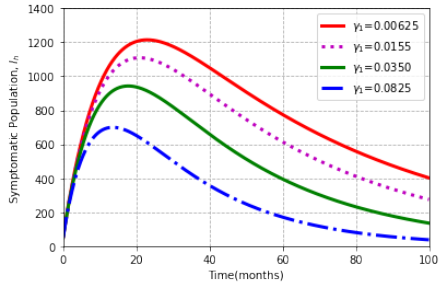

(c)

Fig. 4.3.11. Projections with varying effect of isolation coefficients at values of $\gamma_1 = 0.00625(R_{0i} = 1.084606 > 1)$, $\gamma_1 = 0.0.0155(R_{0i} = 0.967482 < 1)$, $\gamma_1 = 0.0350(R_{0i} = 0.788671 < 1)$ and $\gamma_1 = 0.0.0824(R_{0i} = 0.545427 < 1)$ by using the parameters in table (4.8) except for the varied parameter.

Chapter 5

CONCLUSION AND RECOMMENDATIONS

5.1 Introduction

In this section we give the highlights of the study findings for both models and thereafter give general recommendations as well as the recommendations for further studies.

5.2 Conclusion for Model 1

In this research we have formulated and theoretically analyzed a non-linear deterministic model for COVID-19 transmission dynamics by incorporating the main therapeutic measures such as vaccination of the susceptible and treatment of the infective population. The model has been used to describe the diverse transmission pathways in the infection dynamics and affirms the critical role played by vaccination and early

detection and treatment of the COVID-19 silent spreaders in curtailing the disease outbreak. We obtained the feasible region where the model has been proved to be epidemiologically well posed. We utilized the next generation matrix method to derive the reproduction number R_ν. We have also verified the local stability of the disease free equilibrium point by utilizing the Jacobian matrix, trace determinant method and Routh-Hurwitz criteria. The analytical results points to the fact that COVID-19 free-equilibrium is locally as well as globally asymptotically stable if $R_\nu < 1$ and unstable if $R_\nu > 1$. The global stability of CFE and COVID-19 endemic-equilibrium are investigated via Lyapunov function and LaSalle's Invariance principle. We also proved the condition for the existence of backward bifurcation using the center manifold theory as applied by Castillo-Chavez and Song where this phenomenon is driven by the rate of reinfection of the recovered individuals. From epidemiological view point, the implication of this is the possible coexistence of both CFE and CEE points even after the classical requirement of reducing the reproduction number below unit for the disease eradication has been met. This would frustrate the government and the policy makers' efforts to reduce infections. In the segment of parameter estimation, the model is fitted with real data of COVID-19 infected cases in Kenya as reported from March 30, 2020, to March 30, 2022. In the sensitivity analysis, the normalized sensitivity indices of R_ν reveals that the most sensitive parameters are β and ξ with positive sign which implies that decreasing contact rate between the susceptible and the infectives through maintaining social distance, use of face masks and washing hands with soap water among other non-pharmaceutical measures would decrease R_ν. Moreover, the

parameters θ, α and κ are the most sensitive parameters with negative sign. This signifies that to reduce transmission, a concerted efforts towards vaccinating the susceptible and early detection and treatment of the asymptomatic individuals should be prioritized by public health policy makers. From the numerical simulations, it is evident that to abase the reproduction number below unity, the transmission rate must be kept as low as possible via adherence to NPMs, administering booster vaccine to vaccinated population as well as early detection and treatment of the asymptomatic persons. This would ultimately lead to the reduction in the number of COVID-19 patients requiring specialized treatment and hence decongesting health care facilities.

5.3 Conclusion for Model 2

In model 2, we formulated a deterministic model incorporating imperfect vaccine, detection and treatment of asymptomatic as well as isolation of the symptomatic individuals. The feasible region derived revealed that the model is epidemiologically and mathematically well posed. Utilizing the next generation matrix, the basic reproduction R_{0i} is computed. Liénard-Chirpart method is utilized in establishing the local stability of DFE while the global stability of DFE is obtained using the technique by Chastillo-Chavez and Song. Considering the basic reproduction as the threshold quantity, we establish that COVID-19 free equilibrium point is both locally and globally asymptotically stable for $R_{0i} < 1$ and unstable when $R_{0i} > 1$. Utilizing the center manifold theory, we established the condition for existence of backward bifurcation which according to this

study it is dependent on vaccine efficacy. The global stability of endemic equilibrium is determined using Lyapunov function and LaSalle's invariance principle. On sensitivity analysis segment, normalized sensitivity index of R_{0i} is utilized in order to examine the contribution of individual parameter on the basic reproduction number. The parameters with positive sign such as β, φ and η causes COVID-19 to spiral in a population while the parameters such as σ, θ, γ_1 and κ with negative sign decelerates COVID-19 growth. This implies that the tripartite measures i.e vaccination of the susceptible individuals, early detection and treatment of the asymptomatic patients and isolation of the symptomatic individuals would curtail COVID-19 infections from burgeoning to catastrophic levels that would overwhelm our health care support system. Finally, on simulation, the result shows that COVID-19 persist in the community whenever $R_{0i} > 1$. This supports the fact that increase in transmission coefficient β leads to the corresponding increase in R_{0i}. It is also evident that increasing the waning coefficient of vaccine causes increase R_{0i}. This underscores the importance of administration of COVID-19 booster vaccine to the vaccinated population if R_{0i} is to be brought below unity.It is imperative from simulation results that COVID-19 can be managed via minimizing contact rate of infected and the susceptible, early detection and treatment of asymptomatic individuals, isolation of symptomatic as well as administration of vaccines with higher efficacy.

5.4 Recommendations

Utilizing the results obtained we do recommend the following to the policy makers in the heath sector;

(i) The government should increase the rate of sensitization of the general public on the need to observe non-pharmaceutical measures in order to stem the spread of COVID-19 infections. This can be done via the social media platforms and broadcasting stations.

(ii) The government via the ministry of health should make COVID-19 vaccine easily accessible to the susceptible population as well as encourage the vaccinated people to receive the booster vaccine.

(iii) The symptomatic population should be isolated expeditiously in order to alleviate COVID-19 transmission.

(iv) There should be earnest prioritization of mass testing to the at risk population for example the commercial trucks drivers. This encourages prompt identification and treatment of the asymptomatic persons hence mitigating escalation of COVID-19 transmission as well as severe cases.

(iv) The government of Kenya should give prominence to vaccinating the most vulnerable population which comprises of the elderly and people with compromised immune system in order to immensely avert critical COVID-19 illnesses and deaths.

We now make the following recommendations for further research:

(i) Inclusion of quarantine class as well as carrying out optimal control analysis for both models is paramount.

(ii) We need to consider incorporating contaminated environment class in $S_hV_hE_hI_{hA}I_hJ_hR_h$ model.

(iii) Future research should consider age dependent $S_hV_hE_hI_{hA}I_hJ_hR_h$ model to determine the appropriate vaccine for each age group. This is because studies have explicitly divulged that COVID-19 evidently affects distinctive age sets differently for instance, young people appear to experience placid COVID-19 infections.

References

[1] **Abdulamir A.S.**and **Hafidh R.R.** The Possible Immunological Pathways for the Variable Immunopathogenesis of COVID-19 Infections among Healthy Adults, Elderly and Children. *Electron J Gen Med. 17(4), (2020):em202*. https://doi.org/10.29333/ejgm/7850

[2] **Abdul-rahman J. M** and**Alfred K. H** Mathematical modelling on COVID-19 transmission impacts with preventive measures: a case study of Tanzania, *Journal of Biological Dynamics*, 14(1),(2020), 748-766, DOI: 10.1080/17513758.2020.1823494

[3] **Alligood K.T., Sauer T. D.** and **Yorke J. A.**, *Chaos: An Introduction to Dynamical Systems*, 1st ed. Springer-Verlag New York, 1996.

[4] **Alshammari S.**,A Mathematical Model to Investigate the Transmission of COVID-19 in the Kingdom of Saudi Arabia, *Computational and Mathematical Methods in Medicine*, (2020):9136157, https://doi.org/10.1155/2020/9136157

[5] **Agusto F.B.**, Optimal isolation control strategies and cost-effectiveness analysis of a two strain avian influenza model, *Biosystems*,(113): (2013). 10.1016/j.biosystems.2013.2013.06.004

[6] **Amirudin A., Syamsul M., Marnani C.S.,Rahmah N.A.** and **Wilopo**, Positive impacts among the negative impacts of the

COVID-19 pandemic for community life, *International Conference on Disaster Mitigation and Management (ICDMM 2021)*, (331): 01008 (2021). https://doi.org/10.1051/e3sconf/202133101008.

[7] **Anderson R. M.** and **May R. M.**, Infectious Diseases of Humans: *Dynamics and Control*. Oxford, 1991

[8] **Anggriania N.** and **Beay L.K**,Modeling of COVID-19 spread withself-isolation at home and hospitalized classes, *Results in physics*, (36): 105378 (2022). https://doi.org/10.1016/j.rinp.2022.105378

[9] **Arnold V. I.**, *Ordinary Differential Equations*. Massachusetts Institute of Technology Press, 1973.

[10] **Arrowsmith D.K.** and **Place C.M.** *Dynamical systems*. London-Chapman and Hall, 1992.

[11] **Asamoah J.K, Oduro F.T** and **Seidu B.**, Modeling of Rabies Transmission Dynamics Using Optical Control Analysis, *Journal of Applied Mathematics*, 2017:2451237, (2017), 1-22. https://doi.org/10.1155/2017/2451237.

[12] **Asha H.**and **Nyimvua S.**, Onchocerciasis dynamics: modelling the effects of treatment, education and vector control, *Journal of Biological Dynamics*, 14:1, (2020), 245-268, DOI: 10.1080/17513758.2020.1745306

[13] **Attila D.** and **Abba B. G**, Modeling the impact of quarantine during an outbreak of Ebola virus disease, *Infectious Disease Modelling*, 4(2019):12-27. https://doi.org/10.1016/j.idm.2019.01.003.

[14] **Bai Y., Yao L., Wei T. et al**, Presumed asymptomatic carrier transmission of COVID-19, *JAMA*, 323(14),(2020), 1406–1407. https://doi.org/10.1001/jama.2020.2565

[15] **Balloux F.,** and **van Dorp L.**, What are pathogens, and what have they done to and for us? *BMC biology*, 15(1),(2017), 91. doi: 10.1186/s12915-017-0433-z.

[16] **Barquet N.** and **Domingo P.**, Smallpox: The triumph over the most terrible of the minsters of death, *Annals of Internal Medicine*, 127.(1997), 635-642. 10.7326/0003-4819-127-8-Part-1-199710150-00010.

[17] **Baxby D.**Edward Jenner inquiry; a bicentenary analysis, *Vaccine*, 17(4),(1999), 301–307. https://doi.org/10.1016/s0264-410x(98)00207-2

[18] **Booth A.,Reed A.B,Ponzo S.,Yassaee A., Aral M.,Plans D.,etal.**,Population risk factors for severe disease and mortality in COVID19: A global systematic review and meta-analysis. *PloS one*, 16(3):e0247461,(2021). https://doi.org/ 10.1371/journal.pone.0247461

[19] **Boyce W.E** and **DiPrima R.C.**, *Elementary differential equations and boundary value problems*. Wiley, 2012.

[20] **Brauer F.** and **Castillo C.**, *Mathematical Models in Population Biology and Epidemiology*, 2nd ed. New York: Springer, 2012.

[21] **Brimnes N.**. Variolation, vaccination and popular resistance in early colonial South India. *Med Hist*, 48(2), (2004), 199–228. https://doi.org/10.1017/s0025727300000107

[22] **Bugalia S., Bajiya V.P., Tripathi J.P, Li M.T.** and **Sun G.Q.**, Mathematical modelling of COVID-19 transmission: The roles of intervention strategies and lockdown, *Mathematical biosciences and engineering : MBE*, 17(5),(2020),5961–5986. https://doi.org/10.3934/mbe.2020318

[23] **Buonomo B.**, Analysis of a malaria model with mosquito host choice and bed-net control, *International Jounal of Biomathematics*, (2013). 8. 10.1142/S1793524515500771.

[24] **Callender L.A., Curran M., Bates S.M., Mairesse M., Weigandt J.** and **Betts CJ**, The Impact of Pre-existing Comorbidities and Therapeutic Interventions on COVID-19.*Frontiers in immunology*, 11, (1991). https://doi.org/10.3389/fimmu.2020.01991

[25] **Cascella E.F.**,Features, Evaluation and Treatment Coronavirus (COVID-19). In StatPearls[Internet]. *StatPearls Publishing*. (2020).

[26] **Castillo-Chavez C** and **Song B**.Dynamical models of tuberculosis and their applications, *Mathematical biosciences and engineering : MBE*, 1(2),(2004), 361–404. https://doi.org/10.3934/mbe.2004.1.361

[27] **Centers for Disease Control and Prevention(CDC)**.Symptoms of coronavirus. Available from:https://www.cdc.gov/coronavirus/2019-ncov/about/symptoms.html.

[28] **Centers for Disease Control and Prevention(CDC)**. Vaccines and Immunizations: The Basics. *Washington, DC: Government Printing Office (2012).*

[29] **Chan J., Yuan S.** and **Kok K.** A familiarl cluster of pneumonia associate with the 2019 novel corona virus indicating person to person transmission: a study of family cluster, *Lancet (London, England)*, 395(10223), (2020), 514–523. https://doi.org/10.1016/S0140-6736(20)30154-9

[30] **Chan J.F. , Choi G.K. , Tsang A.K. , Tee K.M. , Lam H.Y. , Yip C.C. , et al.** Development and evaluation of novel real-time reverse transcription-PCR Assays with locked nucleic acid probes targeting leader sequences of human-pathogenic Coronaviruses. *Journal of clinical microbiology*, 53(8), (2015), 2722–2726. https://doi.org/10.1128/JCM.01224-15

[31] **Chavez C.C, Feng Z.** and **Huang W.**, On the computation of R_0 and its role on global stability, *Mathematical Approaches for Emerging and Reemerging Infectious Diseases: An Introduction, Springer, Berlin*, 229.(2002). https://doi.org/10.1007/978-1-4757-3667-0-13

[32] **Chitnis N, Hyman JM** and **Cushing JM**. Determining important parameters in spread of malaria through the sensitivity analysis of a mathematical model.*Bull Math Biol*, 70(5),(2008),1272-1296. https://dx.doi.org/10.1007/s11538-008-9299-0.

[33] **Chowell G.** and **Fenimore P.W.**, SARS outbreaks in Ontario, Hong Kong and Singapore: The role of diagnosis and isolation as a

control mechanism; *Journal of theoretical biology*, 224(1),(2003), 1–8. https://doi.org/10.1016/s0022-5193(03)00228-5

[34] Coronavirus Pandemic in Kenya.https://www.worldometers.info/coronavirus/country/

[35] **Deressa C.T, Mussa Y.O.** and **Duressa G.F.**, Optimal control and sensitivity analysis for transmission dynamics of Coronavirus, *Results in physics*, 19:103642, (2020). https://doi.org/10.1016/j.rinp.2020.103642

[36] **Diagne M. L., Rwezaura H., Tchoumi S.Y.** and **Tchuenche J.M**, "A mathematical model of COVID-19 with vaccination and treatment, *Computational and Mathematical Methods in Medicine*,(2021): 1250129, 1-16 .https://doi.org/10.1155/2021/1250129.

[37] **Diekmann O., Heesterbeek H.** and **Britton T.**, *Mathematical Tools for Understanding Infectious Disease Dynamics*. Princeton University Press, 2013.

[38] **Diekmann O.J., Heesterbeek H. P.** and **Roberts M. G.**, The construction of next-generation matrices for compartmental epidemic models,*Journal of the Royal Society, Interface*, 7(47), (2010), 873–885. https://doi.org/10.1098/rsif.2009.0386

[39] **Driessche P.V** and **Watmough J.**, Reproduction numbers and sub-threshold endemic equilibria for compartmental models for disease transmission, *Mathematical biosciences*, 180,(2002), 29–48. https://doi.org/10.1016/s0025-5564(02)00108-6

[40] **Edridge W.D, Kaczorowska J., Hoste A.R., Bakker M., Klein M., Jebbink M.F., Matser A., Kinsella C., Sastre P., Rueda P., Prins M., Deijns M.** and **Hoek L.**, Coronavirus protective immunity is short-lasting, 2020, https://www.medrxiv.org/content/10.1101/2020.05.11.20086439v2.

[41] **Ega T.T. , Luboobi L.S.** and **Kuznetsov D.**, Modeling the dynamics of rabies transmission with vaccination and stability analysis, *Appl. Comput. Math.*, 4(6),(2015),409-419. DOI: 10.11648/j.acm.20150406.13.

[42] **Ezzinbi K.**, *Lecture Note on ODEs.* AUST, 2018.

[43] **Fenner F., Henderson D. A., Arita I., Jezek Z.** and **Ladnyi I. D.**, Smallpox and its eradication, *World Health Organization*, 1988.

[44] **Fox J. P., Elveback L., Scott W., Gatewood L.** and **Ackerman E.** Herd immunity: basic concepts and relevance to public health immunization practices, *American journal of epidemiology*, 94(3),(1971), 179–189. https://doi.org/10.1093/oxfordjournals.aje.a121310

[45] **Ge F., Zhang L.W** and **Mu H.** Predicting psychological state among Chinese undergraduate students in the COVID-19 epidemic: A longitudinal study using a machine learning. *Neuropsychiatric disease and treatment*, 16, 2111–2118, (2020). https://doi.org/10.2147/NDT.S262004

[46] **Ghostine R., Gharamti M., Hassrouny S.** and **Hoteit I.** An Extended SEIR Model with Vaccination for Fore-

casting the COVID-19 Pandemic in Saudi Arabia Using an Ensemble Kalman Filter.*Mathematics*, 9(6), 636,(2021). https://doi.org/10.3390/math9060636

[47] **Guckenheimer J.** and **Holmes P.**, *Nonlinear oscillations, dynamical systems, and bifurcations of vector fields*, Springer Science and Business Media; 2013.

[48] **Gumel A.B.**, Causes of backward bifurcations in some epidemiological models, */J.Math.Anal.Appl.*,395(1), (2012),355-365. doi:10.1016/j.jmaa.2012.04.077

[49] **Gumel A.B.**, Modelling strategies for controlling SARS outbreaks; *Proceedings of the Royal Society of London - B* 271 (2004) 2223-2232.

[50] **Hale J.K**, *Ordinary Differential Equations*, John Wiley and Sons, New York, 1981.

[51] **Hammer W.**, Epidemic disease in england-the evidence of variability and the persistence of type, *The Lancet* Vol.(II), (1906), 733-739.

[52] **Heesterbeek J.**, A brief history of Ro and a recipe for its calculation, *Acta Biotheoretica*, 50, (2002),189-204. https://doi.org/10.1023/A:1016599411804

[53] **Hodgson S., Mansatta K., Mallett G., Harris V., Emary R. and Pollard J.**, What defines an efficacious covid-19 vaccine? a review of the challenges assessing the clinical efficacy of vaccines against sars-cov-2. *The Lancet. Infectious diseases*, 21(2), (2021), e26–e35. https://doi.org/10.1016/S1473-3099(20)30773-8

[54] **Huang, C., Wang, Y., Li, X., Ren, L., Zhao, J., Hu, Y., Zhang, L., Fan, G., Xu, J., Gu, X., Cheng, Z., Yu, T., Xia, J., Wei, Y., Wu, W., Xie, X., Yin, W., Li, H., Liu, M., Xiao, Y.** and **Cao, B.**, Clinical features of patients infected with 2019 novel coronavirus in Wuhan, China, *Lancet (London, England)*, 395:10223, (2020), 497–506. https://doi.org/10.1016/S0140-6736(20)30183-5.

[55] **Idris A, Goni U.M., Abdullahi Y., Poom K.** and **Ibrahim Y.**,A mathematical model of Coronavirus Disease (COVID-19) containing asymptomatic and symptomatic classes, *Results in physics*, 21: 103776, (2021). https://doi.org/10.1016/j.rinp.2020.103776

[56] **Isaacs, D., Flowers, D., Clarke, J. R., Valman, H. B.** and **MacNaughton, M. R.**, Epidemiology of coronavirus respiratory infections, *Archives of disease in childhood*, 58(7), (1983), 500–503. https://doi.org/10.1136/adc.58.7.500.

[57] **Karunathilake K.** Positive and negative impacts of COVID.19, an analysis with special reference to challenges on the supply chain in South Asian countries, *Journal of social and economic development*, 23(Suppl 3), (2021), 568–581. https://doi.org/10.1007/s40847-020-00107-z

[58] **Kassa S. M., Njagarah H.J.** and **Terefe Y. A.**, Analysis of the mitigation strategies for COVID-19, *From mathematical modelling perspective. Chaos, solitons, and fractals*, 138:109968, (2021). https://doi.org/10.1016/j.chaos.2020.109968

[59] **Kawski M**, *Introduction to Lyapunov Theory*, 2009.

[60] **Keeling M.J** and **Rohnai P.**, *Modeling infectious diseases in humans and animals*, Princeton University Press; 2008 p. 313-320

[61] Kenya Population.Available online, *https.//www.worldometers,info/world-population/Kenya-population/.* assessed on (12th December 2022).

[62] **Keno T. D** and **Etana H. T**, Optimal control strategies of COVID-19 dynamics model, *Journal of Mathematics*, 2023:2050684. https://doi.org/10.1155/2023/2050684

[63] **Kermack W.** and **Mckendrick A.**, Contribution to mathematical theorem of epidemics, *Bulletin of mathematical biology*, 53(1-2),(1991), 33–55. https://doi.org/10.1007/BF02464423

[64] **Khalil H.K**(1996), *Nonlinear Systems*, Second Edition, Prentice Hall.

[65] **Khan, M. D., Thi V., Lai Q. T.** and **Ahn J. W.**, Aggravation of Human Diseases and Climate Change Nexus. *International journal of environmental research and public health*, 16(15), 2799,(2019). https://doi.org/10.3390/ijerph16152799.

[66] **Krammer F.**. SARS-CoV-2 vaccines in development. *Nature*, 586(7830), (2020), 516–527. https://doi.org/10.1038/s41586-020-2798-3

[67] **Kroger A. T., Atkinson W. L., Marcuse E. K.,** and **Pickering L.K.**. General recommendations on immunization: recommendations of the Advisory Committee on Immunization Practices (ACIP),*MMWR. Recommendations and reports : Morbidity*

and mortality weekly report. Recommendations and reports, 55(RR-15),(2006), 1–48.

[68] **Kumar V.,Alshazly H., Idris S.A.** and **Bourouis S.** Impact of COVID-19 on Society, Environment, Economy and Education. *Sustainability* 13(24):13642, (2021). https://doi.org/10.3390/su132413642

[69] **LaSalle J.P.**, *The stability of dynamical systems*, Regional Conference series in Applied Mathematics, SIAM, Philadelphia, PA; 1976

[70] **Layek G.C.**, *An introduction to Dynamical Systems and Chaos*; Springer, India 2015.

[71] **Wu, J. T., Leung, K.** and **Leung, G. M.**, Nowcasting and forecasting the potential domestic and international spread of the 2019-nCoV outbreak originating in Wuhan, China: a modelling study. *Lancet (London, England)*, 395(10225),(2020), 689–697. https://doi.org/10.1016/S0140-6736(20)30260-9

[72] **Li, Q., Guan, X., Wu, P., Wang, X., Zhou, L., Tong, Y., Ren, R., Leung, K., Lau, E., Wong, J.Y., Xing, X.. Xiang, N., Wu, Y., Li, C., Chen, Q., Li, D., Liu, T., Zhao, J., Li, M.** and **Feng, Z.**, Early Transmission Dynamics in Wuhan, China, of Novel Coronavirus–Infected Pneumonia. *New England Journal of Medicine*, 382, (2020). 10.1056/NEJMoa2001316.

[73] **Liu R., Wu J.** and **Zhu H.**, Media/psychological impact on multiple outbreaks of emerging infectious diseases,

Comput. Math.Methods Med. 8(3):612372, (2007), 153-164. https://doi.org/10.1080/17486700701425870

[74] **Matthew O.A, Akindele A. O., Farah A. A., Funmilayo K.** and **Ahmad I. M.**, Modeling the Dynamics of COVID-19 in Nigeria, *International journal of applied and computational mathematics*, 7(3), 67, (2021). https://doi.org/10.1007/s40819-021-01014-5

[75] **McMichael A.J.** and **Lindgren E.**, Climate change: Present and future risks to health, and necessary responses. *Journal of internal medicine*, 270(5), (2011), 401–413. https://doi.org/10.1111/j.1365-2796.2011.02415.x

[76] **Morens, D. M., Folkers, G. K.** and **Fauci, A. S.**,. What is a pandemic?. *The Journal of infectious diseases*, 200(7), (2009), 1018–1021. https://doi.org/10.1086/644537

[77] **Mugisha Y.T., Ssebuliba J., Nakakawa J.N., Kikawa C.R.** and **Ssematimba A.**, Mathematical modeling of COVID-19 transmission dynamics in Uganda: Implications of complacency and early easing of lockdown, *PloS one*, 16(2), e0247456, (2021). https://doi.org/10.1371/journal.pone.0247456

[78] **Murray R.M.**, **Li Z.** and **Stastry S.S.**, *A Mathematical Introduction to Robotic Manipulation*, CRC Press, London, 1994.

[79] **Nainggolan J.** and **Ansori M.F.**, Stability and Sensitivity Analysis of the Covid-19 Spread with Cormorbid Diseases, *Symmetry*,14: 2269, (2022). 10.3390/sym14112269.

[80] **Masuda, N., Konno, N.** and **Aihara, K.** Transmission of severe acute respiratory syndrome in dynamical small-world networks. *Physical review. E, Statistical, nonlinear, and soft matter physics*, 69(3 Pt 1), 031917, (2004). https://doi.org/10.1103/PhysRevE.69.031917

[81] **Newville M., Stensitzki T., Allen D., Michal R., Antonino I.** and **Andrew N.** Lmfit: Non-linear least-square minimization and curve-fitting for python. Astrophysics Source Code Library; 2016, ascl:1606.014, 2016ascl.soft06014N.

[82] **Norman T.** and **Bailey J.** *The mathematical theory of epidemics*, Charles Griffin and Co. Ltd, London, (1957).

[83] **Nyaberi H.O** and **Wkwabubi V.W**, Mathematical Modeling of the Dynamics of Infectious Diseases with Relapse, *Asian Journals of Mathematics and Computer Research*, ISSN:2395-4205

[84] **Okuonghae D.** and **Omame A.** Analysis of a mathematical model for COVID-19 population dynamics in Lagos, Nigeria. *Chaos, solitons, and fractals*, 139:110032, (2020). https://doi.org/10.1016/j.chaos.2020.110032.

[85] **Olaniyi s., Obabiyi O.S., Okosun K.O., Oladipo A.T.** and **Adewale S.O.**, Mathematical modelling and optimal cost-effective control of COVID-19 transmission dynamics.*European physical journal plus*, 135(11), 938, (2020). https://doi.org/10.1140/epjp/s13360-020-00954-z

[86] **Olumuyiwa J. P., Hasan S. P., Afeez A., Mayowa M. O.** and **Festus A. O.**. Mathematical Model of COVID.19 pandemic with double dose vaccination, *Acta biotheoretica*, 71(2), 9, (2023). https://doi.org/10.1007/s10441-023-09460-y

[87] **Ong, S. W. X., Tan, Y. K., Chia, P. Y., Lee, T. H., Ng, O. T., Wong, M. S. Y.** and **Marimuthu, K.** , Air, Surface Environmental, and Personal Protective Equipment Contamination by Severe Acute Respiratory Syndrome Coronavirus 2 (SARS-CoV-2) From a Symptomatic Patient. *JAMA*, 323(16), (2020), 1610–1612. https://doi.org/10.1001/jama.2020.3227

[88] **Naaber, P., Tserel, L., Kangro, K., Sepp, E., Jürjenson, V., Adamson, A., Haljasmägi, L., Rumm, A. P., Maruste, R., Kärner, J., Gerhold, J. M., Planken, A., Ustav, M., Kisand, K.** and **Peterson, P.**, Dynamics of antibody response to BNT162b2 vaccine after six months: a longitudinal prospective study. *The Lancet regional health. Europe*, 10: 100208, (2021). https://doi.org/10.1016/j.lanepe.2021.100208.

[89] **Plotkin S.** History of vaccination,*Proceedings of the National Academy of Sciences*, vol. 111, no. 34, 2014. [Online]. Available: http://www.pnas.org/cgi/doi/10.1073/pnas.1400472111

[90] **Rabiu M., Willie R.** and **Parumasur N.**, Mathematical analysis of a disease-resistant model with imperfect vaccine, quarantine and treatment, *Ricerche di Matematica*, 69:(2020), 603–627. https://doi.org/10.1007/s11587-020-00496-7.

[91] **Riedel S.**. Edward Jenner and the history of smallpox and vaccination, *Proceedings (Baylor University Medical Center)*, vol. 18, no. 1, pp. 21-25, 2005.

[92] **Ross R.**, *The prevention of malaria*. London: John Murray, 1911; 651-686.

[93] **Rothan H. A.** and **Byrareddy, S. N.**, The epidemiology and pathogenesis of coronavirus disease (COVID-19) outbreak. *Journal of autoimmunity*, 109, 102433, (2020). https://doi.org/10.1016/j.jaut.2020.102433.

[94] **Rothe, C., Schunk, M., Sothmann, P., Bretzel, G., Froeschl, G., Wallrauch, C., Zimmer, T., Thiel, V., Janke, C., Guggemos, W., Seilmaier, M., Drosten, C., Vollmar, P., Zwirglmaier, K., Zange, S., Wölfel, R.** and **Hoelscher, M.**, Transmission of 2019-nCoV Infection from an Asymptomatic Contact in Germany. *The New England journal of medicine*, 382(10), (2020), 970–971. https://doi.org/10.1056/NEJMc2001468

[95] **Safi A.M** and **Gummel A.B.**, Mathematical Analysis of a Disease Transmission Model with Quarantine, Isolation and an Imperfect Vaccine, *Computers and Mathematics with Applications*, 61, (2011), 3044-3070. https://doi.org/10.1016/j.camwa.2011.03.095 .

[96] **Sasmita, N.R., Ikhwan, M., Suyanto, S. et al.**, Optimal control on a mathematical model to pattern the progression of coronavirus disease 2019 (COVID-19) in Indonesia. *glob health res policy*, 5, 38, (2020). https://doi.org/10.1186/s41256-020-00163-2

[97] **Seydel R.**, *Practical Bifurcation and Stability Analysis*. Springer-Verlag New York, 2010.

[98] **Scholarpedia.** Equilibrium. Available at:http://www.scholarpedia.org/article/Equilibrium. [Online; accessed on March 04, 2015].

[99] **Shi, H., Han, X., Jiang, N., Cao, Y., Alwalid, O., Gu, J., Fan, Y.** and **Zheng, C.**, Radiological findings from 81 patients with COVID-19 pneumonia in Wuhan, China: a descriptive study. *The Lancet. Infectious diseases*, 20(4), (2020), 425–434. https://doi.org/10.1016/S1473-3099(20)30086-4

[100] **Shrestha S.** and **Lloyd-Smith J. O.** Introduction to mathematical modeling of infectious diseases. Modeling Paradigms and Analysis of Disease Transmission Models, 75:1, 2010.

[101] **Small M.** and **Tse C.K.**, Small world and scale free model of transmission of SARS; *International Journal of Bifurcation and Chaos*. 15. (2015), 1745-1755. 10.1142/S0218127405012776.

[102] **Stern A. M.** and **Markel H.**, The history of vaccines and immunization: familiar patterns, new challenges, *Health Affairs*, vol. 24, no. 3, 2005.

[103] **Strogast S.H**, *Nonlinear Dynamics and Chaos*, Westview press, 2015.

[104] **Sun T.C., DarAssi M.H., Alfwzan W.F., Khan M.A., Alshahrani A.S., Alqahtani S.S.** and **Muhammad T.**, Mathematical Modeling of COVID-19 with Vaccination Using Fractional Deriva-

tive: A Case Study. *Fractal Fract.*, 7, 234, (2023). https://doi.org/10.3390/fractalfract7030234

[105] **Takasar H., Muhammad O., Farhad A., Sajid R.,Taghreed A. and Emad E.E.**, Sensitivity analysis and optimal control of COVID-19 dynamics based on SEIQR model, *Results in physics*, 22:103956, (2021). https://doi.org/10.1016/j.rinp.2021.103956

[106] **Tchoumi S.Y, Rwezaura H.** and **Tcheunche J.M**, Dynamics of a two-strain COVID-19 model with vaccination, *Results in physics*, 39: 105777, (2022). https://doi.org/10.1016/j.rinp.2022.105777

[107] **Tulu A.M.** and **Koya P.R.**, The impact of infective migrants on the spread of dog rabies, *Am.J.Appl.Math.*,5(3), (2017). Available at doi:10.11648/j.ajam.20170503.12.

[108] **Vitaly V., Malay B.** and **Sergei P.**, On a quarantine model of Covid-19 infection and data analysis, *Mathematical Modelling of Natural Phenomena*, 15, 24, (2020). 10.1051/mmnp/2020006.

[109] **Wan H, Cui JA** and **Yang GJ.** Risk estimation and prediction by modeling the transmission of the novel coronavirus (COVID-19) in mainland China excluding Hubei province. *medRxiv.* 2020 Jan 1 https://doi.org/10.1101/2020.03.01.20029629

[110] **Wang Z., Bauch C. T., Bhattacharyya S., Onofrio A., Manfredi P., Perc M., Perra N., Salathe M.** and **Zhao D.** Statistical physics of vaccination, *Physics Reports*, 664, (2016), 1-113. https://doi.org/10.1016/j.physrep.2016.10.006

[111] **Webb G.** A COVID-19 Epidemic Model Predicting the Effectiveness of Vaccination in the US. *Infectious Disease Repository*, 13, (2021), 654 667. https://doi.org/10.3390/idr13030062.

[112] **Wölfel R., Corman V.M., Guggemos W., Seilmaier M., Zange S., Müller M.A, Niemeyer D, Jones T.C, Vollmar K.P., Rothe C., Hoelscher M., Bleicker T., Brünink S., Schneider J., Ehmann R., Zwirglmaier K., Drosten C.** and **Wendtner C.**, Virological assessment of hospitalized patients with COVID-2019. *Nature*, 581(7809),(2020), 465–469. https://doi.org/10.1038/s41586-020-2196-x

[113] **World Health Organization**, Draft landscape of COVID-19 candidate vaccines. *WHO https://www.who.int/publications/m/item/draft-landscape-of-covid19-candidate-vaccines (2020)*

[114] **World Health Organization**, Statement on the second meeting of the international health regulations (2005): emergency committee regarding the outbreak of novel coronavirus (2019-ncov) *https://www.who.int/news-room/detail/30-01-2020*(2005)(2019-ncov), January 2020.

[115] **Wu J.T, Leung K.** and **Leung G.M.** Nowcasting and forecasting the potential domesstic and international spread of the COVID-19 outbreak originating in Wuhan, China. a modelling study.*Lancet (London, England)*, 395(10225),(2020), 689–697. https://doi.org/10.1016/S0140-6736(20)30260-9

[116] **Wu, L. P., Wang, N. C., Chang, Y. H., Tian, X. Y., Na, D. Y., Zhang, L. Y., Zheng, L., Lan, T., Wang, L. F.** and **Liang, G. D.**, Duration of antibody responses after severe acute respiratory syndrome. *Emerging infectious diseases*, 13(10), (2007), 1562–1564. https://doi.org/10.3201/eid1310.070576.

[117] **Xie, X., Zhong, Z., Zhao, W., Zheng, C., Wang, F.** and **Liu, J.**, Chest CT for Typical Coronavirus Disease 2019 (COVID-19) Pneumonia: Relationship to Negative RT-PCR Testing. *Radiology*, 296(2), (2020), E41–E45. https://doi.org/10.1148/radiol.2020200343.

[118] **Yan, X.** and **Zou, Y.**, Optimal and sub-optimal quarantine and isolation control in SARS epidemics. *Mathematical and computer modelling*, 47(1), (2008), 235–245. https://doi.org/10.1016/j.mcm.2007.04.003

[119] **Xu, X., Yu, C., Qu, J., Zhang, L., Jiang, S., Huang, D., Chen, B., Zhang, Z., Guan, W., Ling, Z., Jiang, R., Hu, T., Ding, Y., Lin, L., Gan, Q., Luo, L., Tang, X.** and **Liu, J.**, Imaging and clinical features of patients with 2019 novel coronavirus SARS-CoV-2, *European journal of nuclear medicine and molecular imaging*, 47(5), (2020), 1275–1280. https://doi.org/10.1007/s00259-020-04735-9.

[120] **Sun, C., Yang, W., Arino, J.** and **Khan, K.**, Effect of media-induced social distancing on disease transmission in a two patch setting. *Mathematical biosciences*, 230(2), (2011), 87–95. https://doi.org/10.1016/j.mbs.2011.01.005

[121] **Yin Y.** and **Wunderink R.G**, Mers, sars and other coronaviruses of pneumonia, *Respirology (Carlton, Vic.)*, 23(2), (2018), 130–137. https://doi.org/10.1111/resp.13196

[122] **Yusuf T.T** and **Benyah F.**, Optimal control of vaccination and treatment for a SIR epidemiological model, *World Journal of Modelling and Simulation*, 8, (2012), 194-204.

[123] **Kifle, Z. S.** and **Obsu, L. L.**, Mathematical modeling for COVID-19 transmission dynamics: A case study in Ethiopia. *Results in physics*, 34:105191, (2022). https://doi.org/10.1016/j.rinp.2022.105191

[124] **Zhao, S., Lin, Q., Ran, J., Musa, S. S., Yang, G., Wang, W., Lou, Y., Gao, D., Yang, L., He, D.** and **Wang, M. H.**, Preliminary estimation of the basic reproduction number of novel coronavirus (2019-nCoV) in China, from 2019 to 2020: A data-driven analysis in the early phase of the outbreak. *International journal of infectious diseases : IJID : official publication of the International Society for Infectious Diseases*, 92, (2020), 214–217. https://doi.org/10.1016/j.ijid.2020.01.050

[125] **Zheng, Y., Chen, Y., Yu, K., Yang, Y., Wang, X., Yang, X., Qian, J., Liu, Z. X.** and **Wu, B.**, Fatal Infections Among Cancer Patients: A Population-Based Study in the United States. *Infectious diseases and therapy*, 10(2), (2021), 871–895. https://doi.org/10.1007/s40121-021-00433-7

APPENDICES

A. PYTHON CODES FOR MODEL 1

import numpy as np

import matplotlib.pyplot as plt

from scipy.integrate import odeint

$linestyle_str = [('solid','solid'), ('dotted','dotted'),$

$('dashed','dashed'), ('dashdot','dashdot')]$

t=np.linspace(0, 100, num=1000)

beta=0.30000025

gamma=0.001

mu=1/(67.21*12)

pi=1000/(67.21*12)

epsilon=0.18696757

eta=0.01075081

alpha=1/15delta=0.5887305

varphi=0.000225

theta=0.6785

omega=1/7

kappa=0.11032736

tau=0.00145

params=[beta, gamma, mu, pi, epsilon, eta, alpha, delta, varphi, omega,

kappa, theta, tau]

$V_{h_{initial}} = 600$

$E_{h_{initial}} = 5500$

$A_{h_{initial}} = 550$

$I_{h_{initial}} = 50$

$R_{h_{initial}} = 600$

$S_{h_{initial}} = 54027487 - V_{h_{initial}} - E_{h_initial} - A_{h_{initial}} - I_{h_{initial}} - R_{h_{initial}}$

$x_{h_{initial}} = S_{h_{initial}}, V_{h_{initial}}, E_{h_{initial}}, A_{h_{initial}}, I_{h_{initial}}, R_{h_initial}$

$N_h = S_{h_{initial}} + V_{h_{initial}} + E_{h_{initial}} + A_{h_{initial}} + I_{h_{initial}} + R_{h_{initial}}$

$x_{h_{initial}} = S_{h_{initial}}, V_{h_{initial}}, E_{h_{initial}}, A_{h_{initial}}, I_{h_{initial}}, R_{h_{initial}}$

def sim(variables, t, params):

$S_h = variables[0]$

$V_h = variables[1]$

$E_h = variables[2]$

$A_h = variables[3]$

$I_h = variables[4]$

$R_h = variables[5]$

    beta=params[0]

    gamma=params[1]

    mu=params[2]

    pi=params[3]

    epsilon=params[4]

    eta=params[5]

    alpha=params[6]

    delta=params[7]

    varphi=params[8]

    theta=params[9]

    omega=params[10]

    kappa=params[11]

    tau=params[12]

def deriv(x, t, params):

    $S_h, V_h, E_h, A_h, I_h, R_h = x$

$dS_h dt = pi + varphi * V_h + tau * R_h - beta * (eta * A_h + I_h) * S_h - (mu + theta) * S_h$

$dV_h dt = theta * S_h - (mu + varphi) * V_h$

$dE_h dt = beta * (eta * A_h + I_h) * S_h - (mu + omega) * E_h$

$dA_h dt = (1 - epsilon) * omega * E_h - (mu + alpha) * A_h$

$dI_h dt = epsilon * omega * E_h + (1 - kappa) * alpha * A_h - (mu + gamma + delta) * I_h$

$dR_h dt = gamma * I_h + alpha * kappa * A_h - (mu + tau) * R_h$

$return([dS_h dt, dV_h dt, dE_h dt, dA_h dt, dI_h dt, dR_h dt])$

$x_{initial} = S_{h_{initial}}, V_{h_{initial}}, E_{h_{initial}}, A_{h_{initial}}, I_{h_{initial}}, R_{h_{initial}}$

$soln = odeint(deriv, x_{initial}, t, args = (params,))$

$S_h, V_h, E_h, A_h, I_h, R_h = soln.T\ defplotdata(t, V_h, E_h, A_h, I_h, R_h) :$

fig = plt.figure(facecolor='w')

$ax = [fig.add_subplot(111, axisbelow = True)]$

fig = plt.figure(figsize=(12,6))

$ax[0].plot(t, V_h, lw = 2.5, linestyle = '-', color = "k", label = 'Vaccinated')$

$ax[0].plot(t, E_h, lw = 2.5, linestyle = '-.', color = "b", label = 'Exposed')$

$ax[0].plot(t, A_h, lw = 2.5, color = "m", label = 'Asymptomatic')$

$ax[0].plot(t, I_h, lw = 2.5, linestyle = '-', color = "r", label = 'Symptomatic')$

$ax[0].plot(t, R_h, lw = 2.5, linestyle = '-.', color = "g", label = 'Recovered')$

$ax[0].spines['left'].set_position('zero')$

$ax[0].spines['bottom'].set_position('zero')$

$ax[0].set_title('')$

$ax[0].set_xlabel('Time(Months)')$

$ax[0].set_ylabel('POPULATION')$

$ax[0].set_xlim(0, 100)$

$forainax:$

$ax[0].grid(linestyle = "dashed")$

$a.legend()$

$plt.tight_layout()$

$plotdata(t, V_h, E_h, A_h, I_h, R_h)$

B. PYTHON CODES FOR MODEL 2

import numpy as np

import matplotlib.pyplot as plt

from scipy.integrate import odeint

$linestyle_str = [('solid','solid'), ('dotted','dotted'), ('dashed','dashed'), ('dashdot','dashdot')]$

t=np.linspace(0, 100, num=1000)

$N_h = 54027487$

$beta = 0.150000025$

$gamma_1 = 0.0125$

$gamma_2 = 0.05$

$gamma_3 = 0.001$

$mu = 1/(67.21 * 12)$

$pi = N_h * mu$

$epsilon = 0.18696757$

$eta = 0.01075081$

$alpha = 1/15$

$delta_1 = 0.018$

$delta_2 = 0.0107$

$varphi = 0.00225$

$theta = 0.6785 omega = 1/7$

$kappa = 0.11032736$

$sigma = 0.7$

$params = [beta, gamma_1, gamma_2, gamma_3, mu, pi, epsilon, eta, alpha,$

$delta_1, delta_2, varphi, omega, kappa, theta, sigma]$

$V_{h_{initial}} = 500$

$E_{h_{initial}} = 6500$

$A_{h_{initial}} = 560$

$I_{h_{initial}} = 50$

$J_{h_{initial}} = 20$

$R_{h_{initial}} = 60$

$S_{h_{initial}} = 54027487 - V_{h_{initial}} - E_{h_{initial}} - A_{h_{initial}} - I_{h_{initial}} - J_{h_{initial}} - R_{h_{initial}}$

$x_{h_{initial}} = S_{h_{initial}}, V_{h_{initial}}, E_{h_{initial}}, A_{h_{initial}}, I_{h_{initial}}, J_{h_{initial}}, R_{h_{initial}}$

$N_h = S_{h_{initial}} + V_{h_{initial}} + E_{h_{initial}} + A_{h_{initial}} + I_{h_{initial}} + J_{h_{initial}} + R_{h_{initial}}$

$x_{h_{initial}} = S_{h_{initial}}, V_{h_{initial}}, E_{h_{initial}}, A_{h_{initial}}, I_{h_{initial}}, J_{h_{initial}}, R_{h_{initial}}$

def sim(variables, t, params):

$S_h = variables[0]$

$V_h = variables[1]$

$E_h = variables[2]$

$A_h = variables[3]$

$I_h = variables[4]$

$J_h = variables[5]$

$R_h = variables[6]$

$beta = params[0]$

$gamma_1 = params[1]$

$gamma_2 = params[2]$

$gamma_3 = params[3]$

$mu = params[4]$

$pi = params[5]$

$epsilon = params[6]$

$eta = params[7]$

$alpha = params[8]$

$delta_1 = params[9]$

$delta_2 = params[10]$

$varphi = params[11]$

$theta = params[12]$

$omega = params[13]$

$kappa = params[14]$

$sigma = params[15]$

def deriv(x, t, params): $S_h, V_h, E_h, A_h, I_h, J_h, R_h = x$

$dS_hdt = pi + varphi * V_h - beta * (eta * A_h + I_h) * S_h/(N_h - J_h) - (mu + theta) * S_h$

$dV_hdt = theta * S_h - (1 - sigma) * beta * (eta * A_h + I_h) * V_h/(N_h - J_h) - (mu + varphi) * V_h$

$dE_hdt = (1 - sigma) * beta * (eta * A_h + I_h) * V_h/(N_h - J_h) + beta * (eta * A_h + I_h) * S_h/(N_h - J_h) - (mu + omega) * E_h$

$dA_hdt = (1 - epsilon) * omega * E_h - (mu + alpha) * A_h$ $dI_hdt = epsilon * omega * E_h + (1 - kappa) * alpha * A_h - (mu + gamma_1 + gamma_2 + delta_1) * I_h$

$dJ_hdt = gamma_1 * I_h - (mu + delta_2 + gamma_3) * J_h$

$dR_hdt = alpha * kappa * A_h + gamma_2 * I_h + gamma_3 * J_h - mu * R_h$

$return([dS_hdt, dV_hdt, dE_hdt, dA_hdt, dI_hdt, dJ_hdt, dR_hdt])$

$x_{initial} = S_{h_{initial}}, V_{h_{initial}}, E_{h_{initial}}, A_{h_{initial}}, I_{h_{initial}}, J_{h_{initial}}, R_{h_{initial}}$

$soln = odeint(deriv, x_{initial}, t, args = (params,))$

$S_h, V_h, E_h, A_h, I_h, J_h, R_h = soln.T$

$defplotdata(t, S_h, V_h, E_h, A_h, I_h, J_h, R_h)$:

fig = plt.figure(facecolor='w')

$ax = [fig.add_subplot(111, axisbelow = True)]$

$fig = plt.figure(figsize = (12, 6))$

$ax[0].plot(t, S_h, lw = 2.5, color = "c", label =' Susceptible')$

$ax[0].plot(t, V_h, lw = 2.5, linestyle =' -', color = "k", label =' Vaccinated')$

$ax[0].plot(t, E_h, lw = 3, linestyle =' -.', color = "b", label =' E_h')$

$ax[0].plot(t, A_h, lw = 3, linestyle =' --', color = "m", label =' I_{hA}')$

$ax[0].plot(t, I_h, lw = 3, linestyle =' -', color = "r", label =' I_h')$

$ax[0].plot(t, J_h, lw = 3, linestyle =' -', color =' 00FF00', label =' J_h')$

$ax[0].plot(t, R_h, lw = 3, linestyle =' -.', color = "g", label =' R_h')$

$ax[0].spines['left'].set_position('zero')$

$ax[0].spines['bottom'].set_position('zero')$

$ax[0].set_{title}('')$

$ax[0].set_xlabel('Time(Months)')$

$ax[0].set_ylabel('POPULATION')$

$ax[0].set_xlim(0, 100)$

$ax[0].set_ylim(0, 8000)$

for a in ax: ax[0].grid(linestyle = "dashed")

a.legend()

$plt.tight_{layout()}$

$plotdata(t, S_h, V_h, E_h, A_h, I_h, J_h, R_h)$